**T.R.**
**ONDOKUZ MAYIS UNIVERSITY**
**INSTITUTE OF GRADUATE STUDIES**
**DEPARTMENT OF NANOSCIENCE AND NANOTECHNOLOGY**

# PHARMACEUTICAL PREPARATION AND CHARACTERIZATION OF LISINOPRIL DRUG NANOCRYSTALS BY USING ANTI-SOLVENT CRYSTALLIZATION METHOD

Ph.D. Thesis

**Abdulmohsin AL AIROA**

Supervisor

**Assist. Prof. Dr. İbrahim İNANÇ**

.

SAMSUN
2024

## .ACCEPTANCE AND APPROVAL OF THE THESIS

The study entitled **"PHARMACEUTICAL PREPARATION AND CHARACTERIZATION OF LISINOPRIL DRUG NANOCRYSTALS BY USING ANTI-SOLVENT CRYSTALLIZATION METHOD"** prepared by **Abdulmohsin AL AIROA** and supervised by **Assist. Prof. Dr. İbrahim İNANÇ** was found successful and unanimously accepted by committee members as Ph.D thesis following the examination on the date 14.8.2024.

| | **Title Name SURNAME<br>University<br>Department/Art** | **Final Decision** |
|---|---|---|
| **Chairman** | Prof. Dr. Oğuzhan YAVUZ<br>Cukurova University<br>Department of Preclinical Sciences | ☒ Accept<br>☐ Reject |
| **Member** | Asisst. Prof. Dr. İbrahim İNANÇ<br>Ondokuz Mayıs University<br>Department of Metallurgical and Materials Engineering | ☒ Accept<br>☐ Reject |
| **Member** | Assoc. Prof. Dr. Sinem ÇEVİK<br>Ondokuz Mayıs University<br>Department of Metallurgical and Materials Engineering | ☒ Accept<br>☐ Reject |
| **Member** | Asisst. Prof. Dr. Suna AVCIOĞLU<br>Yıldız Technical University<br>Department Of Metallurgical And Materials Engineering | ☒ Accept<br>☐ Reject |
| **Member** | Asisst. Prof. Dr. Aydemir Güralp URAL<br>Samsun University<br>Department of Aeronautical and Space Engineering | ☒ Accept<br>☐ Reject |

This thesis has been approved by the committee members that already stated above and determined by the Institute Executive Board.

.

Prof. Dr. Ahmet TABAK
Head of Institute of Graduate Studies

## DECLARATION OF COMPLIANCE WITH SCIENTIFIC ETHIC

I hereby declare and undertake that I complied with scientific ethics and academic rules in all stages of my Ph.D. thesis, that I have referred to each quotation that I use directly or indirectly in the study, and that the works I have used consist of those shown in the sources, that it was written in accordance with the institute writing guide and that the situations stated in the article 3, section 9 of the Regulation for TÜBİTAK Research and Publication Ethics Board were not violated.

Is Ethics Committee Necessary?

Yes ☐ (If it necessary, please add appendices.)

No ☒

14/08/2024
Abdulmohsin AL AIROA

## DECLARATION OF THE THESIS STUDY ORIGINALITY REPORT

**Thesis Title:** (PHARMACEUTICAL PREPARATION AND CHARACTERIZATION OF LISINOPRIL DRUG NANOCRYSTALS BY USING ANTI-SOLVENT CRYSTALLIZATION METHOD)

As a result of the originality report taken by me from the plagiarism detection program on 21/06/2024 for the thesis titled above,

Similarity ratio: 18%

Single resource rate: 1% has been released.

14/08/2024
Assist. Prof. Dr. İbrahim İNANÇ

# ÖZET

ANTİ-SOLVENT KRİSTALİZASYON YÖNTEMLERİ KULLANILARAK LİSİNOPRİL İLAÇ NANOKRİSTALLERİNİN FARMASÖTİK HAZIRLANMASI VE KARAKTERİZASYONU

Abdulmohsin AL AIROA
Ondokuz Mayıs Üniversitesi
Lisansüstü Eğitim Enstitüsü
Nanobilim ve Nanoteknoloji Ana Bilim Dalı
Doktora, Ağustos /2024
Danışman: Dr. Öğr. Üyesi İbrahim İNANÇ

Kalp hastalıkları ve yüksek tansiyon, günümüzün en tehlikeli, önemli ve yaygın hastalıkları arasında yer almakta olup, kontrol altına alınması için hızlı tedavi uygulanması gerekmektedir. Nanoteknoloji, ilaç endüstrisi alanında büyük bir gelişmeye katkıda bulunarak, geleneksel ilaçların hastalıkların tedavisindeki performansının kontrol edilmesi ve iyileştirilmesi üzerindeki olumlu etkisini artırmıştır. Nanotıp, geleneksel ilaçların ulaşamadığı hücreleri yüksek oranda hedefleyebilme avantajına sahiptir.

Lisinopril nanokristalini ve kolloidal nanoparçacıkları üretmek için Antisolvent kristalizasyon tekniği kullanıldı. Üç farklı numune hazırlandı; birinci numune, 25 mg/ml Lisinopril tozunun saf su içinde çözülmesiyle hazırlandı ve antisolvent solüsyonu olarak Tween 20'nin mevcudiyetinde aseton içerisinde çökertildi. İkinci numune, 50 mg/ml Lisinopril tozunun saf su ve aseton, asetonitril, dimetilformamid ve Tween 80 içeren bir anti-solvent solüsyonu içinde çözülmesiyle hazırlandı.

Üçüncüsü, 100 mg/ml Lisinopril tozunun sulu solüsyonunun asetonitril, dimetilformamid ve PVP'den oluşan bir antisolvent solüsyonu ile kullanılmasıyla hazırlandı. Ham Lisinopril ve elde edilen kolloidal nanopartiküller ve yeniden kristalize edilmiş tozlar SEM, XRD ve FTIR, kullanılarak karakterize edilmiştir ve ayrıca aktif madde oranları Faz-Yüksek Performanslı Sıvı Kromatografisi (RP-HPLC) ile belirlenip, üretilen yeniden kristalize edilmiş tozların su içeriği de incelenmiştir.

Son aşamada ise üretilen tüm Lisinopril ilaç nanokristalleri için stabilite çalışması yapıldı ve üretilen tüm numuneler, ilaç endüstrisinde kullanım için stabilitelerinin sağlanması amacıyla tersine mühendislik farmasötik testleri ile tespit edilen referans hammadde ile karşılaştırıldı. Numuneler, WHO sınırlamalarına göre 6 aylık stabilite çalışması boyunca stabil bir farmasötik formüle sahiptir.

**Anahtar Sözcükler:** Anti-solvent kristalizasyonu, anti-hipertansif, Lisinopril nanokristal, nanoilaç, karakterizasyon

## ABSTRACT

PHARMACEUTICAL PREPARATION AND CHARACTERIZATION OF LISINOPRIL DRUG NANOCRYSTALS BY USING ANTI-SOLVENT CRYSTALLIZATION METHOD

Abdulmohsin AL AIROA
Ondokuz Mayıs University
Institute of Graduate Studies
Department of Nanoscience and Nanotechnology
Ph.D., August/2024
Supervisor: Assist. Prof. Dr. İbrahim İNANÇ

Heart disease and high blood pressure are among the most dangerous, significant, and widespread diseases in the present time, which need rapid treatment to control them. Antihypertensive drugs comprise several compounds with the therapeutic intention of preventing, controlling, or treating hypertension.

Nanotechnology has contributed to significant development in the pharmaceutical industry, improving its positive effect on controlling and improving the performance of traditional medicines in treating diseases. Nanomedicines have the advantage of targeting cells that traditional drugs cannot reach at a high rate.

The Antisolvent crystallization technique produced the Lisinopril nanocrystal and colloidal nanoparticles. Three different samples were prepared; sample one was prepared by dissolving 25 mg/ml of Lisinopril powder in distilled water. as a solvent solution and precipitated in acetone with the presence of Tween 20 as the antisolvent solution. Sample two was prepared by dissolving 50 mg/ml of Lisinopril powder in distilled water.. as a solvent solution with acetone, acetonitrile, dimethylformamide, and Tween 80 as antisolvent solutions. The third one was prepared using 100 mg/ml of a solvent solution with an antisolvent solution consisting of acetonitrile, dimethylformamide, and PVP. The raw Lisinopril and obtained colloidal particles and re-crystallized powders were characterized by using SEM, XRD, and FTIR, and also the ratio of the active substance by Phase-High Performance Liquid Chromatography (RP-HPLC) as well as the water content of the produced re-crystallized powders was also examined.

In the last stage, a stability study was conducted for all produced Lisinopril drug nanocrystals, and all produced samples were compared with the reference raw material detected by reverse engineering pharmaceutical tests to ensure their stability for use in the pharmaceutical industry. Samples have a stable pharmaceutical formula during 6 months of stability study according to the limitation of WHO.



**Keywords:** Anti-solvent crystallization, anti-hypertensive, Lisinopril nanocrystal, nanodrug, characterization

# ACKNOWLEDGEMENT

First of all, I convey appreciation to my supervisor, **Dr. İbrahim İNANÇ**, for his assistance in procuring the required equipment and devices, which were essential for the successful completion of this project. Furthermore, I appreciate his provision of the necessary resources and granting me the autonomy to carry out my work. Without his valuable advice and guidance, this project would not have achieved its desired result. **Dr. İbrahim İNANÇ,** my supervisor, has regularly communicated with me during all stages of our work. I consider myself privileged to be one of his students.

Throughout the research process, I am grateful to **Dr. Senim ÇEVİK** and **Dr. Aydemir Güralp URAL** for their important help and wise counseling.

I express my gratitude to the entire faculty of Ondokuz Mayıs University's Department of Nanoscience and Nanotechnology, as well as the Engineering Department, for their invaluable support during the project.

I thank to my friends **Mohammed AL SAMARRAI**, **Ahmad ALBAYATI,** and **Rafid AL DORI** for their invaluable assistance during the study and work stages.

Ultimately, I may only convey my profound love and admiration to my family, as it is solely because of their unwavering support that I have overcome all the challenges in my life.

Abdulmohsin AL AIROA

# CONTENTS

# SYMBOLS AND ABBREVIATIONS

| | |
|---|---|
| API | : Active Pharmaceutical Ingredients |
| ACE | : Angiotensin-Converting Enzyme |
| CV | : Cardiovascular |
| D.W. | : Distilled Water |
| DMF | : Dimethylene Formamide. |
| DSC | : Differential Scanning Calorimetry |
| FDA | : Food And Drug Administration |
| FTIR | : Fourier Transform Infrared Spectroscopy. |
| ICH | : International Council for Harmonisation |
| KFT | : Karl Fischer Titration |
| PVP | : Polyvinylpyrrolidone |
| SEM | : Scanning Electron Microscopy |
| TGA | : Thermogravimetric Analysis |
| USP | : United State Pharmacopoeia |
| WHO | : World Health Organization |
| XRD | : X-Ray Diffraction |

# FIGURES LEGENDS

# TABLES LEGENDS

# 1. INTRODUCTION

Hypertension, often known as high blood pressure, impacts almost one billion people globally and is a serious and potentially fatal health disease (Go et al., 2013). Annually, the incidence of hypertension is projected to rise, resulting in substantial healthcare expenses and diminished worker productivity, amounting to billions of dollars. Numerous long-term health problems, including cardiovascular disorders (such as heart attacks, heart failure, and strokes) and renal diseases, have hypertension as their root cause or a substantial risk factor (Rapsomaniki et al., 2014). Hypertension is a significant global health problem, as evidenced by its economic expenses, high prevalence, and long-term health problems it is associated with.

Antihypertensives are drugs prescribed for the treatment of elevated blood pressure, sometimes known as hypertension. Antihypertensive therapy aims to mitigate the adverse effects of hypertension. The primary advantage of any antihypertensive treatment is reducing blood pressure, which is mostly unaffected by the specific type of medication employed (Medicine, 2000).

After deciding to start antihypertensive treatment, the selection of medication should be determined by the patient's specific characteristics, such as their age and any other existing medical conditions (Law et al., 2003).

Lisinopril, with the molecular formula $C_{21}H_{31}N_3O5$, is an extremely advantageous medicine for treating hypertension, according to its wide range of uses and effectiveness in therapy. It is prescribed as an angiotensin-converting enzyme inhibitor and has been on the market for more than thirty years. Lisinopril exhibits unique attributes that differentiate it from enalapril and captopril: (1) It has a long half-life, (2) it has hydrophilic characteristics, and (3) the liver does not break it down (Warner et al., 1988).

Nanoscience is the scientific investigation of materials at the nanoscale, which refers to dimensions on the order of one billionth of a meter; transforming a large quantity of material into nanoscale dimensions enhances its properties, including physicochemical, biological, mechanical, optical, electrical, and others.

The recently obtained unique features of nanoengineered materials can be employed for several important applications. Therefore, it is a technology that facilitates and supports different sectors, including chemicals, consumer items, health, energy, and other businesses, as well as the environment. The utilization of this technology is experiencing rapid and significant growth in the pharmaceutical industry (Ai et al., 2011).

Nanotechnology is a technology that allows for the development of both little improvements and major breakthroughs in numerous fields. The utilization of this technology holds immense potential in the pharmaceutical sector, as it can enhance the treatment effectiveness by precisely delivering the medicine to the specific location of the ailment. Concomitant reduction of the drug dosage may result in a decrease in toxicity (Ragelle et al., 2017).

Pharmaceuticals engineered on the nanoscale, i.e., nanopharmaceuticals, which are pharmaceuticals designed at the nanoscale, are a developing area that integrates nanotechnology with pharmaceutical and biomedical science. Their purpose is to enhance drug delivery, perhaps leading to improved effectiveness and safety (Fatehi et al., 2012).

Drug nanocrystals refer to drug crystals with less than 100 nm dimensions. Decreasing the particle size to the limit of the nanoscale increases the surface area, which in turn promotes disintegration. Nanocrystal preparations have been formed to enhance the solubility created to enhance the oral distribution of pharmaceuticals with low solubility, enhancing their oral bioavailability and reducing their pharmacokinetics (Shen et al., 2018; Xie et al., 2018).

A number of oral medicinal treatments utilizing nanocrystals have been effectively commercialized (Y. Lu et al., 2017). The majority of these products utilize drug nanocrystals that are created using the top-down strategy, specifically by grinding bigger drug crystals. In order to decrease the dimensions and preserve the uniformity of nanocrystals, it is commonly necessary to apply surfactants to the surface of the nanocrystals. However, this practice raises safety issues due to the potential adverse effects caused by the surfactants (Pramanick et al., 2013).

Moreover, the utilization of stabilized materials amplifies the total chemical load on the patient, leading to a decrease in drug loading and intensifying the risk of potential hazardous reactions.

Nanoparticles can be manufactured using top-down or bottom-up approaches (Zhang et al., 2009). The top-down approach employs many technologies, including jet milling, pearl milling, spiral media milling technology, and high-pressure homogenization, to mechanically reduce pre-existing larger particles. Nevertheless, these approaches suffer from inefficiency caused by the substantial energy required and the denaturation during milling (Cho et al., 2010).

In contrast, the "bottom-up" strategy, which involves the use of anti-solvent precipitation technology, is rarely employed. Anti-solvent crystallization, as a bottom-up approach, is a more direct, economical, and easily expandable technology in comparison to milling and high-pressure homogenization, which are top-down procedures (Kakran et al., 2012).

Anti-solvent crystallization is an efficient technique for preparing micro-to-nano-sized drug particles, which is a separation and purification process (Xia et al., 2010). This technique produces crystals through the manipulation of solutions and controls the properties of the crystals, such as their particle size and shape (Park et al., 2012). Using an anti-solvent throughout the crystallization process diminishes the solubility of a solute inside the solution, prompting fast crystallization. The properties of the anti-solvent, both in terms of its physical and chemical characteristics, can alter the speed at which it combines with the solutions. As a result, this has an effect on the formation of nuclei and the rate at which crystals grow in the chemical solution. Additionally, the variables of crystallization experiments have a substantial impact on the process of particle formation and dictate the dimensions and distribution of crystals (Park et al., 2010).

In most cases, the antisolvent is composed of hydrophilic stabilizers, also known as surfactants, that are absorbed into the surface of the crystal to prevent its growth. Nanocrystals have clear advantages in terms of solubility and dissolution rate when the particle size is reduced and the surface area is raised. Nevertheless, a larger surface area results in a higher surface free energy. Nanocrystals have a

tendency to spontaneously come together in clusters in order to reduce the amount of energy on their surfaces (Müller et al., 2011).

The majority of products that use nanocrystals are usually produced as nanosuspensions or solid dosage forms.

The process of combining particles presents considerable difficulties in the development of products based on nanocrystals. Nano-crystal aggregation can occur at many stages, such as during nano-crystal formation, nanosuspension storage, and the dissolution of solid dosage forms containing nanocrystals. The most prevalent approach to counteract aggregation in colloidal systems is to incorporate stabilizers into the formulation. Conventional colloid science provides strategies for solving the aggregation issue, such as using surface charges or capping agents to stabilize nanocrystals against aggregation (Li et al., 2006).

Colloidal particles are solid microscopic particles that can be suspended in a liquid. Colloids are of a size that allows thermal energy to drive their movement and keep them in balance with the surrounding fluid. However, they are also large enough to enable accurate determination of their positions and motions using optical techniques. Colloidal suspensions serve as an excellent model system for investigating various phenomena in condensed matter physics due to the similar phase behavior shown by the solid particles in these systems and other condensed systems ( Lu et al., 2013).

Analytical chemistry has greatly benefited from the use of High-Performance Liquid Chromatography. Any substance that can dissolve in a liquid can have its chemical components separated, differentiated, and quantified using this method (Rao et al., 2015). The process includes the injection of a solution containing the sample into a column composed of a permeable material (stationary phase), followed by the application of high pressure to pump a liquid (mobile phase) through the column. The sample separation is determined by the discrepancies in migration rates inside the column, which arise from the distinct distribution of the sample between the stationary and mobile phases.

It is increasingly being used to estimate bioavailability and, in certain instances, to replace clinical investigations in determining bioequivalence. The

dissolution characteristics of a medicine have a substantial impact on its pharmacological efficacy (Ganesh et al., 2010).

Quantifying the amount of water is a crucial element in the pharmaceutical sector. It is essential in the many stages of pharmaceutical development, including technique, production, and quality control. It is essential to comprehend the moisture content and hygroscopic properties of a medicinal substance, as well as its existence in the end result. Water can negatively affect the solubility activity and therapeutics of the active pharmaceutical ingredients (APIs), as well as the potency, effectiveness, and longevity (Warner et al., 2007). Hence, it is crucial to establish precise requirements and employ accurate techniques for quantifying water content in pharmaceuticals during their developmental phases.

One of the most considerable investigations of functional groups is of various components of Fourier transform infrared spectroscopy (FTIR), including gaseous, liquid, and solid ones. It measures the amount of infrared radiation a molecule absorbs, resulting in a spectrum. IR light absorbs less energy and longer wavelengths than microwave radiation (Khan et al., 2018).

Dissolution refers to the incorporation of a solid solute into a solution. In the pharmaceutical industry, dissolution refers to the speed at which a pharmacological substance dissolves in a solution within a defined timeframe based on predetermined factors such as the solid and liquid interaction, temperature, and the composition of the solvent. Dissolution is a crucial quality assurance test performed on pharmaceutical dosage forms.

This study successfully produced Lisinopril nanocrystals using three separate samples, employing various solvents, stabilizers, and synthesis settings. The antisolvent crystallization method was utilized, incorporating a stabilizer to prevent clumping and serve as a lubricant. Sample 1 was prepared by dissolving 100 mg/ml of Lisinopril powder in distilled water (D.W.) to form a solvent solution. The precipitation was performed by incorporating an antisolvent solution that consisted of a mixture of acetonitrile, dimethylformamide, and PVP.

Sample 2 was generated by dissolving 50 mg/ml of Lisinopril powder in distilled water (D.W.). The solution was subsequently precipitated using an

antisolvent solution composed of a mixture of acetonitrile, acetone, dimethylformamide, and Tween 80.

A 25 mg/ml of Lisinopril powder in distilled water (D.W) was the solvent solution to produce Sample 3. The solvent solution is subsequently separated from the antisolvent solution, which is a mixture of acetone and Tween 20, forming a solid precipitate. To facilitate SEM examination, colloidal samples were prepared and maintained at a temperature of 5 ℃ for a duration of 2 hours. The size and morphology of particles are analyzed using SEM.

# 2. THEORETICAL PART

## 2.1. High Blood Pressure (Hypertensıon)

### 2.1.1. Definition

Hypertension is typically characterized by the long-term increase in the pressure of the arteries throughout the body, surpassing a specific threshold value. However, there is growing evidence that a significant increase in the risk of cardiovascular disease (CVD) is associated with blood pressure (BP) levels exceeding 115/75 mm Hg (Kannel, 1996; Klag et al., 1996; Vasan et al., 2001). People can be diagnosed as antihypertensive patients whose blood pressure readings over were between 120/80 mm Hg (Roth et al., 2006).

Hypertension is a cardiovascular condition that develops gradually and is caused by a combination of various factors. The illness often exhibits early indicators before sustained elevation of blood pressure. Hence, hypertension cannot be completely categorized based on specific blood pressure thresholds. Cardiac and vascular abnormalities cause damage to organs like kidneys, brain, heart, and blood arteries, leading to early sickness and mortality (Giles et al., 2005). Lowering blood pressure (BP) when damage to a specific organ is visible or when a functional precursor to that damage is apparent and still reversible usually lowers the risk of cardiovascular (CV) events. Keep in mind that we distinguish between hypertension (the disease) and increased BP (a symptom of the condition.

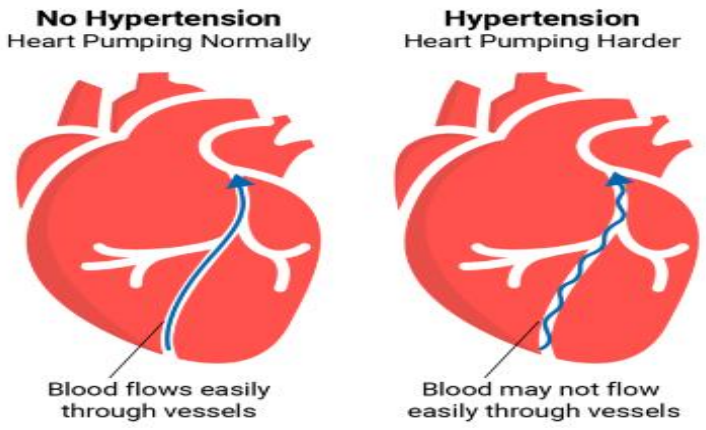


Figure 2.1. Difference representation between no hypertension and hypertension (Kikuya et al., 2007)

### 2.1.2. Damage Associated with Hypertension Organ

If inadequately treated, hypertension increases the risk of vascular damage. These lesions result in morbidity and mortality in the heart, kidneys, and brain. The occurrence of these various abnormalities is also influenced by the presence of additional risk factors, such as high levels of cholesterol in the blood, diabetes, and smoking tobacco (Kannel, 1991).

Due to the frequent correlation between hypertension and atherosclerosis, hypertensive patients often exhibit atherosclerotic plaques in their epicardial coronary arteries, particularly if they also have other risk factors for atherosclerosis, such as high plasma lipids and smoking.

Prevention or correction of coronary atherosclerosis should not be limited to lowering blood pressure but should also include active interventions against these other risk factors (Zanchetti et al., 1993).

Systolic function is often preserved in hypertension, but untreated hypertension may lead to congestive heart failure. Prior to the development and widespread use of antihypertensive medication, congestive heart failure was a frequent consequence of hypertension. Progressive enlargement of the left ventricle, in cases when the thickening of the heart muscle is linked to the presence of coronary artery blockages or narrowing, indicates the onset of heart failure. A meta-analysis of controlled clinical trials, which includes studies on hypertension in older adults, has shown that antihypertensive medication can decrease the occurrence of congestive heart failure by approximately 50 % (Yusuf et al., 1989)

One of the organs most vulnerable to hypertension-induced injury is the kidney. Renal insufficiency typically develops after a few years of the onset of severe and malignant hypertension, mostly as a consequence of fibrinoid necrosis of small renal arteries. In less severe forms of hypertension, renal damage due to arteriosclerosis is mild and develops more slowly (de Leeuw, 2002).

Stroke can be caused by various factors; however, the most significant risk factor that can be modified is hypertension. Hypertension is related to all forms of stroke, including hemorrhagic, lacunar, and thrombotic strokes. Studies have demonstrated that antihypertensive medication is highly efficient in decreasing the occurrence of strokes. A decrease of 5–6 mmHg in diastolic blood pressure can lead

to a reduction of around 409 cases of stroke (Collins et al., 1990).

### 2.1.3. Antihypertensive Drug

Antihypertensive drugs are a group of chemical compounds used to prevent, manage, or treat hypertension. Antihypertensive drugs exhibit diversity in terms of their structure and function. People frequently use antihypertensive drugs to treat a range of unrelated diseases. In contrast to angiotensin-converting enzyme inhibitors (ACEIs), which are used to treat heart failure, antihypertensive drugs manage anxiety and thyrotoxicosis.

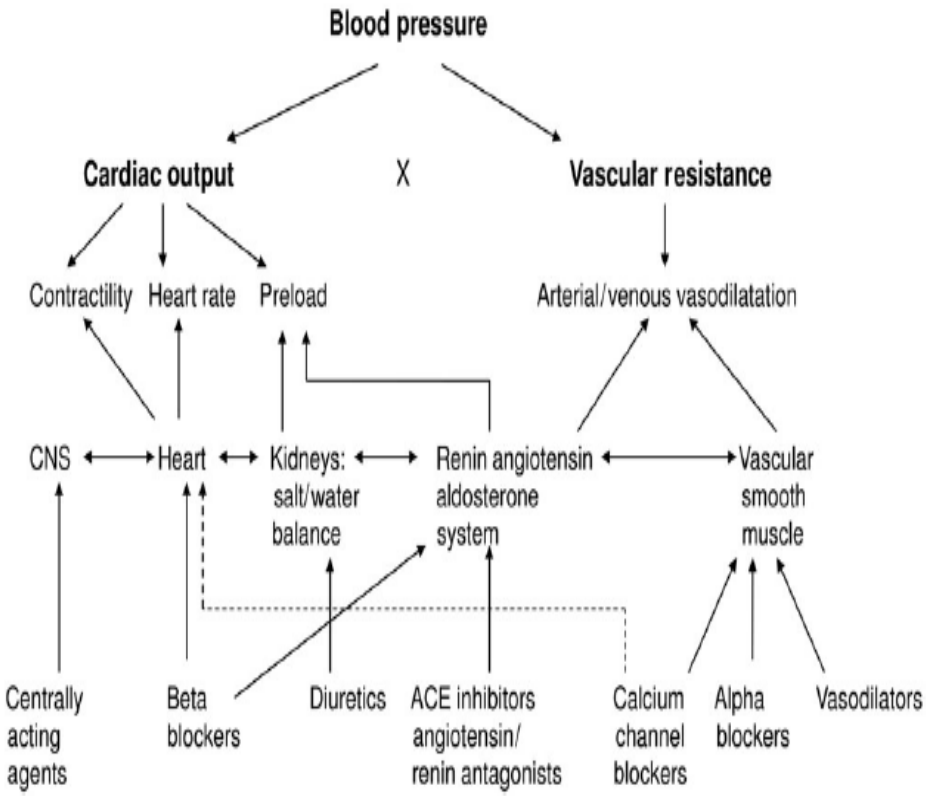


Figure 2.2. A summary of common kinds of antihypertensive drugs' mechanisms of action (Jackson et al., 2015)

The medication and its recommended use are crucial elements in anesthesia administration, as shown in Figure 2.2 (Jackson & Bellamy, 2015).

Antihypertensives can be broadly classified into two groups. Medications that lower blood pressure by influencing the renin-angiotensin system (RAS) in some way make up one category. Among these, you can find ACEIs, ARAs, DRIs, and, to a lesser degree, -blockers. The primary effect of these medications is to cause vasodilation, however they do so in a variety of ways. To reduce intravascular

volume, the second group of drugs works by increasing the excretion of water and sodium. On the other hand, they can dilate blood vessels through non-renin-angiotensin systems such as calcium channel blockers (CCBs) and diuretics. Drugs that target and suppress the RAS are made more effective by the actions of the second category, which enhance RAS activity through negative feedback. When choosing an antihypertensive drug, it is important to choose the pharmacological class that effectively lowers blood pressure while minimizing side effects, including organ damage.

#### 2.1.3.1. Drugs that Target the Renin-Angiotensin System (RAS)

The RAS pathway is the intended target of three distinct classes of medications. The peptide hormone angiotensin II is inhibited in its synthesis or interaction with receptors by these substances (Fig. 2.3). Systemic vascular resistance (SVR) and arteriole stiffness are both increased when angiotensin II binds firmly to AT1 G protein-coupled receptors, activating these receptors. Also, it may cause activation of the sympathetic nervous system, the pituitary gland to make more antidiuretic and adrenocorticotrophic hormones, and the adrenocortical glands to release more aldosterone (Peck et al., 2021). Antagonizing the RAS pathway leads to a decrease in SVR (systemic vascular resistance) and arterial pressure. Decreased aldosterone release and reduced salt and water retention in the kidneys enhance this impact. The juxtaglomerular apparatus produces more renin in response to negative input.

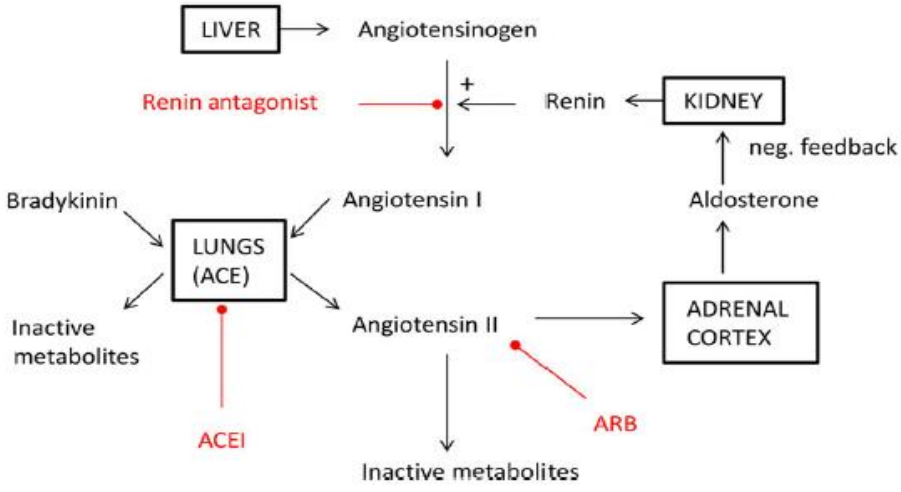


Figure 2.3. A summary of common kinds of antihypertensive drugs' mechanisms of action (Jackson and Bellamy, 2015)

#### 2.1.3.2. Angiotensin-Converting Enzyme Inhibitor (ACEI) Drugs

For patients with ages below 55 years, ACEIs can be considered the main primary hypertension treatment (Dumbreck et al., 2015). A reduction in arterial pressure alone would not have the same beneficial benefits on the kidneys and heart as an ACEI (Van Vark et al., 2012).

The primary location of the metallopeptidase enzyme ACE is in the pulmonary vasculature. Bradykinin's enzymatic conversion to inert molecules and the enzymatic breakdown of angiotensin I into angiotensin II are both decreased by ACE inhibition.

The decrease in angiotensin II accounts for the majority of the therapeutic effects. The accumulation of bradykinin has certain therapeutic benefits by causing blood vessels to widen, but it also leads to a dry cough in sensitive people. ACE inhibitors can damage the kidneys by weakening the tone of the renal efferent arterioles, which lowers the effective renal perfusion pressure. This is especially risky for individuals with renal artery stenosis. Some of the other bad effects are Hyperkalemia from less aldosterone production, agranulocytosis, skin eruptions, and problems with taste and smell.

#### 2.1.3.3. Renin-Angiotensin System (RAS) Drugs

ARAs are commonly administered to persons who are unable to tolerate angiotensin-converting enzyme inhibitors (ACEIs) because they are less likely to cause a dry cough. Like ACE inhibitors, this medicine can have both beneficial and adverse effects. People with chronic renal disease have a lower risk of developing diabetes, stroke, worsening heart failure, and death overall, according to the available studies. Orally used angiotensin receptor antagonists (ARAs) block the physiological effects of the peptide hormone angiotensin II by binding to AT1 G-protein-coupled receptors. Losartan and valsartan act as competitive antagonists, whereas candesartan and telmisartan show irreversible binding. There may be advantages to directly targeting angiotensin II receptors rather than ACE inhibition. Other mechanisms, such as the chymase enzyme in ACEI-resistant kidney tissue, can synthesize angiotensin II. Angiotensin receptor antagonists (ARAs) do not impede the breakdown of bradykinin, and the occurrence of coughing is significantly lower compared to angiotensin-converting enzyme inhibitors (ACEIs).

ARAs significantly reduce the risk of angioedema when compared to ACEIs. ARAs, like ACEIs, increase the risk of hypotension during anesthesia induction, especially when used with diuretics (Smith et al., 2010).

#### 2.1.3.4. Direct Renin Inhibitors

Direct renin inhibition has emerged as a novel focus for developing antihypertensive drugs, filling a gap of two decades without significant advancements in this field. Despite this, there is still a remaining therapeutic need that has not been completely met. The unique mechanism of action is based on the specific suppression of renin activity and its potential effect on recently identified renin receptors. Aliskiren is an effective medication for treating hypertension. It can be taken with all classes of current antihypertensive medicines, which helps increase the number of patients who are able to achieve blood pressure control. Given that a significant number of patients with high blood pressure are currently not effectively managing their condition, the introduction of this new class of antihypertensive medication is seen as a valuable resource for successfully treating and regulating hypertension.

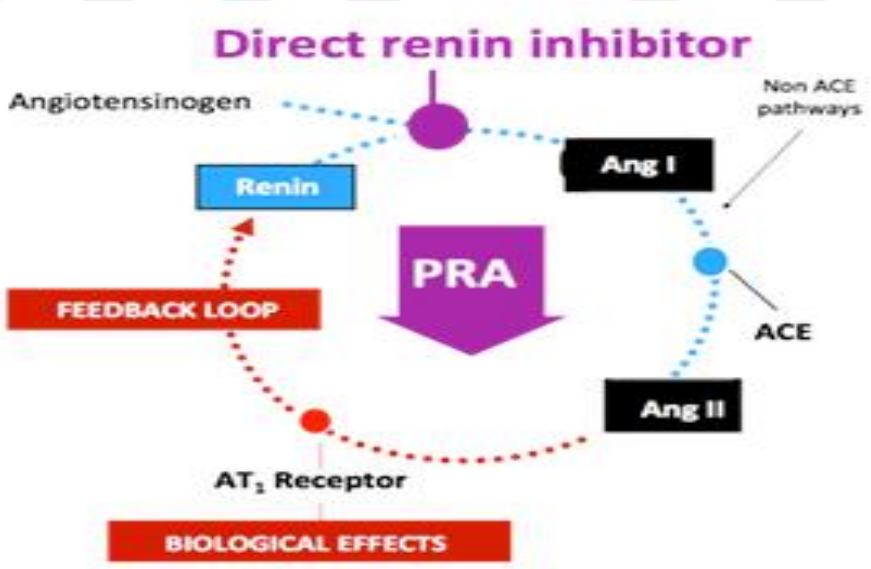


Figure 2.4. Direct renin suppression works (Brown, 2008)

Aliskiren is likely to become a more important part of treating high blood pressure in the future, maybe even along with other drugs. There is limited evidence about the effects of aliskiren therapy on aesthetic conduct. However, there have been

case reports of patients experiencing extended and difficult-to-treat low blood pressure after receiving general anesthesia (Brown, 2008).

### 2.1.4. Adrenoceptor Antagonists

#### 2.1.4.1. Beta-Blockers

Beta-blockers inhibit catecholamine effects by blocking beta-adrenoceptors in the heart, kidneys, lungs, blood vessels, and muscles. They reduce arterial pressure, heart rate, and contractility and impact the chronotropic and inotropic systems.

Metoprolol, esmolol, and atenolol exhibit increased binding affinity towards Beta 1 receptors compared to Beta 2 rt therapeutic levels (selectivity diminishes at higher doses). This contrasts with non-cardio-selective medicines like propranolol and sotalol.

Beta-blockers are mostly pure antagonists, with some having agonist or sympathomimetic activity. Some, like timolol and pindolol, act as partial antagonists. Propranolol and metoprolol inhibit sodium channels and stabilize membranes.

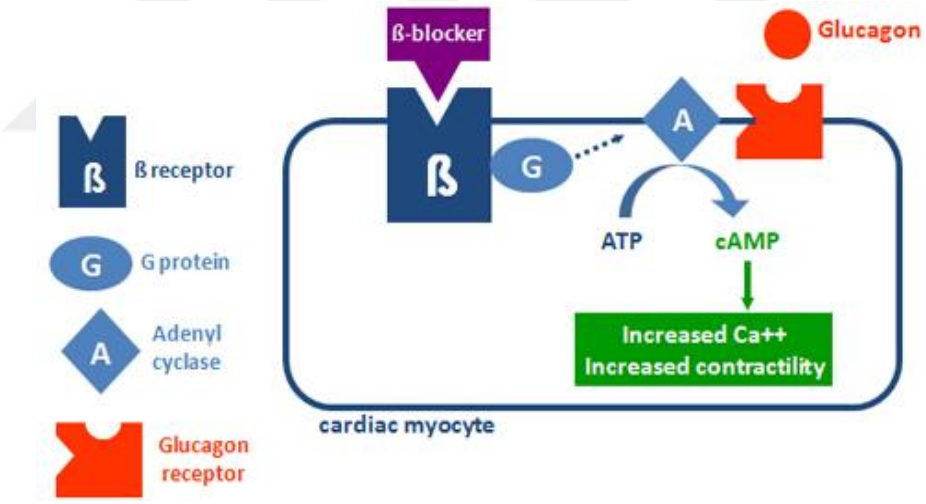


Figure 2.5. Beta-blockers mechanism of action (do Vale et al., 2019)

#### 2.1.4.2. Alpha-Blockers

Alpha-blockers are used for people who have hypertension and do not respond well to or cannot tolerate other forms of treatment. Labetalol is specifically indicated for the treatment of preeclampsia in secondary hypertension, while phentolamine is used in the perioperative management of phaeochromocytoma. Alpha-blockers, such as tamsulosin, are frequently prescribed to enhance urine flow in cases of benign prostatic hyperplasia (Yu et al., 2017).

The alpha-adrenergic receptors can be either alpha-1 or alpha-2. Catecholamines like epinephrine and norepinephrine (NE) activate the vast majority of alpha-1 adrenergic receptors on vascular smooth muscle, which leads to vasoconstriction in various tissues, including skin, gastrointestinal sphincters, kidneys, and the brain (Nash, 1990).

Reducing the potency of vasodilation generated by blocking alpha-1 transmitters is achieved by increasing the release of NE through blocking alpha-2 receptors. These medications work best in situations where the sympathetic nervous system is overactive, including when stress levels or blood catecholamines are high. Therefore, pheochromocytoma patients benefit from these treatments. By blocking the activation of the alpha-1 receptor in the nervous system.

Alpha-1 adrenergic antagonists that are selective in nature induce vasodilation, resulting in a subsequent reduction in blood pressure. Due to this characteristic, alpha-1 blockers have a positive effect on the treatment of hypertension. Alpha-1 blockers cause the smooth muscles of the prostate to relax, which helps urine flow through the urethra. These medications have a feature that makes them useful for treating benign prostatic hyperplasia (BPH) (Cui et al., 2015). Selective alpha-2 adrenergic antagonists increase activity in the sympathetic nervous system by inhibiting NE's negative feedback inhibition. However, studies examining the significance of this mechanism of operation in human medicine are few.

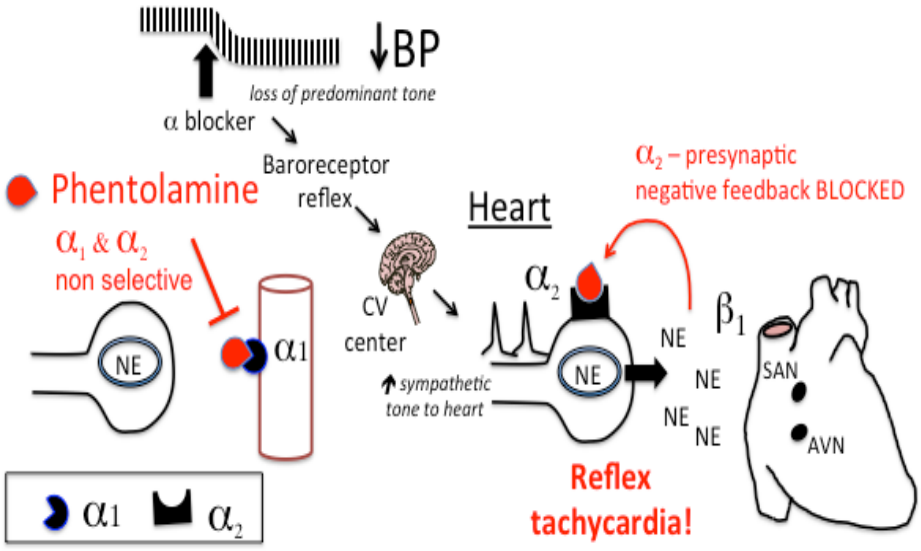


Figure 2.6. Alpha -Blocker's mechanism of action (Mulvihill-Wilson et al., 1983)

### 2.1.4.3. Calcium Channel Blockers (CCBs)

Medical applications for calcium channel blockers, known clinically (CCBs), are well-established. Non-dihydropyridines and dihydropyridines are the two main classes into which these drugs are often divided.

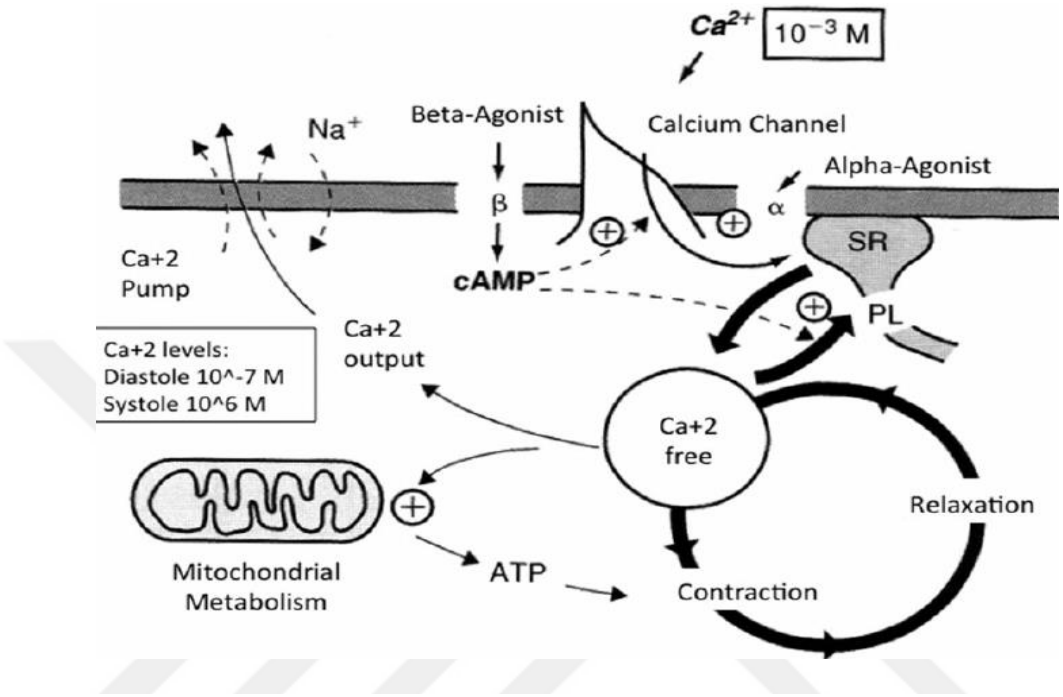


Figure 2.7. Illustration depicting the chemical pathways by which calcium channel blockers (CCBs) exert their effects (Tocci et al., 2015)

The cardiovascular indications include pulmonary hypertension, supraventricular dysrhythmias, angina pectoris, hypertension, and coronary spasm. Moreover, they are administered to treat subarachnoid hemorrhage, migraine headaches, and the Raynaud phenomenon. The mechanism of action, adverse event profile, toxicity, dosage, pharmacodynamics, and monitoring of calcium channel blockage are all thoroughly reviewed in this activity. It is designed to help clinicians and other interprofessional team members recognize and effectively use these agents for their therapeutic purposes (Pavasini et al., 2019). The primary physiological effects of calcium channel antagonists allow us to divide them into two categories. The non-dihydropyridines inhibit the sinoatrial node (Lin et al., 2018).

### 2.1.5. Diuretics

Diuretics are a pharmaceutical intervention that controls and treats both edematous and non-edematous medical problems. Diuretics belong to a category of medications. As a successful treatment for heart failure, hypertension, ascites, and other pertinent conditions, this exercise looks at diuretics' indications, mechanism of action, and contraindications. This activity will concentrate on elucidating the mechanism of action, potential adverse effects, alternative applications, suggested dosage, the impact on the body, the body's processing of the treatment, monitoring strategies, and any pertinent interactions with other substances. This information is important for healthcare professionals who are involved in treating patients with heart failure and related conditions (Popkin et al., 2010).

Diuretics are all attached to albumin. The glomerulus does not filter albumin, so the diuretic agents must actively secrete into the lumen to function. As ARAs enter the distal tubule from the bloodstream, they bind to and interact with the mineralocorticoid receptor (MR), which is found in the main cells' cytoplasm (Cannavo et al., 2018). Diuretics, such as loop, thiazides, and acetazolamide, can be either acidic or basic. The acidic diuretics are secreted through the organic anion transporters (OATs), whereas the basic diuretics are secreted through the organic cation transporters (OCTs). These transporters are found on the basolateral surface of cells in the straight segment of the proximal tubule (PT) (Klein and Cherrington, 2014).

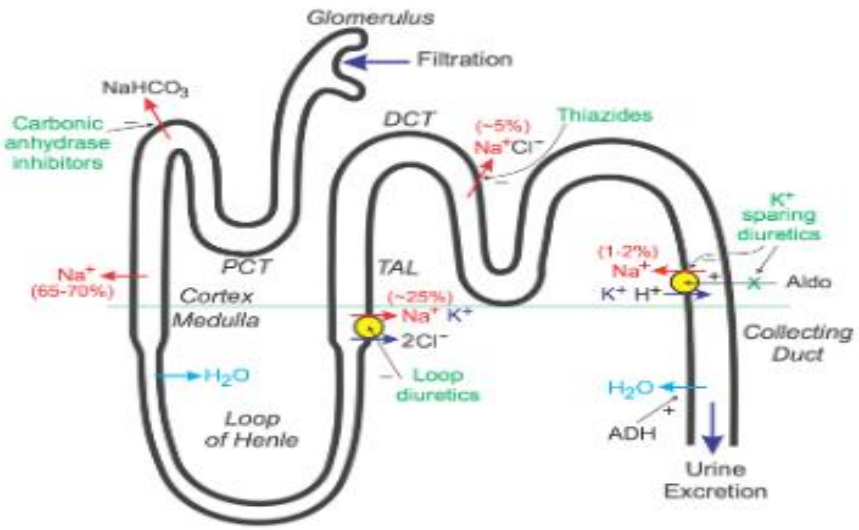


Figure 2.8. Diuretics's mechanism of action (D. M. Klein et al., 2014)

## 2.2. Lisinopril

### 2.2.1. Description

The molecular weight of Lisinopril is 441.53, and the powder is white to off-white in color. It decomposes and melts at around 160 degrees (Zaky et al., 2014). It dissolves somewhat in water but almost completely in methanol and ethanol. Oral Lisinopril is an inhibitor of angiotensin-converting enzymes. The chemical formula for lisinopril, $C_{21}H_{31}N_3O_5.2H_2O$, is its empirical formula, and Figure 2.9 shows its structural formula.

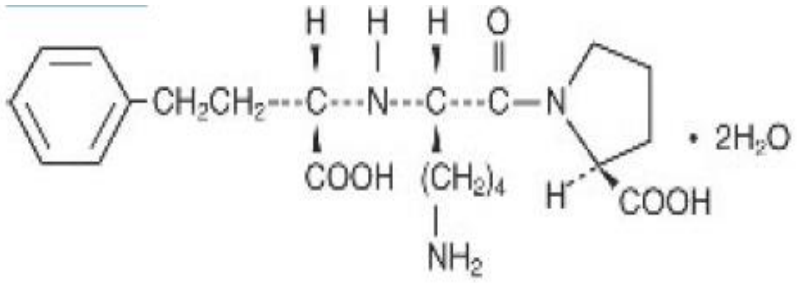


Figure 2.9. Lisonopril structural formula (Zaky et al., 2014)

### 2.2.2. Indications

For patients aged six and up, the FDA has given the green light to Lisinopril for the treatment of heart failure and the control of hypertension (Chen et al., 2018). The FDA also authorizes the treatment of hemodynamically stable patients with ST-segment elevation myocardial infarction (STEMI) within 24 hours to improve survival. The subsequent drop in sodium and potassium excretion is due to a reduction in aldosterone secretion (Whelton et al., 2018).

### 2.2.3. Indications

For patients aged six and up, the FDA has given the green light to Lisinopril for the treatment of heart failure and the control of hypertension (Chen et al., 2018). The FDA also authorizes the treatment of hemodynamically stable patients with ST-segment elevation myocardial infarction (STEMI) within 24 hours to improve survival. The subsequent drop in sodium and potassium excretion is due to a reduction in aldosterone secretion (Whelton et al., 2018).

### 2.2.4. Mechanism of Action of Lisinopril

The powerful vasoconstrictor angiotensin II cannot be produced by the angiotensin-converting enzyme (ACE), which Lisinopril inhibits by acting as a competitive inhibitor. As Lisinopril lowers angiotensin II levels, aldosterone secretion drops as well, leading to less salt absorption; consequently, blood potassium levels may rise somewhat with lisinopril treatment. Eliminating angiotensin II's negative feedback loop, Lisinopril raises serum renin activity (Regulski et al., 2015).

ACE also reduces bradykinin, though, which is the mechanism by which ACE inhibitors might cause angioedema (Bezalel et al., 2015).

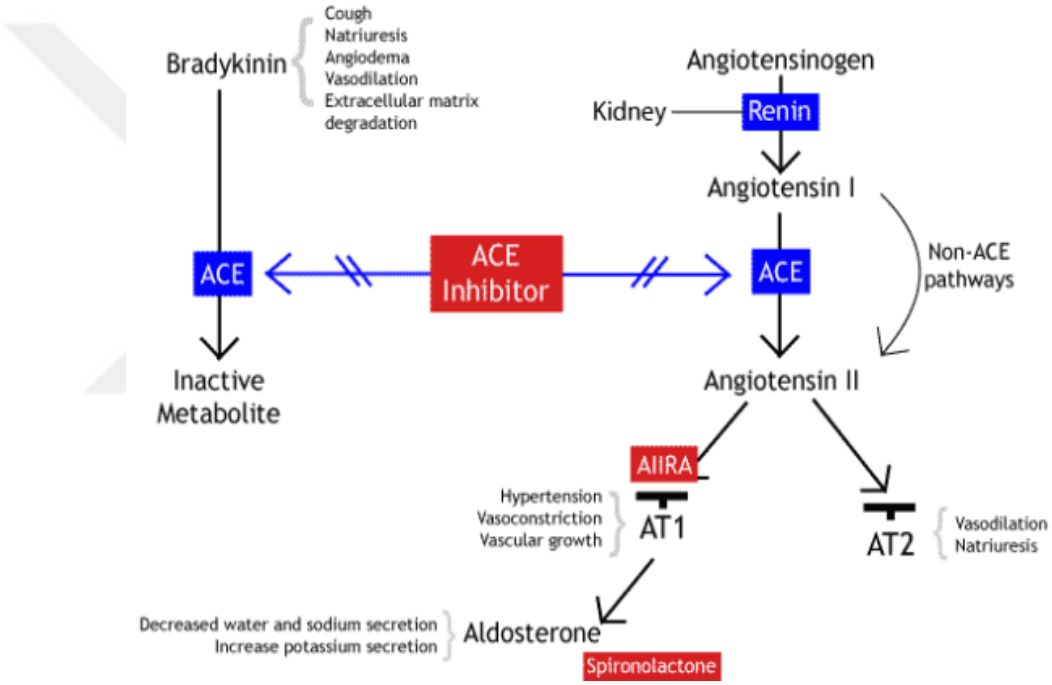


Figure 2.10. Schematic representation of the working mechanism of lisinopril (Bezalel et al., 2015; Regulski et al., 2015)

### 2.2.5. Pharmacokinetics of Lisinopril

The absorption of Lisinopril is not affected by food, and the drug is excreted unchanged in the urine. Lisinopril has poor bioavailability (anything from 10 % to 30 %) when taken orally. Reaching maximal concentration can take anywhere from six to eight hours. Patients with heart failure have restricted medication dispersion because the drug does not bind to albumin or other proteins (Bezalel et al., 2015).

## 2.3. Nanoscience and Nanomedicines

### 2.3.1. Definition

Nanoscience is the scientific investigation of materials that exist within the nanoscale range. The physiochemical, biological, mechanical, optical, electrical, and other properties of any substance are altered when it is converted to nanoscale dimensions. The innovative characteristics of these materials, which are the result of their transformation into nanoscales, can be effectively utilized in a variety of practical applications.

In many different industries, nanotechnology has been a driving force behind incremental and even revolutionary improvements. With the ability to optimize pharmaceutical delivery through active or passive targeting, sustained release, controlled release, triggered release, enhanced delivery, or delayed release.

Minimizing the drug's side effects and enhancing its bioavailability are all achievable goals simultaneously.

Developing in order to improve and concentrate drug delivery, nanomedicine combines nanotechnology with biomedical and pharmaceutical research. Using the five R's framework which comprises "right target/efficacy," "right tissue/exposure," "right patients," "right safety," and "right commercial potential"—can significantly help nanopharmaceuticals to be effectively advanced (Hare et al., 2017).

After analyzing nanotechnology's potential applications in healthcare, the US National Institutes of Health coined the term "nanomedicine" to describe this field. Nanotechnology aims to construct and combine new materials in order to enable personalized therapy by fine-tuning the engineering of atoms and molecules to create new molecular assemblies on the size of individual cells, organelles, or even smaller components (Dou et al., 2007).

A nanopharmaceutical (Pharmaceuticals engineered on the nanoscale) refers to a pharmaceutical product specifically designed and produced at the nanoscale. It incorporates nanomaterials and serves both internal and external applications for humans. The objective of nano pharmaceutics with particle size agnostic and health advantages. Nanomaterials are typically characterized as materials with particle sizes ranging from 1 to 100 nm in at least one dimension. Consequently, any pharmaceutical that contains such material should likewise be classified as a nanopharmaceutical (REDDY et al., 2021).

Nanopharmaceuticals's particle size dispersion. The product specification should include a declaration of the nano-size range. Additionally, the particles must maintain their nano-size range under all testing conditions during the stated stability period and in the final product (REDDY et al., 2021). A drug's entry onto the market following its first discovery or development may take up to two decades (Bawa et al., 2008). Factors to be considered include having enough qualified medical and scientific staff members prepared to devote ten or even twenty years to a single project, having a novel scientific premise protected by intellectual property, and having an economic business plan that can persuade investors of future profits.

Nanopharmaceuticals use nanocrystals, liposomes, polymers, and protein-based and metallic nanoparticles to create new drugs with improved solubility, faster dissolution, oral bioavailability, and therapeutic action. Size reduction is limited to micron ranges, but nanometers work better in various dosage types. Benefits include more surface area, faster onset of therapeutic action, lower dose needed, and less variation between fed and fasted states (Gangapure et al., 2019).

### 2.3.2. Drug Nanocrystal

Crystals of a size in the nanometer range are known as drug nanocrystals. This describes nanoparticles that have a crystalline nature. Stabilized by suitable excipients, drug nanocrystals are APIs in their purest form (Junghanns et al., 2008). Presently, there are ongoing disputes regarding the exact delineation of a nanoparticle. The categorization of a particle as a nanoparticle is prone to variation based on the specific field or discipline. In the field of colloid chemistry, particles are categorized as nanoparticles only if their size is less than 100 nm or even less than 20 nm. In the pharmaceutical industry, nanoparticles are defined as particles with dimensions ranging from a few nanometers to 1000 nm (equal to 1 μm).

On the other hand, microparticles have a size ranging from 1 μm to 1000 μm. The dispersion of drug nanocrystals in liquid media results in the formation of "nanosuspensions" as opposed to "microsuspensions" or "macrosuspensions" (Jog and Burgess 2017). Typically, it is necessary to stabilize the scattered particles, for instance, through the use of surfactants or polymeric stabilizers. The dispersion medium might consist of water, aqueous solutions, or nonaqueous media such as liquid polyethylene glycol or oils. (Jog et al., 2017).

Stabilizing the dispersed particles is usually a must, and one common way to do this is via surfactants or polymeric stabilizers. Water, aqueous solutions, or nonaqueous media like oils or liquid polyethylene glycol (PEG) can all make up the dispersing medium. The final form of drug nanoparticles, derived from drug microcrystals, could be crystalline or amorphous, depending on the manufacturing process employed, particularly in the case of precipitation. Amorphous drug nanoparticles should not be referred to as nanocrystals from a technical standpoint. On the other hand, "nanocrystals in the amorphous state" is a popular way to explain it (Tran et al., 2014).

### 2.3.3. Properties of Drug Nanocrystal

#### 2.3.3.1. Increase in Dissolution Velocity

A modified version of the Noyes-Whitney equation, the Nernst-Brunner equation (equation-2.1) contains the integration of Fick's second law and sheds light on the enhanced rate of dissolution of the nanocrystals.

$$\frac{dC}{dt} = \frac{Ds}{vh}(Cs - C) \qquad \textbf{(2.1)}$$

dC/dt denotes the rate of change of the concentration of a material with respect to time, particularly in the context of dissolution. The term "D" refers to the diffusion coefficient, which quantifies the ability of a material to flow through a medium. S is the efficacious surface area, which corresponds to the extent of the particles that are in direct contact with the solvent during the process of dissolution. V represents the volume of the solvent in which the substance is being dissolved. The variable "h" denotes the magnitude of the diffusion layer's thickness. CS refers to the saturation solubility, which represents the concentration of the drug at the surface where it is undergoing dissolution. The variable C denotes the drug concentration in the solvent at a specific moment. Equation (1) states that decreasing the particle size from micro to nano levels results in a significant increase in surface area, leading to a higher dissolving velocity (dC/dt). Furthermore, the presence of a very thin layer of diffusion encompassing the nanocrystals augments the pace at which they dissolve, as elucidated by the Prandtl equation (Junyaprasert et al., 2015).

### 2.3.3.2. Increase in Saturation Solubility

The mechanism of nanocrystals increasing pharmacological saturation solubility can be explained by the following pair of equations. The Kelvin equation offers the first clarity in this sense:

$$ln\left(\frac{P_r}{P\infty}\right) = \frac{2\gamma v_m}{rRT} \quad \textbf{(2.2)}$$

In this particular equation, the variables are: The variables Pr, P, Vm, R, and T stand for several variables such as vapor or dissolution pressure, interfacial tension, molar volume, gas constant, and absolute temperature, with a particle radius of r and a size of an infinite particle. The changing value of r represents the particle's radius. Equation 2, the Kelvin equation, was originally developed to represent the increase in vapor pressure due to the curvature of the liquid-gas interface; however, it is also applicable to the contact between solids and liquids as well. In this case, we use the vapor pressure at the interface between the liquid and the gas to compensate for the dissolving pressure at the solid-liquid contact. Figure 2.10 shows that the maximum amount of solute that may be dissolved increases as the particle size is reduced to less than 1-2 m. This is because raising the pressure for dissolving at the solid-liquid interface makes the particle size smaller.

Ostwald and Freundlich give solubility to increase saturation.

$$\left(\frac{RT}{vm}\right) ln\left(\frac{s}{So}\right) = \frac{2\gamma}{r} \quad \textbf{(2.3)}$$

The variables in the equation are defined as follows: S represents the solubility of the medication at temperature T, Vm represents the molar volume, γ represents the interfacial surface tension, R represents the universal gas constant, and ρ represents the density of the molecule. We derived the equation under the assumption that the dissolution of a solid adheres to the principles of gas laws, substituting the pressure factor for gases with a concentration factor for solids. The underlying premise is that the process by which molecules transition from a liquid state to a gaseous state is essentially the same as the process by which molecules transition from a solid state to a liquid state. Equation 3 predicts that a solubility enhancement of approximately 10-15% will occur in the intestinal fluid of the

medicine with a particle size of 100 nm and a molecular weight of 500 Dalton (Kesisoglou et al., 2007). A strong concentration gradient produced by the enhancement in saturation solubility can help to promote absorption by passive diffusion.

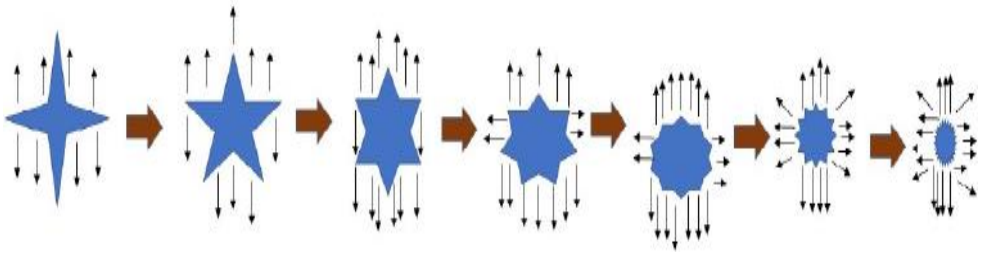

Figure 2.11. Reducing the particle size increases the curvature of the particle, and so is the dissolution velocity (Dhaval et al., 2020)

#### 2.3.3.3. Increased Adhesiveness

Adherence to biological and gastrointestinal mucosa is a natural property of nanocrystals (Khadka et al., 2014). Hydrogen bonds and van der Waals interactions between the surfaces of the particles and the mucus in the gastrointestinal tract bind the suspended nanocrystals to the mucosa. The solid dose form may already have these linkages, or new ones can form when they dissolve. When nanocrystals remain in the GI tract for a longer period of time, the concentration gradient widens, which improves drug absorption and bioavailability (Smart, 2005).

#### 2.3.3.4. Improved Stability

In contrast to other approaches that require a large number of additional excipients to have a stable final formulation, the drug nanocrystal system has a much lower probability of a chemical reaction because it is a very simple formulation that consists primarily of the drug and stabilizers (in the case of nanosuspension, it also includes an appropriate dispersion medium).

#### 2.3.3.5. Improved Bioavailability

Enhancing the rate at which drugs dissolve and their capacity to dissolve completely increases the concentration difference between the drug and the membrane, leading to faster diffusion and ultimately improving bioavailability.

#### 2.3.3.6. The Versatility of Final Dosage Form

The nanocrystals' ability to modify surface properties and control size, together with their simple post-production process, allows them to be integrated into many dosage forms, including tablets, pellets, capsules, dry suspensions, and hydrogels.

### 2.4. Anti-Solvent Crystallization Technique

One way to create pharmaceutical material nanocrystals is by using top-down technology, which involves downsizing particles in size, and bottom-up technology, which involves growing particles in the nanometer range. Another way is to combine the two approaches (Gao et al., 2008).

Wet bead milling and high-pressure homogenization are two key components of top-down technology that can be readily industrialized (Lu et al., 2016).

Disintegration of crystalline species and the emergence of secondary nucleation nuclei occur in tandem with the reduction of drug particles caused by mechanically produced shear and collision stresses (Bitterlich et al., 2015). Top-down technology does not depend on supersaturation for its formation pace. This approach has been used to create the majority of previously documented anticancer medications since it does not require organic solvents and makes production scaling up reasonably simple. (Chen et al., 2020).

The primary foundation of bottom-up technology is evaporation and precipitation (Srivalli et al., 2016). The fundamental concept is to acquire drug nanocrystals by inducing medications to reach a condition of supersaturation and then regulate the size distribution of the nanoparticles using suitable techniques (Ran et al., 2022).

Nucleation is particularly crucial for tiny, uniform nanocrystals to form. The best method for accurately regulating medication particle size is to regulate crystal formation. Numerous physical techniques, such as precipitation under high gravity, have been employed to regulate the formation of crystals. In contrast to top-down approaches, these techniques offer enhanced control over particle characteristics (Chow et al., 2007).

Anti-solvent crystallization, or as known as antisolvent precipitation of liquid (Sinha et al., 2013) is a method used for the separation and purification of drug

particles ranging from micro- to nano-size (Xia et al., 2010). This method facilitates the formation of crystals from solutions and allows for precise control over their crystalline characteristics, including particle size and shape (Park and Yeo, 2012).

In the crystallization process, we employ anti-solvents to reduce a solute's solubility in the solution and accelerate the crystallization process. The characteristics of the anti-solvent, both in terms of its physical and chemical properties, can influence the speed at which it mixes with the solutions. As a result, this can impact the rate at which nucleation occurs and the subsequent formation of crystals in the compounds undergoing crystallization. Furthermore, the parameters used in crystallization studies have a significant impact on the particle creation process and control the shape and distribution of crystal size (Park and Yeo, 2010).

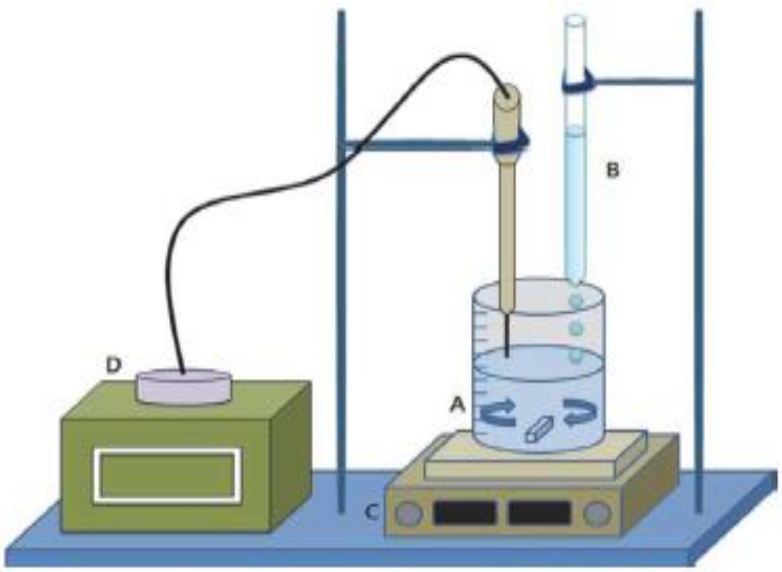


Figure 2.12. Equipment for the liquid anti-solvent crystallization technique:
(A) glass beaker, (B) solution injector, (C) magnetic stirrer, and
(D) ultrasound generator (Teng et al., 2017)

Essentially, the crystal surface absorbs a hydrophilic stabilizer, like a surfactant, from the antisolvent solution to prevent crystal formation. Hydroxypropyl methylcellulose (HPMC), Polyvinylpyrrolidone (PVP), Tween 20, and Tween 80 are non-toxic substances with excellent hydrophilic properties. Food and pharmaceutical formulations commonly use them as thickening, emulsifying, and stabilizing agents (Kim et al., 2012).

### 2.4.1. Effect of Operating Variables of Anti-Solvent Crystallization Technique

#### 2.4.1.1. Effect of Drug Concentration

There is an inverse relationship between the drug concentration and the size of the precipitated particles. As the drug concentration increases, the size of the precipitated drug particles decreases. The drug concentration in crystallization liquids affects crystal formation speed under this equation.

The level of supersaturation can affect the speed at which nucleation occurs, which depends on the drug solution concentration. The rapid nucleation rate is responsible for generating numerous nuclei, resulting in an augmented quantity of crystals and, consequently, a potential reduction in the size of each crystal. However, as the concentration increases further, the precipitation process particles tend to cluster together, leading to an uneven distribution of the final product's size and shape (Sinha et al., 2013).

#### 2.4.1.2. Effect of Stirring Speed

The stirring speed is an essential aspect as it influences the interaction between the solvent and anti-solvent, resulting in a decrease in the solute's solubility in the solvent. Higher stirring speeds generally result in smaller particle sizes due to enhanced micro mixing, a molecular-level mixing between the different phases.

Increasing the micromixing efficiency results in higher mass transfer and diffusion rates between the multiphases, resulting in uniform supersaturation. This, in turn, promotes fast nucleation and the formation of smaller drug particles. As the stirring speed increases, the high intensity generates a significant quantity of thermal energy, resulting in an elevated temperature that increases the size of the nanoparticles ( Zhang et al., 2009).

#### 2.4.1.3. Effect Of Temperature

The temperature and the rate of nucleation are inversely correlated, according to the theory of crystallization.

The temperature is a crucial determinant that governs the final particle size and distribution. Empirical evidence suggests that higher temperatures during crystallization result in the formation of bigger crystals. The drug becomes more supersaturated at lower temperatures because its solubility in the solvent-antisolvent

mixture decreases with decreasing temperature (Zhang et al., 2009). Consequently, the diffusion and growth kinetics at the interface of the crystal boundary layers would be reduced at low temperatures. Because of this, medication particles are reduced in size when processed at low temperatures.

#### 2.4.1.4. Effect of the Solvent to Anti-Solvent (SAS) Volume Ratio

The volume ratio of solvent to antisolvent is a crucial factor that directly affects the particle size growth. As the ratio increases, there is a substantial decrease in particle size. Furthermore, a greater amount of anti-solvent led to an accelerated rate of nucleation and the creation of smaller nuclei while also promoting growth.

In the following stages of growth, an increased amount of anti-solvent leads to a greater distance for the growing particles to diffuse, resulting in diffusion becoming the limiting factor for the growth of nuclei (Kakran et al., 2012; C. Li et al., 2011) .

The nucleation rate, which has a considerable impact on the ensuing particle size distribution, is mostly influenced by the degree of supersaturation rather than the crystal growth rate. The critical size and the logarithm of the supersaturation ratio have an inverse relationship. Therefore, a considerable quantity of nuclei coalesce into minuscule particles under high supersaturation conditions (Paulino et al., 2013).

### 2.5. Drug Stabilizers

Drug stabilizers are organic substances that assist in preserving the desired characteristics of the active pharmaceutical ingredient (API) until the patient ingests it.

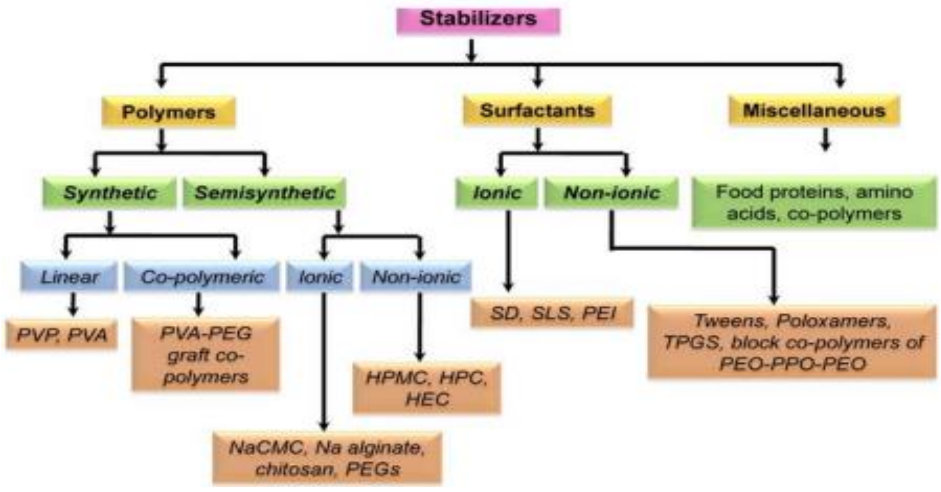


Figure 2.13. Various types of the nanoformulations stabilizers (Shete et al., 2016)

The most prevalent approach to counteract aggregation in colloidal systems is to incorporate stabilizer(s) into the formulation. Strategies for addressing the issue of aggregation rely on established principles of colloid science, wherein capping agents or surface charges are employed to ensure the stability of nanocrystals and prevent their aggregation (Li and Kaner, 2006).

To make drug nanocrystals physically stable, stabilizers lower their free surface energy, decrease their hydrophobicity, prevent their particles from aggregating, alter the crystalline structure of nanosized particles during manufacture and storage, and prevent Ostwald ripening (Chang et al., 2015).

The drug's solubility in the stabilizer solution significantly impacts the selection of the stabilizer. Ostwald ripening refers to the phenomenon where particles with larger sizes grow in size, and smaller particles shrink. The phenomenon occurs as smaller particles, due to their larger surface area and smaller curvature compared to larger particles, enhance the dissolution rate. As the smaller particles dissolve and the larger particles undergo crystallization, the size of the latter particles progressively augments. Minute crystals are assimilated, but larger crystals proliferate. The smaller crystals act as a catalyst for the growth of larger crystals. The molecules on the surface demonstrate less stability in terms of energy compared to those previously arranged and densely packed in the core. The free energy of dispersion reduces as the smaller particles dissolve and the larger particles increase in size (Verma et al., 2009; Verma et al., 2011; Wu et al., 2011).

The stability of colloidal systems relies on the concentration of stabilizers present in the dispersion medium. The quantity of the stabilizer affects the stability of the suspension by altering its absorption affinity on the surface of the medication particles (Wu et al., 2011).

An ideal concentration of stabilizer is required since a low concentration of stabilizer could not sufficiently cover the drug surface, therefore compromising the steric repulsion between the particles (CESARANO III et al., 1988; Ghosh et al., 2012).

Molecular structure of the surfactant controls the required effective concentration for stabilization. Studies have indicated that surfactants with a longer hydrophobic chain and a larger hydrophilic head, which offer more steric hindrance and reduce the inclination to agglomerate, need a lower molar concentration (Rangel-Yagui et al., 2005; Sinha et al., 2013).

### 2.5.1. Tween 20

One of the most common uses for the non-ionic polyoxyethylene surfactant known as tween 20 is an emulsion for water and oil mixtures (Ravindran et al., 2011).

Tween 20 has around 40-60% lauric acid and 14-25% myristic acid, as per EU requirements (T. A. Khan et al., 2015).

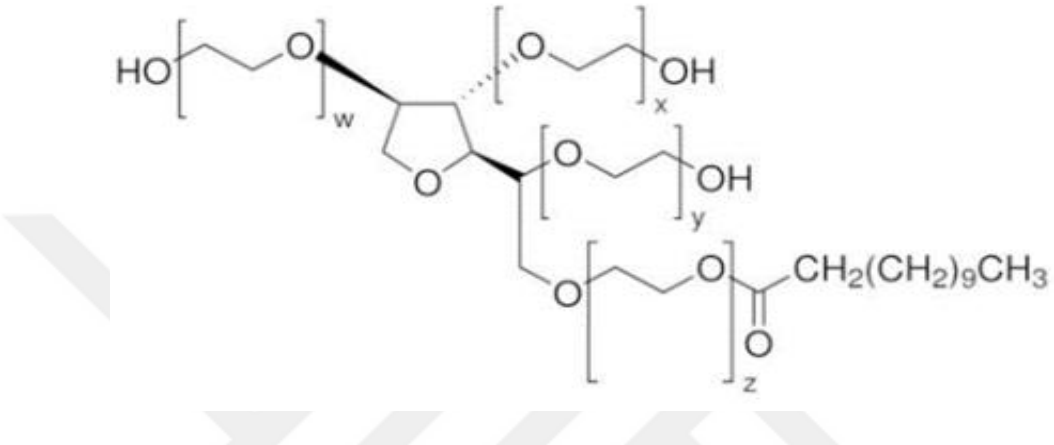


Figure 2.14. Chemical structure of Tween 20 (Winarni et al., 2020)

By improving the accumulation of anticancer medications and by suppressing the multidrug-resistant gene expression at a low dose, Tween 20 can effectively correct the multidrug-resistant phenotype (Yang et al., 2012). The cyto/genotoxicity investigation of Tween 20 on different cell lines has not, as far as we are aware, been thoroughly published.

The Tweens are a group of polyoxyethylene-1,4-sorbitan-monoesters that consist of a combination of fatty acids (Dwivedi et al., 2018; Dwivedi et al., 2020). The Tween 20 and 80 that are currently being used and sold commercially are a combination of molecules that are derived from the main molecule sorbitan polyoxyethylene fatty acid ester, as shown in Figure 2.14.

### 2.5.2. Tween 80

Polysorbate 80, sometimes called Tween 80, is an artificial surfactant made up of fatty acid esters of polyoxymethylene sorbitan (Kerwin, 2008). Oleic acid is the most often occurring fatty acid in the composition. Other fatty acids, including palmitic or linoleic acid, could also be present, albeit as Figure 2.13 shows. Usually

found as a mixed combination of fatty acid esters, polysorbate 80 consists of oleic acid, forming about 58 % of the mixture (Kerwin, 2008; Khan et al., 2015).

Polysorbate 80 mostly consists of polyoxyethylene-20-sorbitan monooleate, which bears a structural resemblance to polyethylene glycols. Polysorbate 80 possesses a molecular weight of 1309.7 Daltons and a density of 1.064 g/ml (ten Tije et al., 2003).

Widely used in the production of food, cosmetics, and medications, Tween 80 is a synthetic nonionic surfactant, either solubilizer, stabilizer, or emulsifier (Kerwin, 2008; ten Tije et al., 2003)

Protein adsorption and aggregation prevention has also made use of it (Khan et al., 2015). Amiodarone is just one of many pharmacological medicines available in formulations containing polysorbate 80 (Souney et al., 2010), vitamin K (Hey, 2003), etoposide (ten Tije et al., 2003), docetaxel (Schwartzberg et al., 2018), various vaccines (Hall et al., 2021), protein biotherapeutics (A. Khan et al., 2015), erythropoietin-stimulating agents (Food et al., 2017; Yoon et al., 2017), and fosaprepitant (Schwartzberg and Navari, 2018).

Polysorbate 80 may directly mediate adverse events or modify the pharmacologic characteristics of the medicine it is formulated with, according to recent data (ten Tije et al., 2003; Van Zuylen et al., 2001).

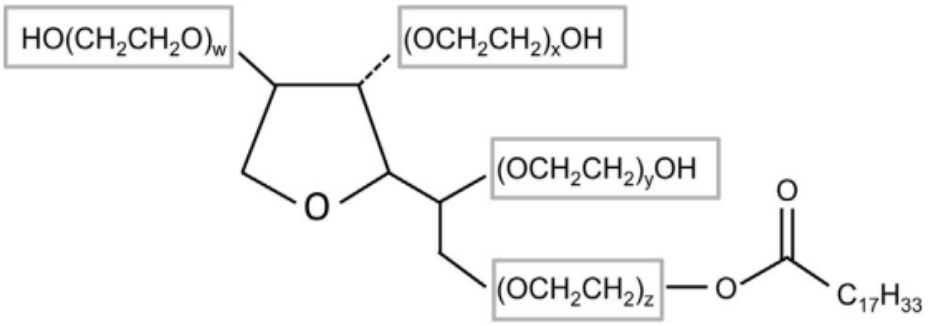


Figure 2.15. Chemical structure of Tween80 (Cabanillas et al., 2021)

Therefore, several of the side effects linked to medications made with polysorbate 80 have been linked to this ingredient specifically.

Polysorbate 80's negative inotropic characteristics may explain why it causes a significant and long-lasting drop in blood pressure in animal experiments (Gough et al., 1982).

Amiodarone formulations that do not contain polysorbate 80 and benzyl alcohol were found to have a much lower incidence of hypotension in clinical investigations (Souney et al., 2010).

### 2.5.3. PVP

PVP, also known as polyvidone or povidone, is a fine, odorless, white to creamy-white powder that is very hygroscopic and may absorb up to 40% of its weight in water from the atmosphere (Sheskey and Quinn 2009). This excipient's low toxicity and affinity for both hydrophilic and hydrophobic compounds are two of its many benefits (Sheskey et al., 2009).

PVP is a polymer that is soluble in water and can be broken down naturally. It is created by using N-vinylpyrrolidone as its monomer. In addition to being hydrophilic, PVP demonstrates exceptional solubility in solvents of different polarities, impressive binding capabilities, and a stabilizing effect on suspensions and emulsions (Folttmann et al., 2008).

Non-toxic and biocompatible, PVP is a polymer. Furthermore, it has been approved by the FDA as being safe for human consumption. For this reason, PVP is not only used in food production but also in cosmetics and medicine, especially for biological and pharmaceutical applications (Folttmann and Quadir, 2008; Martins et al., 2013; Rasekh et al., 2014).

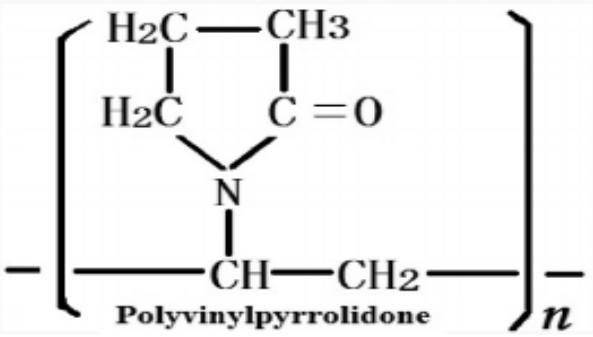


Figure 2.16. Chemical structure of Polyvinylpyrrolidone (PVP) (Ingole et al., 2021)

PVP exhibits specific physical and chemical characteristics, such as being chemically inert, colorless, resistant to high temperatures, and stable under different pH conditions. Chemical structure of PVP illlustrated in Fıgure 2.16.

In the biomedical and pharmaceutical domains, PVP has been used to produce oral, topical, transdermal, and ocular administration techniques, among other drug

delivery systems. Furthermore, beneficial in gene delivery is PVP (Zhang et al., 2009; Zheng et al., 2015). Alternatively, it can be combined with metal particles to enhance its effectiveness in regenerative medicine (Hecold et al., 2017; Hu et al., 2018) and targeted delivery (Ramalingam et al., 2018). Thus, the PVP results also demonstrate the high adaptability of this polymer. Various morphologies utilizing PVP as the polymeric carrier have been suggested for medication delivery.

PVP facilitates a regulated release of drugs, improving the uptake of pharmaceuticals with low water solubility. It also protects the active ingredient from environmental influences like pH, temperature, and oxygen and masks unpleasant aromas and flavors. PVP microparticles and nanoparticles have been infused with a diverse range of active compounds from multiple categories.

From more traditional techniques like spray drying to more cutting-edge ones like procedures assisted by supercritical fluids, a variety of technologies have been employed in the manufacturing of PVP-based particle (Bothiraja et al., 2009; Gupta et al., 2005; Prosapio et al., 2016). Fibers made of PVP, which is a very spinnable polymer, have also been developed that include a variety of active medicinal compounds (Rasekh et al., 2014; Sriyanti et al., 2017).

### 2.6. Physical, Chemical, and Pharmaceutical Characterization Techniques

#### 2.6.1. High-Performance Liquid Chromatography (HPLC)

HPLC has emerged as a highly potent instrument in analytical chemistry. it has the ability to analysis more than one substance in one solvent. One of the most common quantitative and qualitative methods used to analyze pharmaceuticals is high-performance liquid chromatography, or HPLC (Rao et al., 2015).

The separation of HPLC is based on the distribution of the analyte (sample) between the mobile phase (eluent) and the stationary phase (column packing material). Depending on the analyte's chemical structure, the stationary phase slows down the molecules as they transit through it.

Time "on-column" refers to the amount of time that molecules spend in a sample as a result of their unique intermolecular interactions with the packing material. As a result, different parts of the sample are taken and released at different times (Rajan, 2015).

The analytes are identified by an analyte recognition device, such as a UV detector, after they have exited the column. Before being displayed in a chromatogram, the signals are converted and recorded by a data management system (also known as computer software). After passing through the detector unit, the mobile phase may be subjected to additional detection units, such as a fraction collector, or it may be disposed of as refuse.

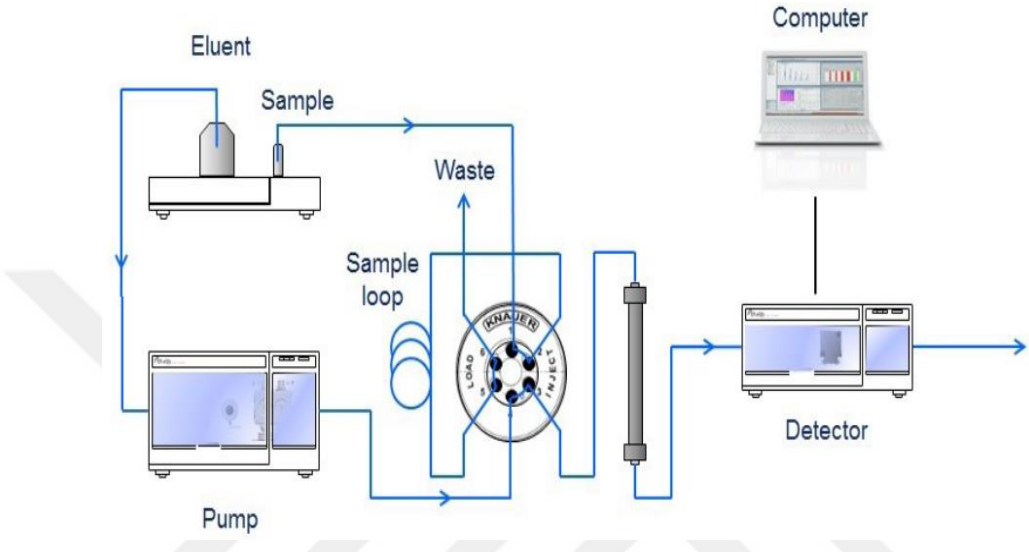


Figure 2.17. Schematic layout of a HPLC system (Moldoveanu et al., 2022)

HPLC system is typically composed of numerous components, including a container for solvent storage, a pumping device for solvent circulation, a valve for sample injection, a column for component separation, a detector for component detection, and a unit for result processing, as shown in Figure 2.17. The pump consistently supplies the system with solvent eluent at a high pressure and speed.

### 2.6.2. Dissolution Test

The process of incorporating a solid solute into a solution is known as dissolution. In the pharmaceutical industry, dissolution refers to the rate at which a pharmacological component dissolves in a solution over a specific period of time.

This process was measured under controlled conditions, which include the interface between the liquid and solid, temperature, and the solvent composition.

Pharmaceutical dosage forms undergo a crucial quality control test known as dissolution. People are increasingly using it to forecast bioavailability and, in certain cases, to replace clinical investigations in determining bioequivalence. The

dissolution characteristics of a medicine have a substantial impact on its pharmacological efficacy.

Employing dissolving testing results can provide guidance for the creation of innovative formulations and enhance the efficiency of product development procedures. Furthermore, it can guarantee the continuous quality and efficiency of the manufacturing process. Moreover, dissolution is a necessary condition for acquiring regulatory approval for product promotion and a crucial component of a thorough quality assurance program. The process involved the breaking down of a solid medication form (Ummadi et al., 2013).

Figure 2.18 represents a schematic illustration of the dissolving process. A solute molecule is taken out of its solid state in the first two steps (a and b), and a space is made in the solvent for the molecule. In the second step (c), the solute molecules are put into the solvent holes. This makes the solute and solvent molecules stick together (Brittain et al., 1999).

Solubility refers to a thermodynamic parameter that remains constant under specific variables such as temperature, pressure, solvent, and pH. The term dissolving is used to describe a kinetic parameter that represents the rate at which a medication transitions from a solid state to a solvent phase during a specific period of time (Brittain and Grant, 1999).

For a drug to be absorbed after being taken orally, it must dissolve in the fluids of the gastrointestinal tract. The Noyes-Whitney equation, formulated by Noyes and Whitney in 1897, is the predominant theoretical expression used to explain the pace at which dissolution occurs. Despite being over a century old, this equation remains relevant (Noyes et al., 1897).

$$\frac{dm}{dt} = \frac{(D \cdot A)}{h}(C_s - C_t) \qquad \textbf{(2.4)}$$

The diffusion coefficient (D) is the rate of spread at which the drug substance is in a stagnant layer of the medium dissolution surrounding the particle of each drug. This layer has a thickness (h). The drug particle surface area (A) is the total area of the drug particles. Cs refers to saturation solubility, which is the maximum amount of the drug that may dissolve in the medium. Ct represents the drug concentration in the bulk solution.

The USP-NF offers multiple authorized techniques for conducting dissolution tests on tablets, capsules, and other specialized goods (Felton, 2016; Prior et al., 2010).

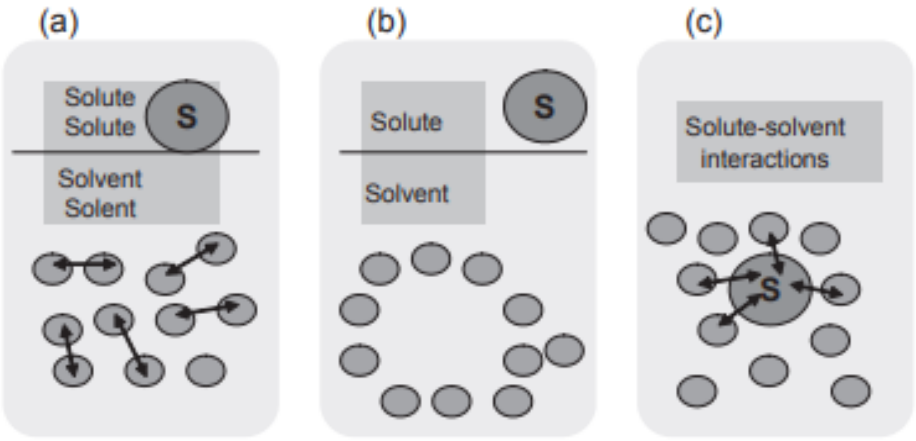


Figure 2.18. Steps of dissolution process (Abraham et al., 2002)

### 2.6.2.1. USP Apparatus 1(Basket Apparatus)

In 1968, Pernarowski and his colleagues initially detailed the basket approach (Barsagade et al.). The evaluation of dissolution was initially introduced in the 13th edition of the U.S. Pharmacopeia in the early 1970s, and it has since become the most often utilized method for this purpose. The methods utilized are called method I(basket) and method II (paddle) according to USP, and they are referred to as "closed-system" procedures since they include the use of a specific amount of dissolving media (Sinko, 2023).

Practically, a rotating basket technique creates a consistent stirring movement in a sizable container containing 1000 mL of liquid, which is submerged in a water media at a controlled temperature. The basket technique is analyzed based on its simplicity, robustness, and ease of standardization. The USP basket method is preferred for conducting dissolution testing of immediate-release or topical formulations. This device is beneficial for administering tablets, capsules, beads, and floating medications. USP Apparatus1 is often used to test drug items, including solids that primarily float, as well as monodisperse tablets and polydisperse encapsulated beads.

### 2.6.2.2. USP Apparatus 2 (Paddle Apparatus)

Levy and Hayes's (1960) description of equipment might be regarded as the precursor to the beaker method. A 400 ml beaker holding 250 ml of 0.1N HCl dissolving fluid was part of the setup (Levy et al., 1960). Inside the beaker, there was a three-blade polyethylene stirrer with a diameter of 5 cm. The stirrer was placed in the center and revolved at a speed of 59 rpm. The tablet was positioned alongside the beaker, and samples were extracted at regular intervals. An alternative to using a basket for agitation is Apparatus 2, which is called the paddle apparatus method. The shaft, like the basket equipment, must revolve freely and firmly without swaying more than 2 mm from the vessel's vertical axis at any angle (Uddin et al., 2011).

The apparatus is beneficial for administering pills, capsules, and suspensions. USP

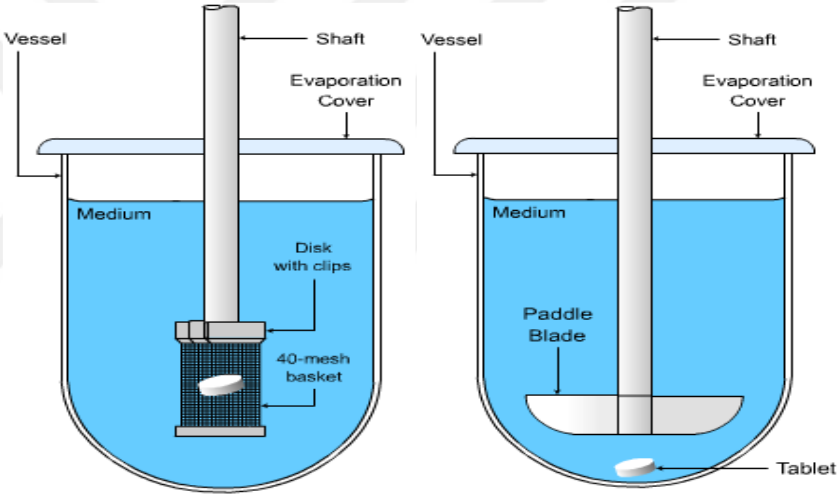


Figure 2.19. Diagrammatic depictions of basket (USP 1) and paddle (USP 2) apparatus (Qureshi, 2004)

### 2.6.3. Water Content Test

Measuring the water content is a crucial factor in the pharmaceutical sector. The pharmaceutical industry relies on it heavily for research, manufacturing, and quality control. It is crucial to have knowledge of the water content and a clear grasp of the hygroscopic properties of a pharmacological material and end product in which it is present. Water can potentially impact the stability of APIs and therapeutic formulations, as well as the sustainability and activity of microbes, potency, efficacy, and shelf life (Warner et al., 2007). Consequently, it is critical to establish reliable

procedures for determining the concentration of water in pharmaceuticals throughout their development phase and to create appropriate standards for this purpose.

The quantity of water contained in a material is referred to as its water content, which is also called its moisture content. For each product in the pharmaceutical industry's process, knowing the maximum moisture content that may be tolerated is crucial.

Water in medications and pharmaceutical preparations provides an ideal habitat for the growth of germs. The gastrointestinal system may cause bacterial death and endotoxin release once a composition containing a specific quantity of bacteria enters the organism. Antibodies against endotoxins are formed in response to even trace amounts of endotoxin in the body. A significant amount of endotoxin can enter the bloodstream during gastrointestinal crises, causing an allergic reaction that ends in severe shock (Warner et al., 2007).

Traditionally, water content in pharmaceutical products is determined by one of two methods: loss on drying (Ma et al., 2018) or Karl Fischer Titration (Talebi et al., 2020) .

#### 2.6.3.1. Loss on Drying (LOD)

Loss on Drying (LOD) refers to the percentage decrease in weight that occurs under defined conditions, often at a temperature of 105 °C for a specified duration. The LOD process was implemented in the pharmaceutical business at the start of the previous century (Talebi and Armstrong, 2020) and still may be considered adequate in some cases. According to the United States Pharmacopeia (USP) General Chapter <731>, LOD (Razvi et al., 2021) may still be used in those cases where the weight loss sustained on heating may not be entirely water. While being a commonly used technique for determining water content, LOD has significant drawbacks. The disparity in weight before and after drying is not necessarily due to the water content but, instead, the reduction in mass caused by the drying process. This phenomenon of mass loss is occasionally referred to as "moisture"; however, this term is problematic since it is widely used to denote water and other volatile liquids. Part of the reduction in bulk may be due to inherent gaseous and volatile substances and breakdown byproducts.

This method can be carried out when the sample material is abundant and will not decompose or melt at 110 °C. In this method, the prescribed quantity of the

substance specified in the appropriate monograph is dried to constant mass or for the prescribed time. Drying can be carried out in a desiccator, in a vacuum, or in an oven within a specified temperature range, as illustrated in Figure 2.20. This method is commonly used to determine water content in excipients, tablets and for stable APIs (Hachmann et al., 2011). Also, accurate LOD values can be determined using thermogravimetric analysis (Villain et al., 2007).

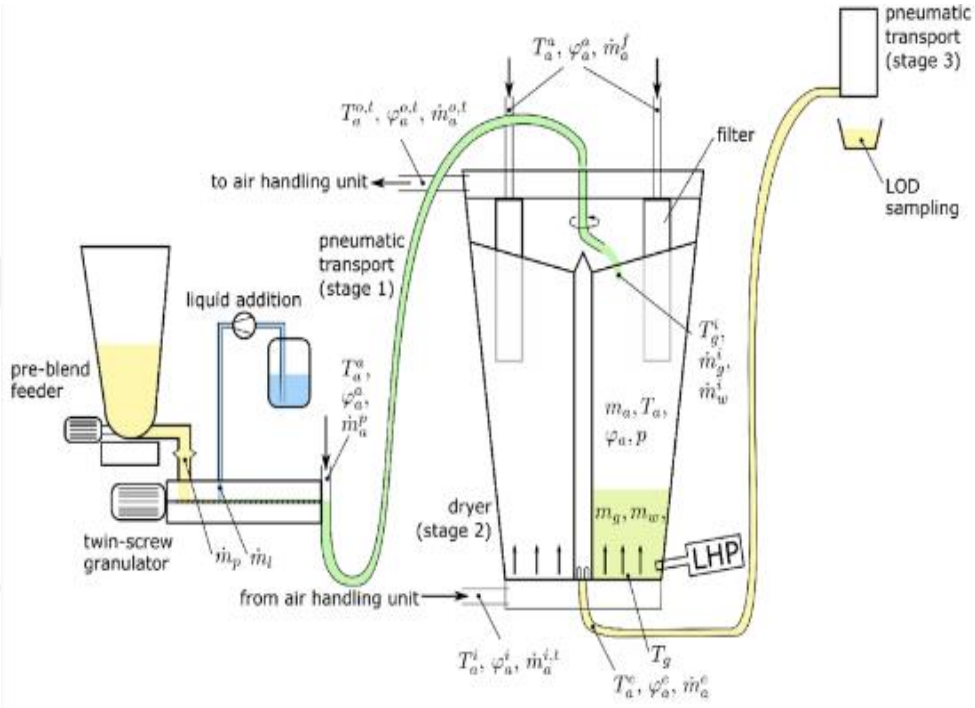


Figure 2.20. Schematic diagram of Loss on Drying (LOD) process (Razvi et al., 2021)

### 2.6.3.2. Karl Fischer Titration (KFT)

At this time, KFT is the method of choice for determining water content (Talebi and Armstrong, 2020) which was first reported in 1935 (Fischer, 1935). The method for water analysis has been widely accepted and used for more than 70 years. It is listed in well-known pharmacopeias such as the USP (Joseph 2019) and European Pharmacopoeia (Ph. Eur.) (Oketch-Rabah et al., 2019). E stimates suggest that 500,000 KF calculations are carried out every day worldwide. The KF technique measures sulfur dioxide concentration in water-based solutions by means of the modified Bunsen reaction.

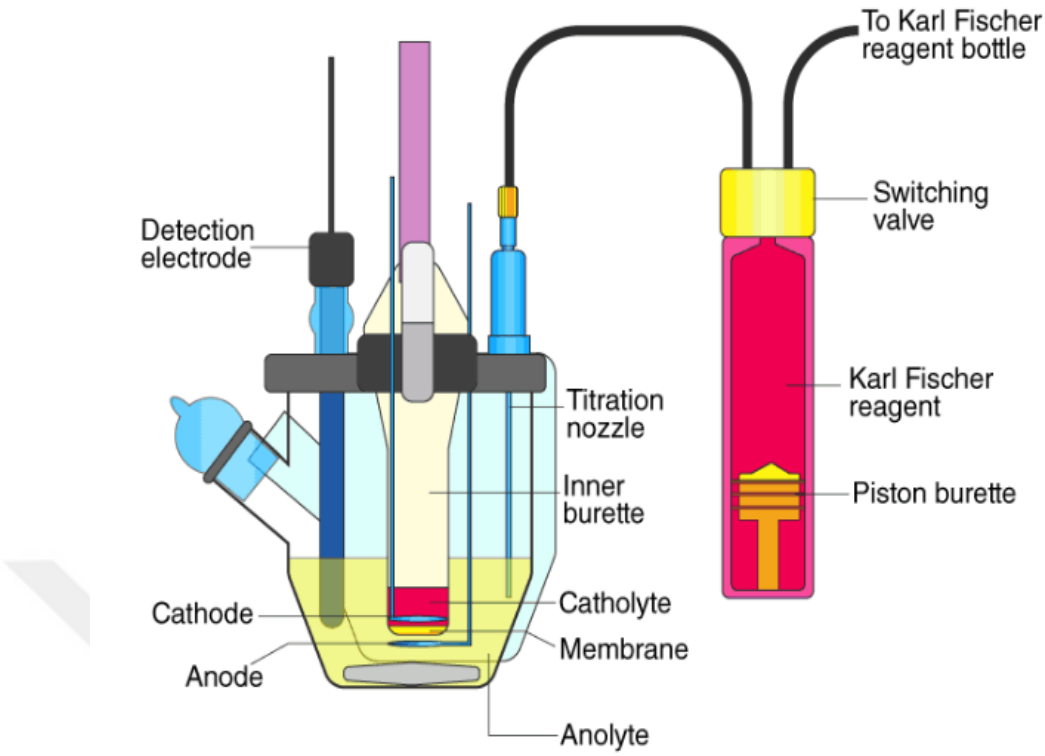


Figure 2.21. Karl Fischer titration (Marković et al., 2018)

The KFT is a very specific chemical reaction that occurs when a dehydrated sulfur dioxide and iodine solution is mixed with water in the presence of a hydrogen ion-interacting buffer. There have been several revisions to the original protocol since it was published, and the conditions and reagent composition could vary greatly depending on the sample type and the method used. First impressions are that the KFT reaction is just a water-based variant of the well-known Bunsen reaction (Eq 2.4).

$$I_2 + 2H_2O + SO_2 \longrightarrow H_2SO_4 + 2HI \quad \textbf{(2.4)}$$

To make sure the reaction is thorough and to neutralize any free protons, the reagent is buffered with pyridine (Py) (Eq. 2.5).

$$2H_2O + (Py)2.SO_2 + I_2 + Py \longrightarrow (Py)_2.H_2SO_4 + 2Py + HI \quad \textbf{(2.5)}$$

A 2:1 M ratio of $H_2O$ to iodine is required according to Fischer's equation (4.2) that was mentioned earlier in order to ascertain the quantity of water. Sulfur dioxide plus Iodine were dissolved in a combination of pyridine and methanol, and the classical KF reagent was the product of this reaction.

### 2.6.4. Scanning Electron Microscopy (SEM)

SEM is a widely used method for analyzing organic and inorganic substances at nanometers to micrometers. With high magnification capabilities, it produces accurate images. Its provided data, when combined with energy-dispersive X-ray Spectroscopy (EDS), enables essential information unavailable through conventional laboratory examinations.

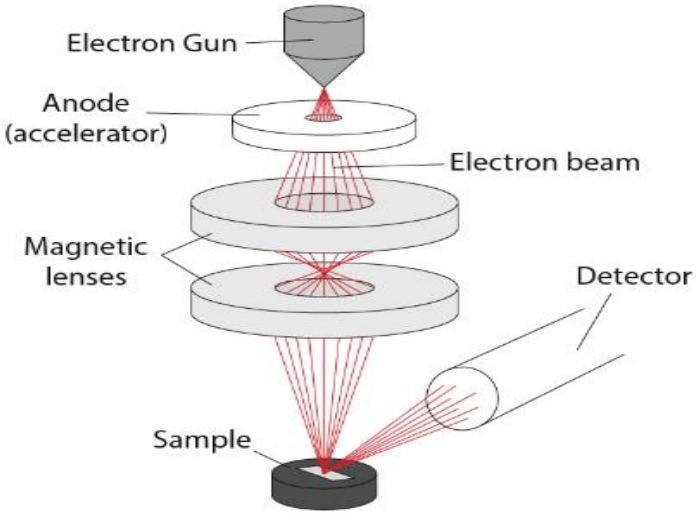


Figure 2.22. Schematic of SEM (Zhou et al., 2007)

SEM is an invaluable instrument. Hence, the approach is widely utilized in almost every science, technology, and industry field. The primary obstacle is ensuring that the seen object can endure the vacuum conditions inside the chamber and the impact of electron bombardment (T. Klein et al., 2012).

In SEM, the electron beam systematically moves across the sample in a raster pattern. Instead of traversing the specimen, electrons are deflected from the surface or can even cause ionization of atoms within the sample by releasing electrons. The secondary and backscattered electrons can be used as signals to construct the final image (Danilatos et al., 1979). SEM images describe the physical structure of a specimen and have the ability to create quasi-three-dimensional visualizations of the specimen's surface. Hence, this technique is primarily employed to acquire a detailed image of surface characteristics and enables inferences about the spatial arrangement of various chemical constituents within the specimen. Contemporary scanning electron microscopes SEMs have the capability to achieve a resolving power superior to one nanometer (Kannan, 2018).

### 2.6.5. X-ray diffractometer (XRD)

XRD can be defined as the most effective technique for investigating the material's crystal structure. Crystalline compounds with domain sizes greater than 3–5 nm can be detected by the instrument. You can use it to find out what chemicals are in a crystal and how its general structure is defined (Iwashita, 2016).

Emissions of electromagnetic radiation with wavelengths between 0.01 and 0.7 nanometers are known as X-rays. The distances between atomic layers in a crystal lattice are analogous to these wavelengths. Metals typically have interatomic spacing between 0.2 and 0.3 nm. An X-ray beam's interaction with an atom in a target causes the photons to scatter in all directions. When there is no change in the energy of the incident and scattered photons, we say that there has been elastic scattering.

During inelastic scattering, the photon that is dispersed experiences a decrease in its energy. When these waves are spread out, they can overlap with one another. If the waves are in sync, the interference is constructive, meaning they reinforce each other. However, if they are out of sync, destructive interference happens, causing them to cancel each other out. The atoms within crystal planes arrange themselves in a regular pattern, creating a coherent scattering effect. Diffraction occurs when light or other waves interact with atoms on distinct planes, resulting in a pattern that reveals details about the arrangement of atoms in a crystal (Speakman, 2011).

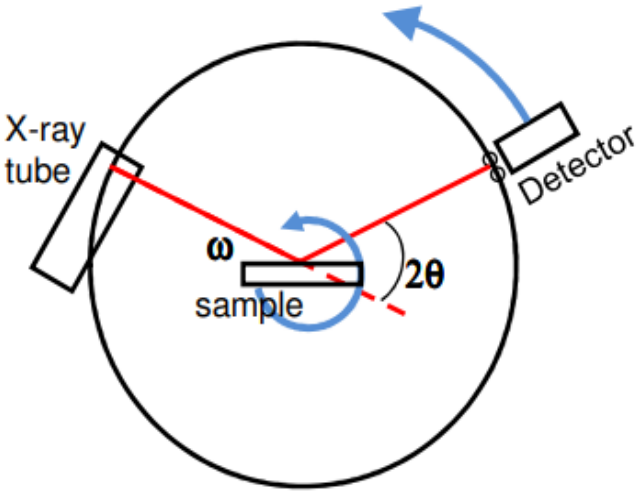


Figure 2.23. Basic components of X-ray diffractometers (Zevin et al., 2012)

An X-ray diffractometer is the name of the instrument. In order to examine the samples, the diffractometer uses a single-color X-ray beam. A diffraction intensity

spectrum can be obtained by measuring the corresponding angle between the incident and diffraction beams and then systematically changing the X-ray beam's incidence angle. The main components of a diffractometer are as follows: (1) an X-ray tube, which is where the X-rays come from; (2) incident-beam optics, which are used to focus the X-rays before they hit the sample; and (3) a goniometer, which is mounting for the sample, optics, detector, and/or tube. holder of the specimen, (5)Optics on the receiving end: these adjust the X-ray beam after it has hit the sample, and (6) Detector: this device measures the amount of X-rays emitted by the material under study (Reynolds, 1989).

### 2.6.6. Fourier-Transform İnfrared Spectroscopy (FTIR)

Infrared spectroscopy, or IR spectroscopy, is an essential instrument that allows the investigation, identification, and classification of functional groups inside a molecule. Moreover, the distinct set of absorption bands may easily determine the properties of pure substances and identify certain contaminants. Infrared spectroscopy operates on the assumption that molecules exhibit unique vibrational frequencies (Meier, 2005). The infrared (IR) portion of the electromagnetic spectrum contains frequencies between about 4000 and 200 $cm^{-1}$. When IR radiation is directed towards a sample, the sample selectively absorbs radiation that has frequencies that match its molecular vibration frequencies while allowing other frequencies to pass through (Berthomieu et al., 2009).

The absorption of specific frequencies of radiation can be measured using an infrared spectrometer. An infrared spectrum, a plot of absorbed energy against frequency, can be created in this way. It is feasible to identify a particular molecule because various materials have distinct vibrations and generate distinct infrared spectra. A molecule that is not linear and consists of N atoms demonstrates 3N-6 vibrational motions for its atoms, which are also referred to as fundamental vibrations or normal modes. The only molecule vibrations that are present in the IR spectrum are those that are capable of absorbing IR light, often known as being IR active. In order for a mode to be considered IR active, the vibration of the molecule must cause a measurable alteration in its dipole moment. As a result, symmetric vibrations are not observed in the infrared spectrum. In a molecule possessing a center of symmetry, the vibrations that exhibit symmetry in relation to the center are considered to be infrared (IR) passive. Nevertheless, any molecule vibrations that

lack symmetry are considered to be infrared (IR) active and will, therefore, be observed in the spectrum. This leads to the simultaneous identification of all chemical groups contained in the sample. Remarkably, this methodology has the ability to easily identify both amino acids and water molecules, which are challenging to detect using traditional spectroscopic methods. Chemical groups with a persistent dipole, such as polar bonds, have a high level of absorption in the infrared spectrum. Therefore, infrared spectra of proteins exhibit absorption peaks resulting from the presence of carbonyl groups in the polypeptide chains(Baravkar et al., 2011).

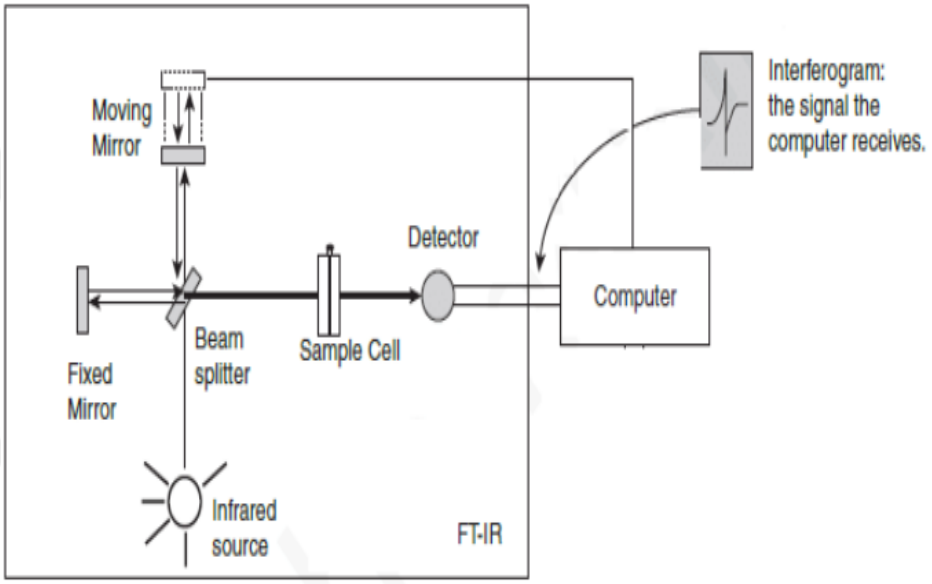


Figure 2.24 Schematic diagram of typical FTIR spectrophotometer (Jalvandi, 2016)

### 2.6.7. The Stability Test of Drug Nanocrystal

One of the most indispensable tests of drug nanocrystals is the stability test (stability study). It must be done depending on the general requirements specified in Clause 5 of the Second Schedule of New Drugs and Clinical Trials Rules, 2019 (Dubey et al., 2019) and ICH guidelines (Pokharana et al., 2018).

Developmental drug nanocrystals should undergo thorough and methodical stability testing. Once a medicine is made using nanoengineered APIs, it must periodically undergo stability testing under typical storage and transportation settings to ensure it remains active in its final form. Functionality, integrity, stability of the carrier material, stability of the drug in encapsulated form, size range of drug

nanocrystals, and identification of degradation products should be the main areas of study.

It is essential to choose appropriate storage conditions for the individual product, and research must be conducted on the suggested packaging for the market. Furthermore, it is necessary to measure and quantify parameters unique to nanoengineered material-based systems at various time intervals. These parameters include particle size, distribution, surface morphology analysis, loading of drug, drug release kinetics, and so on. It is important to employ suitable techniques for this purpose (Ai et al., 2011).

### 2.7. Literature Review

At a higher stirring speed of 1000 rpm, the opposite pattern Particle size decreased as the concentration was increased from 5 to 15 mg/ml. This finding suggests that super saturation, rather than drug concentration aggregation, becomes the most important consequence as the mixing level increases. Increases in stirring speed result in the generation of smaller particles, regardless of the drug concentration (Kakran et al., 2013).

(Kakran et al., 2012) found that the diameter of the curcumin particle did not drop much when the flow rate increased. This is because the crystal development of curcumin happens in a specific direction, resulting in needle-shaped crystals.

(Zhang et al., 2009) was found that the particles formed at a temperature of 30 °C had an average size of approximately 2 μm and had an irregular flake-like shape. On the other hand, the particles obtained at a temperature of 3 °C had a rod-like shape and were around 240nm in size.

The antisolvent crystallization approach was used to crystallize carbamazepine from organic solutions. A solution of carbamazepine in ethanol was prepared using sterile water as the antisolvent. Carbamazepine had been dissolved in the solvent and was causing particle precipitation prior to injection into the antisolvent. Various process factors were tested during the crystallization studies, including solution concentration, temperature, injection rate, and ultrasonic presence/absence. An examination of the produced particles revealed that the process parameters significantly impacted the particles' outward features, including size and dispersion, while having little effect on their internal structures, including crystallinity and thermal stability. The use of solutions with high drug concentrations resulted in the

collection of smaller particles. Crystals grew in size as the temperature rose. Particle size was also affected by the injection rate of the medication solutions. Targeted use of an ultrasonic pulse dramatically decreased carbamazepine particle size (Park & Yeo, 2010)

One of the biggest problems in developing new pharmaceuticals is that hydrophobic medications are insoluble and difficult to dissolve. Many believe that drug nanoparticles will help to solve this issue. In this work, we aimed to manufacture celecoxib nanoparticles by combining soluplus hydrophilic stabilization with antisolvent precipitation and high-pressure homogenization with soluplus in arbitrary proportions. The two procedures used to manufacture celecoxib nanoparticles were antisolvent crystallization followed by freeze-drying (CRS-FD) and high-pressure homogenization followed by freeze-drying (HPH-FD) (Homayouni et al., 2014).

The processing of carrier-free nanocrystals necessitates meticulous nucleation control and, as a result, a detailed understanding of the metastable zone of the appropriate solution. A solution will become metastable if it remains supersaturated without forming nuclei. The metastable zone width is the maximum degree of supersaturation. When nucleation occurs directly from the metastable region, it aids in the formation of homogeneous nuclei that result in uniform nanocrystals (Ren et al., 2019).

Colloidal particles are solid microscopic particles that can be suspended in a liquid. Colloidal suspensions are an ideal model for studying other condensed matter physics phenomena since the solid particles' collective phase behavior is comparable to that of other condensed systems. (Ren et al., 2019).

(Hatkar et al., 2012) was mentioned. One can efficiently regulate the average particle size and its distribution by manipulating ultrasound factors like the amount of power and ultrasonic duration throughout the crystallization process. This is for high-energy materials that are prone to friction and impact during mechanical size.

# 3. MATERIALS AND METHODS

## 3.1. Materials

The following ingredients are used: Lisinopril powder (from Harman Finochem Ltd, India), Tween 80 (from Merck Germany), Tween 20 (from Merck Germany), distilled water (D.W.), acetone, acetonitrile, PVP (from Merck Germany), and dimethylformamide (from Sigma Aldrich, Germany).

## 3.2. Methods

Figure 3.1 shows the antisolvent precipitation procedure used to prepare Lisinopril nanocrystal powder and colloidal particles. In order to get three distinct samples, we varied the antisolvent solutions, stabilizers, and other variables.

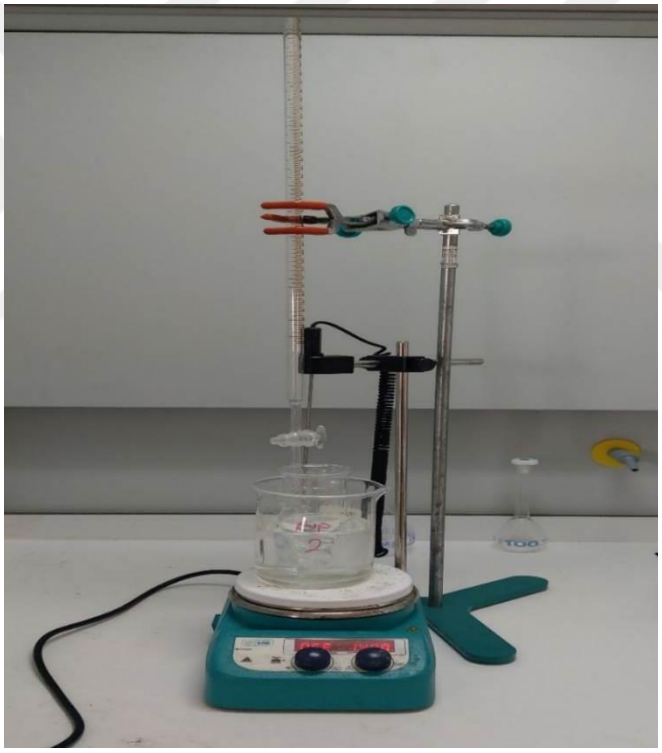

Figure 3.1. The antisolvent's crystilization technique setup

### 3.2.1. Preparation of Sample 1

In Sample 1, 100 mg/ml of Lisinopril powder was dissolved in distilled water. The antisolvent is a mixture of dimethylformamide and acetonitrile at a ratio of 1:0.05:6. The stabilizer is 1 % PVP. An ice bath will be used to prepare a 100 mg/ml solution of lisinopril that has been supersaturated. The next step is to add the solution to a beaker with acetonitrile and dimethylene formamide. The beaker will be stirred

at 1500 rpm as the solution is injected at a 3 ml/min flow rate. An intake filter with a particle size of 0.45 µm is utilized for the injection.

### 3.2.2. Preparation of Sample 2

Sample 2's components include 50 mg/ml of Lisinopril in distilled water, acetonitrile, and acetone in a ratio of (1:3:1) as antisolvents and 1 % of Tween 80 as a stabilizer. In a beaker with acetone, acetonitrile, dimethylene formamide, and 1 % Tween 80 as an antisolvent solution. First, a 0.45 µm inlet filter will be used to filter a 50 mg/ml solution of lisinopril. The solution will be stirred in an ice bath at 1300 rpm with a 2 ml/min flow rate.

### 3.2.3. Preparation of Sample 3

Sample 3 consists of Lisinopril dissolved in distilled water at a concentration of 25 mg/ml. Acetone is used as an antisolvent in a ratio of 1:3, and 1 % of Tween 20 is added as a stabilizer. Lisinopril solutions with a supersaturated concentration of 25 mg/ml will be prepared. These solutions will then be filtered using a 0.45 µm inlet filter. The filtered solution will be injected into a beaker that contains acetone and a 1 % solution of Tween 20, which acts as an antisolvent. The injection will be done at a flow rate of 1.5 ml/min while swirling the solution at a speed of 1300 rpm. The entire process will be carried out in the presence of an ice bath.

During the subsequent synthesis stage, colloidal samples were generated and kept at a temperature of 5 °C for a duration of 2 hours in order to prepare them for SEM analysis, as depicted in figure 3.2(a).

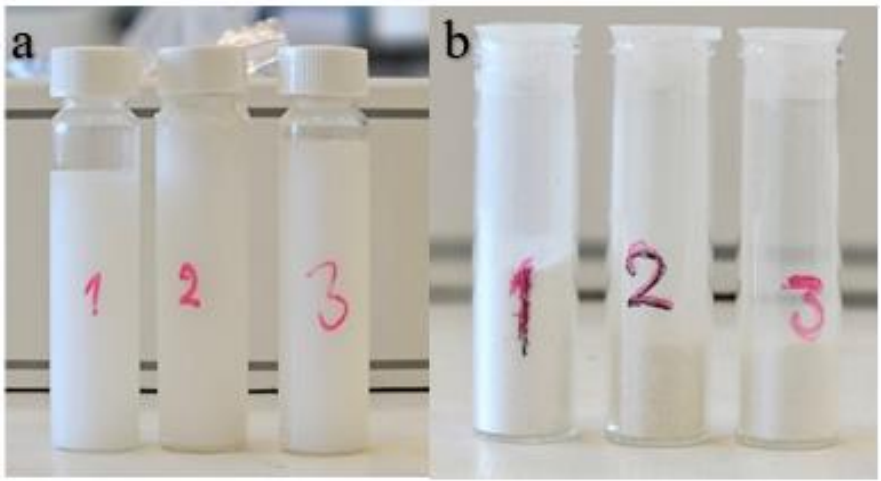


Figure 3.2. (a) Lisinopril colloidal samples and (b) Lisinopril drug nanocrystal samples

The colloidal samples depicted in Figure 3.2(a) were subjected to evaporation in an oven at 90 °C. The resulting powder was then collected for subsequent characterization using various techniques, including XRD, FTIR, assay test, water content test, and dissolution test, as indicated in Figure 3.2(b).

### 3.3. Chemical, Physical, and Pharmaceutical Characterizations

#### 3.3.1. SEM Characterization

The synthesized Lisinopril drug nanocrystals and raw Lisinopril powder were characterized using SEM (Jeol JSM7001F model) in KITAM. The form and size of the particles, as well as their surface appearance, were readily visible using SEM.


Figure 3.3. Scanning electron microscope (Jeol JSM7001F model)

#### 3.3.2. Image J Program

Image J Program was used to measure the particle size of the different nanocrystal samples produced by the lisinopril drug. All particle size measurements are done through the use of images captured by SEM.

#### 3.3.3. XRD Analysis

The crystal structures of the raw Lisinopril powder and the resultant Lisinopril drug nanocrystals were examined using the Rigaku Smart Lab XRD instrument. CuKα radiation was used in the tests, with an X-ray voltage of 40 kV and a current of 40 mA.

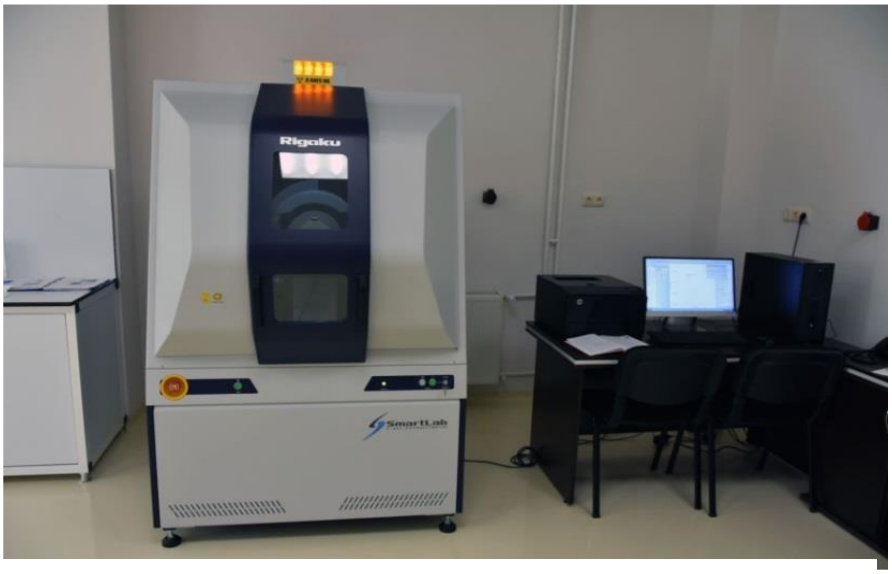


Figure 3.4. X-ray diffraction device (Rigaku. SmartLab model)

### 3.3.4. Fourier Transform Infrared Spectroscopy (FTIR)

Using a Perkin Elmer Spectrum Two FTIR Spectrometer, the chemical compositions of raw Lisinopril APIs and Lisinopril drug nanocrystals were examined. A tiny quantity of the samples was put in a special container and inspected. The required assistance was given via Spectrum software. In a matter of seconds, each spectrum was recorded using four scans with 0.5 mL of material per scan at a resolution of 4 $cm^{-1}$ in the 4000-650 $cm^{-1}$ range. Spectrum was the computer software used to process the scan data.

Figure 3.5. FTIR Spectrometer (Perkin Elmer Spectrum Two)

### 3.3.5. Water Content Test

The Metrohm 787 KF titration was used to analyze the water content of the raw Lisinopril APIs and prepared drug nanocrystals. As a water deterrent sample, 500 mg of each sample was utilized. Following USP 34, method I <921>, it underwent titration using Karl Fischer pyridine-free reagent.


Figure 3.6 Water content tester Metrohm 787 KF titrino

### 3.3.6. Reverse Phase-High Performance Liquid Chromatography(HPLC)

The quantitative assessment of raw Lisinopril APIs and Lisinopril drug nanocrystals was analyzed by the HPLC system (Shimadzu instrument, Model LC 2040 with photodiode array detector) used in an isocratic mode.

Figure 3.7. HPLC system (Shimadzu instrument, Model LC 2040 with photo diode array detector)

### 3.3.7. Dissolution Test

The pharmaceutical test model PTWS 820-MA was used to measure the dissolution rate using Apparatus 2 (Immediate-Release Dosage Forms) and the USP 38 technique (first apparatus). It was set at 50 rpm for the paddle speed and 37.0 ± 0.5 °C for the bath temperature. Separate containers holding 900 ml of sterile water were used to add 10 mg of lisinopril reference standard and lisinopril medication nanocrystal powder, respectively. The results were compared to those obtained from the drug solubility test in filtered water following a further trial with 0.1 N HCl. After 30 minutes, 2.0 ml of the sample was transferred to a 25 ml volumetric flask.

The mobile phase diluted the flask to reach the desired volume. Finally, a 0.45 µm syringe filter was used for raw and prepared samples. Then, a second 25-ml volumetric flask was used to dilute 4.0 ml of this solution to volume with the mobile phase. An HPLC system (equipment made by Shimadzu, Model LC 2040 with a photodiode array detector) was used to measure the sample concentration at 210 nm. (USP 44).

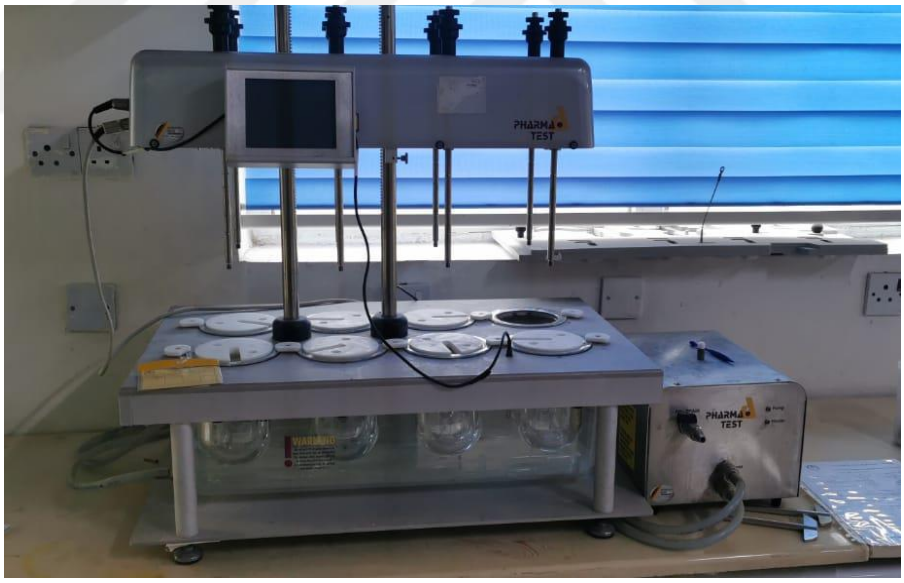


Figure 3.8. Dissolution tester (Pharma test model PTWS 820-MA)

### 3.3.8. Quantitative Analysis of Lisinopril APIs

#### 3.3.8.1. Material and Chemicals Reagent

As analytical reagent grade, monobasic potassium phosphate, dibasic sodium phosphate, and sodium hydroxide were supplied from Sigma Aldrich-Germany. Deionized water and acetonitrile were of HPLC grade. (99.8 % purity) supplied by

Sigma Aldrich-Germany as analytical reagent grade. Raw Lisinopril APIs were supplied by Harman Finochem Ltd, India.

#### 3.3.8.2. Standard and Test Solutions Preparation

Solution A, which was made by dissolving 2.76 g of monobasic sodium phosphate in around 900 mL of distilled water (D.W) in a 1000-mL volumetric flask, and a mobile phase consisting of four parts acetonitrile to ninety-six percent water were the chromatographic conditions recommended. dilute by distilled water (D.W) and pH calibration to 5.0 using 1 N sodium hydroxide. was made to the last stage of analysis

#### 3.3.8.3. Chromatographic Conditions

Solution A, which was made by dissolving 2.76 g of monobasic sodium phosphate in around 900 mL of distilled water (D.W). in a 1000-mL volumetric flask, and a mobile phase consisting of four parts acetonitrile to ninety-six percent water were the chromatographic conditions recommended. dilute by distilled water (D.W) and pH calibration to 5.0 using 1 N sodium hydroxide. was made to the last stage of analysis

Chromatographic system:

- Detector: UV 210 nm.
- Column: 4.6-mm × 25-cm; 5-µm packing L7.
- Column temperature: 50 °C.
- Flow rate: 1 mL/min.
- Injection volume: 20 µm.

#### 3.3.8.4. Assay Calculations

The percentage of lisinopril drug nanocrystals assay was calculated using the following equation:

$$Assay = (r_U/r_S) \times (C_S/C_U) \times 100 \quad \textbf{(3.1)}$$

Where:

$r_U$ = peak response Lisinopril drug nanocrystal solution.

$r_S$ = peak response of Lisinopril drug nanocrystal solution.

$C_S$ = concentration Lisinopril raw material (mg/mL).

$C_U$ = concentration of Lisinopril drug nanocrystal solution (mg/mL).

Acceptance criteria: 98.0 %–102.0 % on the anhydrous.

### 3.3.9. Stability Test

The stability of the Lisinopril drug nanocrystal was assessed per the recommendations provided by the International Council for Harmonisation (ICH) and the World Health Organization (WHO) in their documents titled "Stability testing of new drug substances and products" [Q1A (R2)] and "Impurities in new drug substances" [Q3A (R2)]. These guidelines also specify the stability parameters that member states of the WHO should follow. For six months, Lisinopril drug nanocrystals were kept in a tightly sealed container at a consistent temperature of 30 ± 2 ℃ and a relative humidity of 65 ± 5 %. For this task, we make use of the stability chamber of RU MED-Germany.

Approximately 30 g of each of the prepared Lisinopril drug nanocrystal samples were stored in an appropriate airtight container and subjected to continuous monitoring at a temperature of 30 ℃ and relative humidity of 65 % for 6 months in order to conduct long-term analysis. As per the WHO standard, stability results are considered unsuccessful if there is a substantial change of 5 % or more in the assay from the initial content of the active pharmaceutical ingredient (API).

Figure 3.9. Stability chamber (RU MED Germany)

# 4. RESULTS AND DISCUSSION

## 4.1. SEM Results

The Lisinopril powder and the three manufactured Lisinopril drug nanocrystal samples were characterized using SEM. SEM of the Lisinopril raw materials was captured using a 1µm scale and a 5 KX magnification. Figure 4.1 shows that the Lisinopril raw materials had large particle sizes and lengthy crystal forms at this level.

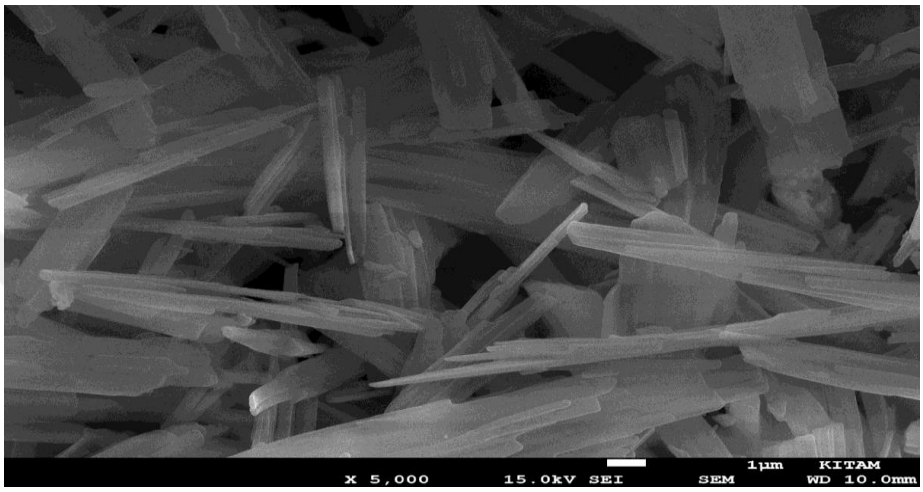


Figure 4.1. SEM image of raw Lisinopril at 1µm

### 4.1.1. SEM Result of Sample 1

An SEM snapshot picture was captured for sample one at a 1 µm scale and 20 KX magnification to examine the Lisinopril drug nanocrystals. At this stage, with 20 K X magnification, the nanoparticles can be clearly seen in Figure 4.2.

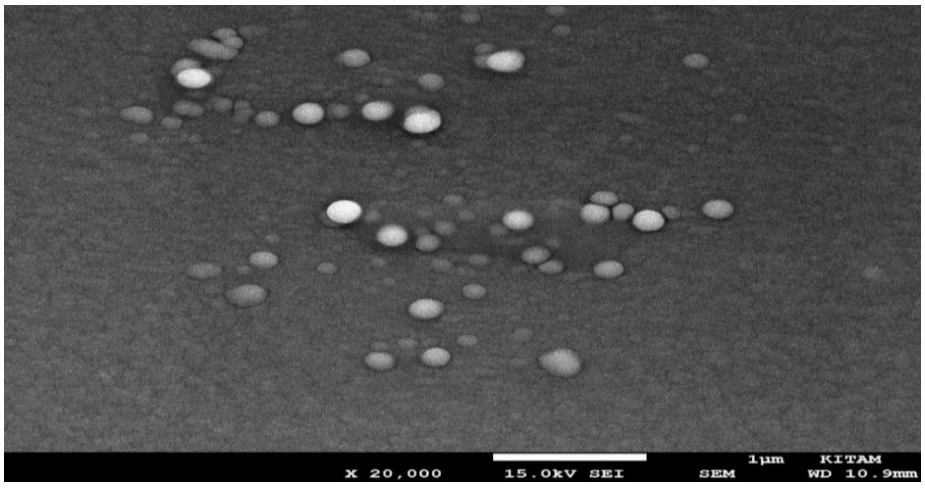


Figure 4.2. SEM image of Lisinopril drug nanocrystals (sample 1) at 1 µm

For sample 1, the scanning electron micrograph was captured at a magnification of 30 KX with a scale of 100 nm. The observed diameters of the produced colloidal Lisinopril drug nanocrystals were chosen at random. Figure 4.3 shows that, at this point, it was easy to measure the diameters of the synthesized colloidal Lisinopril drug nanocrystals. These pictures were captured using a PVP stabilizer on colloidal samples.

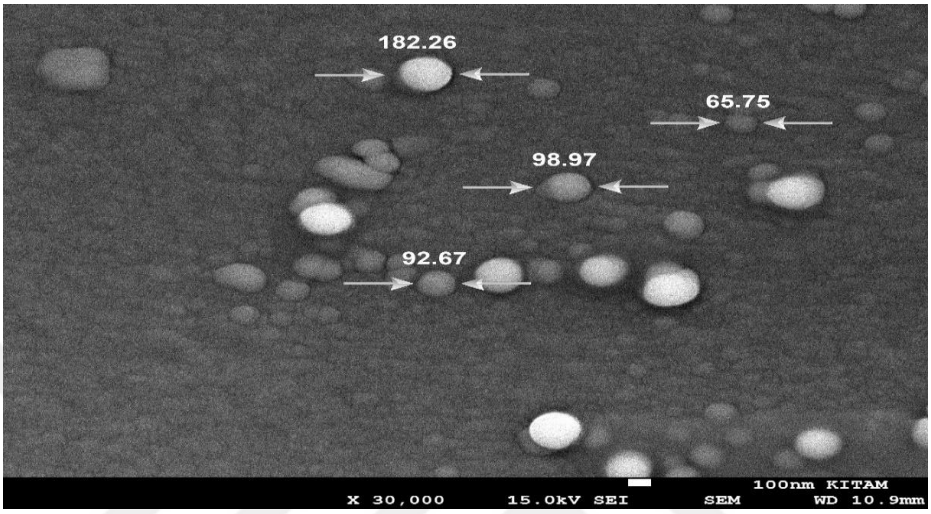


Figure 4.3. SEM image of Lisinopril drug nanocrystals (sample 1) at 1 nm

The Lisinopril drug nanocrystals that were synthesized had particle sizes ranging from 65.75 to 182.26 nm, which is within the size range of nanopharmaceuticals. Based on Figure 4.3. The drug nanocrystals maintained a uniform shape with no agglomeration and became easily distinguishable from one another after PVP was added as a stabilizer to avoid particle aggregation. Figure 4.4 shows that the particle size distribution ranged from 100 nm to 120 nm.

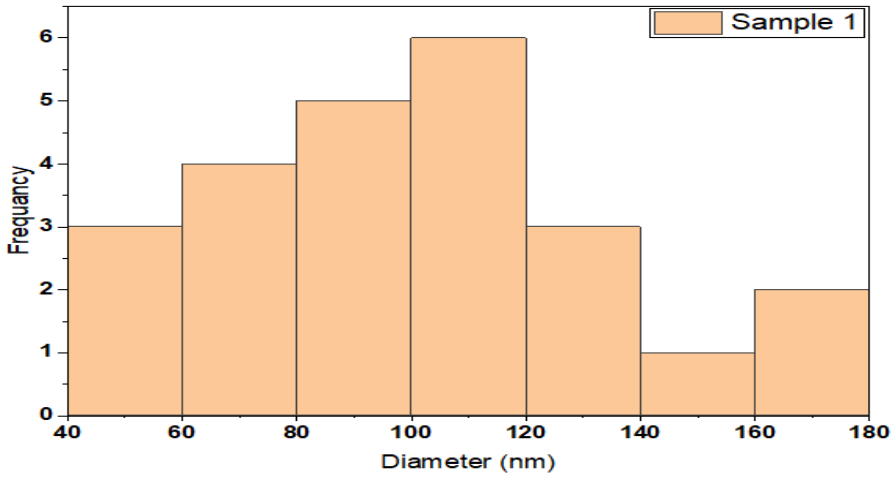


Figure 4.4. Particle size distribution of sample 1

### 4.1.2. SEM Result of Sample 2

The SEM image in Figure 4.5 displays sample 2, which was produced with Tween 80 stabilizers. The image has a scale of 1µm and a magnification of 5 KX. The particle size was readily observable and can be quantified at this magnitude.

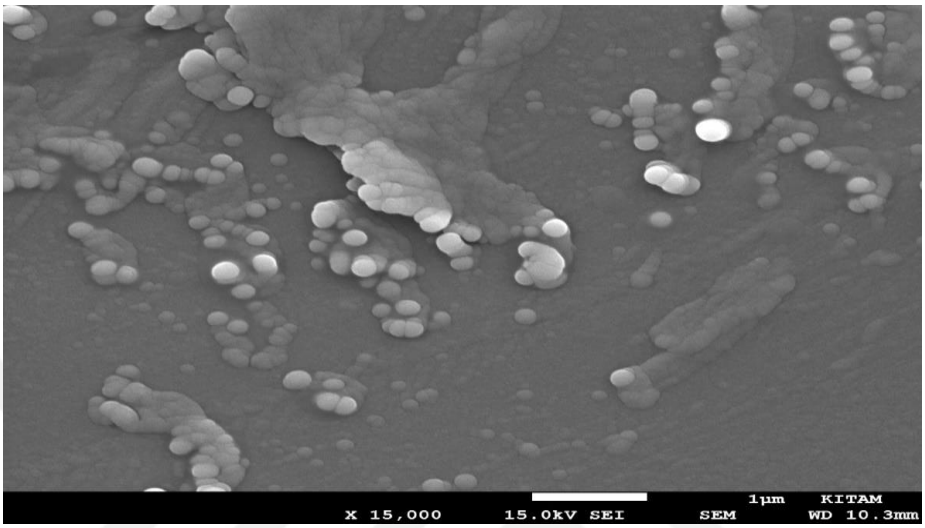


Figure 4.5. SEM image of Lisinopril drug nanocrystals (sample 2) at 1 µm

The SEM image of sample 2 was captured at a 100 nm scale and a 30 KX magnification. At this level, the colloidal Lisinopril drug nanocrystals were distinctly observable, as shown in Figure 4.5. Measuring the diameters of the produced colloidal Lisinopril drug nanocrystals is a straightforward task. The photos were acquired from a colloidal solution that was stabilized using Tween 80.

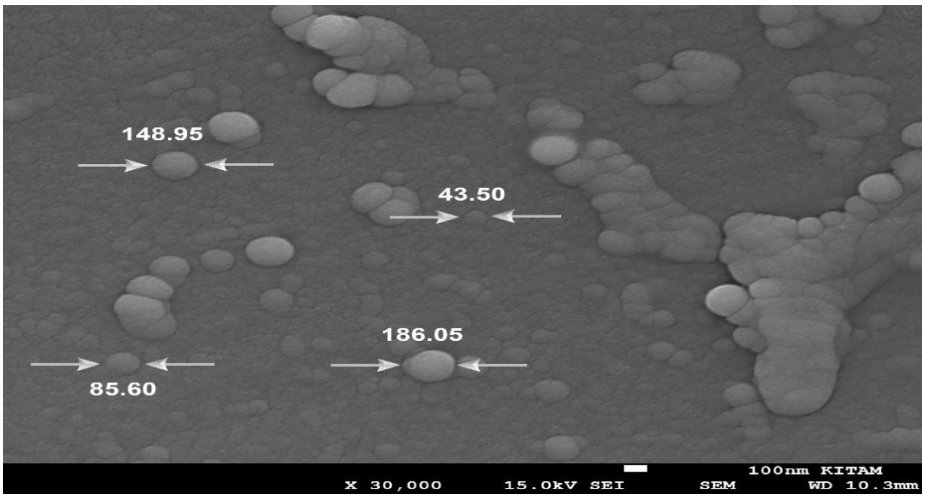


Figure 4.6. SEM image of Lisinopril drug nanocrystals (sample 2) at 1nm

Particle sizes of the synthesized Lisinopril drug nanocrystals were within the nanopharmaceuticals range, measuring 85.60 nm to 197.24 nm.

According to Figure 4.6. The application of Tween 80 as an anti-agglomeration agent (stabilizer) resulted in drug nanocrystals with a regular spherical form that was found to be separated from each other.

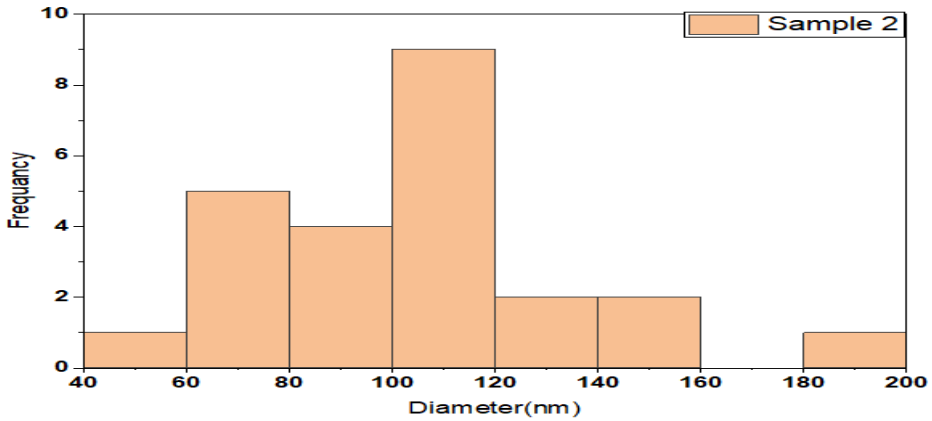


Figure 4.7. Particle size distribution of sample 2

Figure 4.7 represents the amount of particle size distributed from 40 nm to 200 nm of sample 2, which was prepared using 50 mg/ml of Lisinopril raw material with Tween 80 as a stabilizer. The highest amount of prepared nanodrug was between 100 nm and 120 nm, the second amount was between 60 nm and 80 nm, and the third ranged between 80 nm and 100 nm.

### 4.1.3. SEM Result of Sample 3

Figure 4.8 shows an SEM picture of sample 3, which was produced using a Tween 20 stabilizer. The image has a scale of 1µm and a magnification of 20 KX.

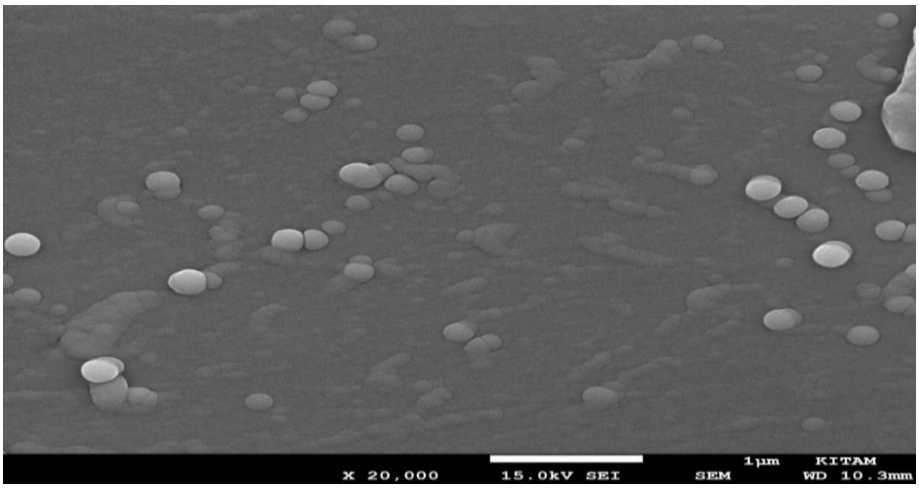


Figure 4.8. SEM image of Lisinopril drug nanocrystals (sample 3) at 1 µm

A100 nm scale and magnification of 30 KX, the SEM image was taken for sample 3; the colloidal Lisinopril drug nanocrystals were clearly visible at this stage, as shown in Figure 4.9. the dimensions of the synthesized colloidal Lisinopril particles can be measured easily. Colloidal Lisinopril drug nanocrystals with Tween 20 stabilizer.

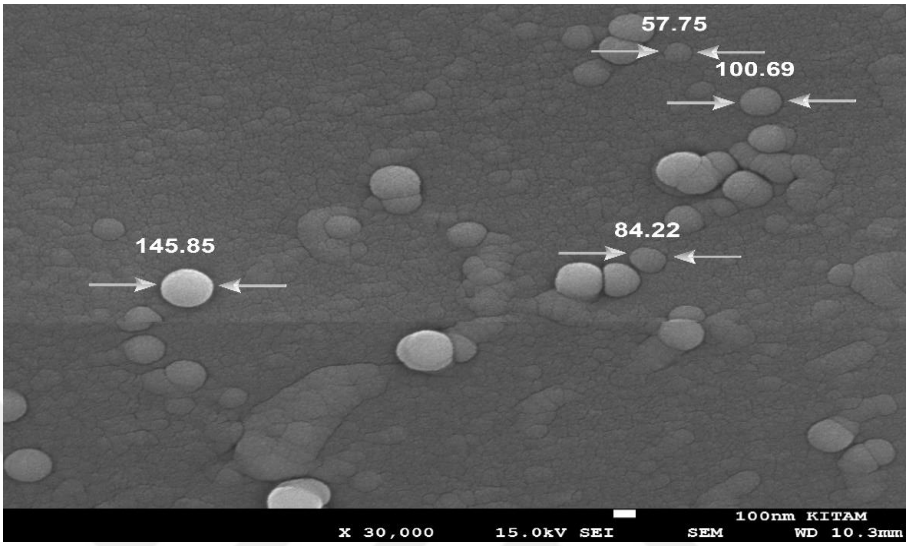


Figure 4.9. SEM image of Lisinopril drug nanocrystals (sample 3) at 1nm

The Lisinopril drugs nanocrystals that formed had particle sizes that fell between 57.75 and 145.85 nm, within the range of nanopharmaceuticals, according to Figure 4.9. Tween 20 was used as an anti-agglomeration agent (stabilizer), and we observed that Tween 20 protected the final product from side reactions and particle adhesion

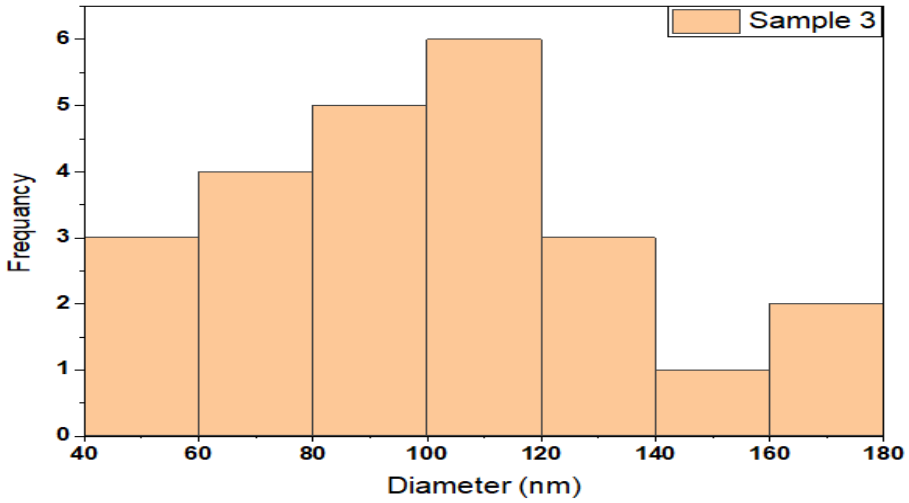


Figure 4.10. Particle size distribution of sample 3

According to the particle size distribution in Figure 4.10, the highest amount of nanoparticle size was between 100 nm and 120 nm, the second between 80nm and 100nm, and the third ranged between 60 nm and 80 nm.

### 4.2. XRD Results

As seen in Figure 4.11(a), the spectrum displays seven significant diffraction intensity peaks of the raw ingredients used to prepare Lisinopril at 7.25°, 12.32°,

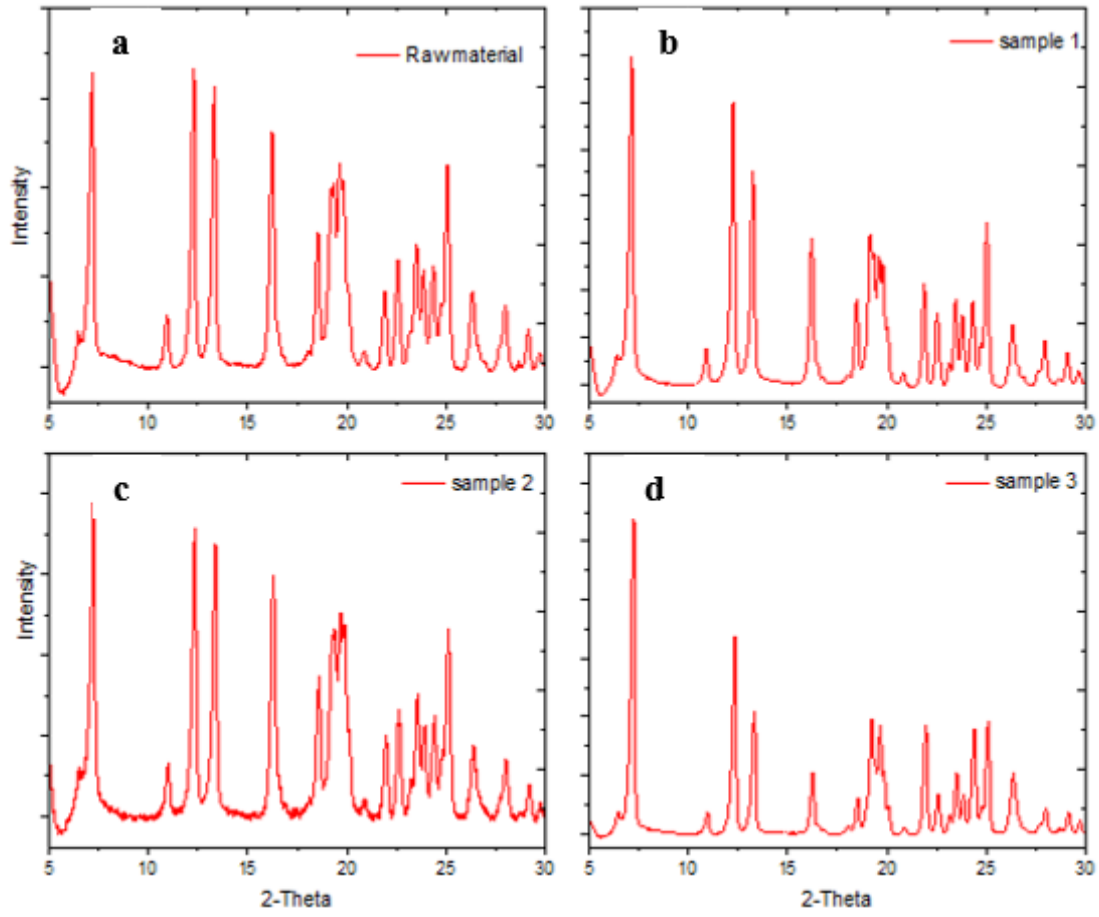


Figure 4.11. XRD pattern of (a)Rwa Lisinopril, (b) Prepared Lisinopril drug nanocrystals (sample 1), (c) Prepared Lisinopril drug nanocrystals (sample 2), and (d) Prepared Lisinopril drug nanocrystals (sample 3)

#### 4.2.1. XRD Result of Sample 1

As illustrated in Figure 4.12, the Lisinopril drug nanocrystals exhibited spectral prominent diffraction intensity peaks at 7.25°, 12.362°, 19.23°, 22.61°, and 25.10°.

Upon comparing the XRD patterns of the raw and prepared drug nanocrystal powder, it was observed that there were no noticeable changes or differences in the diffractograms between Lisinopril raw and prepared drug nanocrystals.

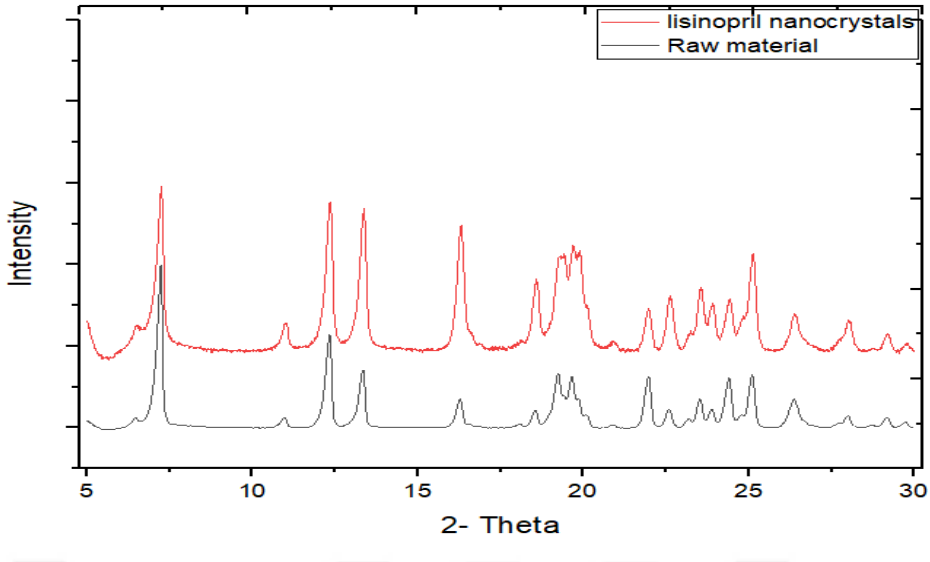


Figure 4.12. Evolution of diffraction patterns comparison raw Lisinopril and prepared Lisinopril drug nanocrystals (sample 1)

Furthermore, the X-ray diffraction (XRD) peaks observed in the raw and produced drug nanocrystal powder (sample 1) exhibit identical diffraction angles without any noticeable shifts or additional/missing peaks, as depicted in Figure 4.12.

### 4.2.2. XRD Result of Sample 2

XRD patterns of the lisinopril drug nanocrystals (sample 2) powder detect that the peak at the seven different diffraction angles were at 7.15°, 12.24°,19.11°, 21.87° and 24.99° as shown in Figure 4.11(c). shows the seven diffraction peaks of Lisinopril drug nanocrystals (sample 2).

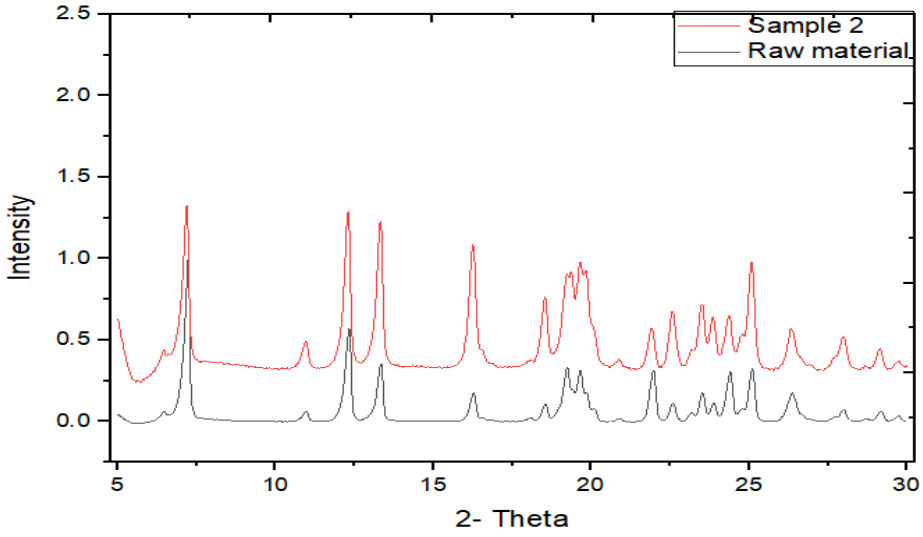


Figure 4.13. Evolution of diffraction patterns comparison raw Lisinopril and prepared Lisinopril drug nanocrystals (sample 2)

In sample 2, there was no discernible difference between the diffractograms of the raw and produced medication nanocrystal powder of lisinopril, as shown in Figure 7.9, which compares the XRD spectra of the two.

### 4.2.3. XRD Result of Sample 3

The spectra depicted in Figure 4.11(d) exhibited seven diffraction peaks corresponding to the Lisinopril raw materials. These peaks were observed at angles of 7.22°, 12.35°, 12.15°, 19.33°, 21.97°, 23.72°, and 25.19°.

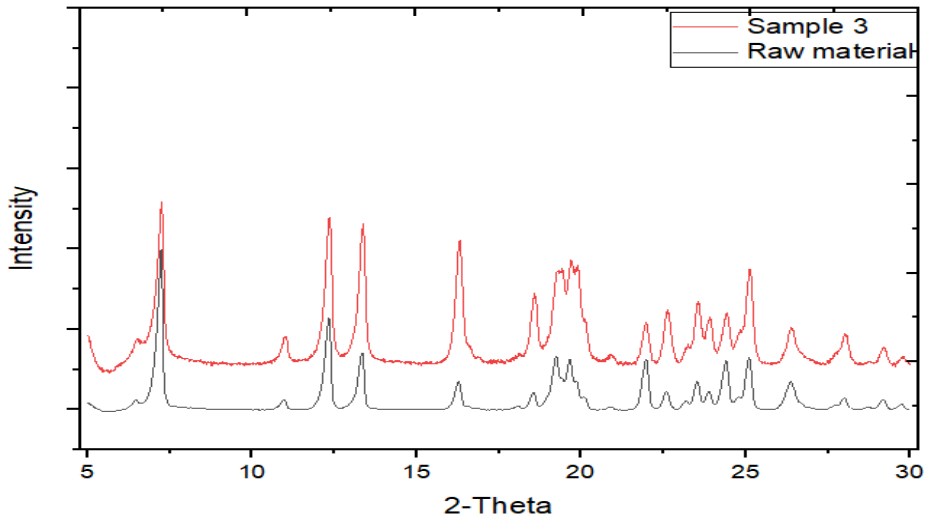


Figure 4.14. Evolution of diffraction patterns comparison raw Lisinopril and prepared Lisinopril drug nanocrystals (sample 2)

The XRD patterns of the raw and prepared drug nanocrystal powders were compared, and the same peaks at the same 2-theta were observed that our operating parameters and additives kept the crystalline structure of final with no change compared to the raw material in the diffractograms between the raw and prepared Lisinopril drug nanocrystals. Furthermore, the X-ray diffraction (XRD) peaks observed in the raw and produced drug nanocrystal powder (sample 3) exhibit identical diffraction angles without any noticeable shifts or additional/missing peaks, as depicted in Figure 4.14.

The X-ray diffraction (XRD) peaks of both the raw and produced drug nanocrystal powder (sample 1, sample 2, and sample 3) exhibit identical diffraction angles, indicating no peak displacement or presence of additional or missing peaks.

The XRD analysis confirmed no alterations in the crystalline structures of the raw and processed samples. Furthermore, the inclusion of additives such as solvent,

antisolvent, and stabilizers did not adversely impact the physical structure of the prepared drug nanocrystals.

### 4.3. FTIR Results

FTIR spectra of the raw and produced drug nanocrystal powder (sample 1, sample 2, and 3) were obtained and are presented in Figure 4.15. All powders exhibit identical absorption peaks within the frequency range of 650–4000.

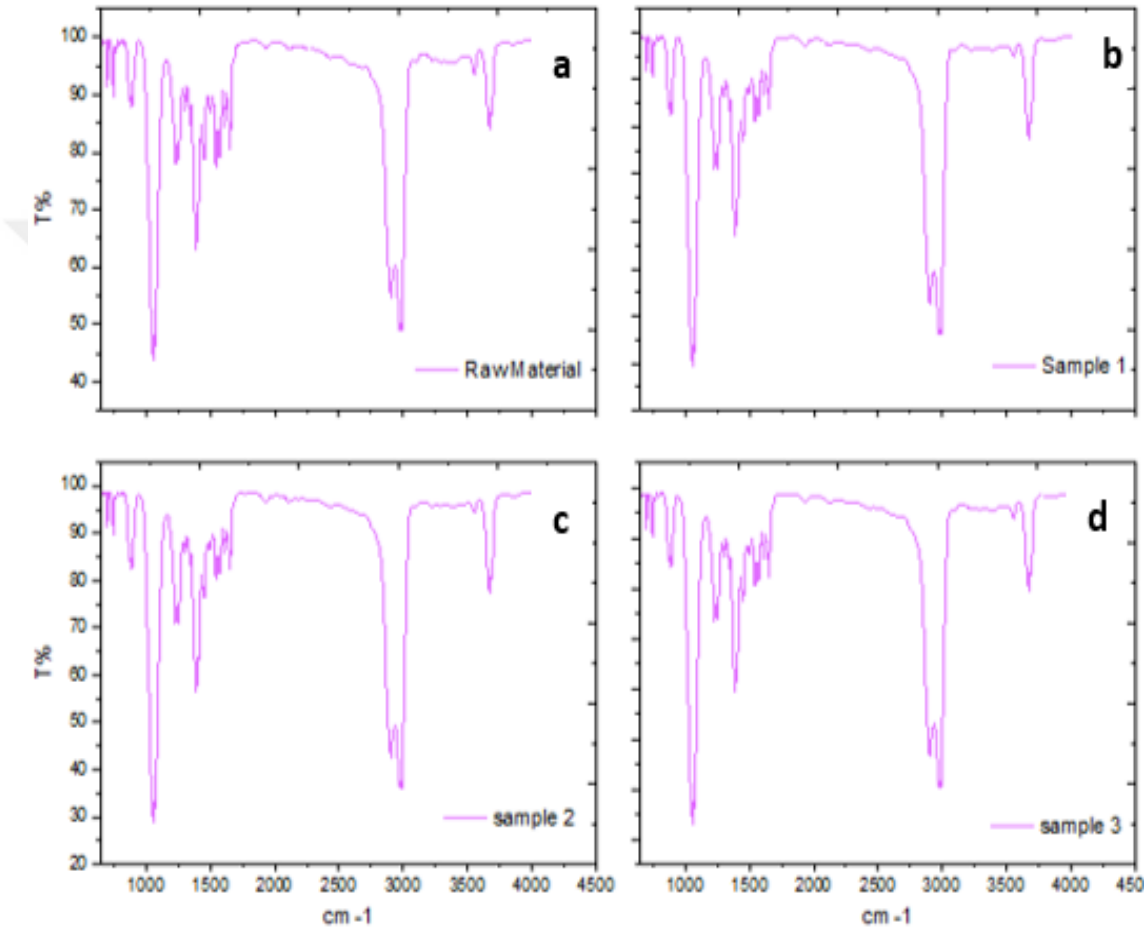


Figure 4.15. IR chart of (a) raw Lisinopril, (b)Lisinopril drug nanocrystals (sample 1), (c) Lisinopril drug nanocrystals (sample 2), and (d) Lisinopril drug nanocrystals (sample 3)

#### 4.3.1. FTIR Result of Sample 1

Figure 4.16 represents the FTIR peaks comparison between raw Lisinopril figure 4.15 (a) and (b) Lisinopril drug nanocrystals (sample 1).

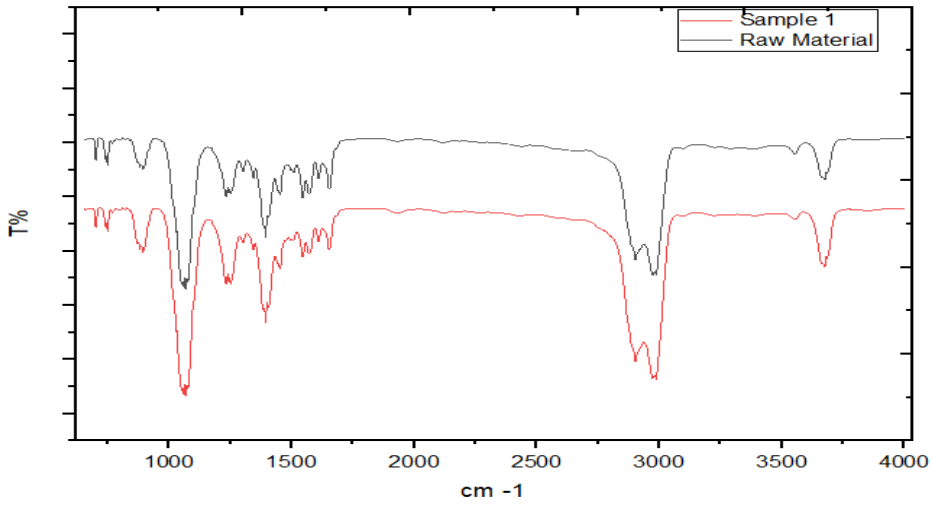


Figure 4.16. IR comparison between raw Lisinopril and prepared Lisinopril drug nanocrystals (sample 1)

There is no discernible variation in the FTIR spectra between raw Lisinopril and Lisinopril drug nanocrystals (sample 1) of both raw and recrystallized nanoparticles (sample 1). The peaks are identical, and the diffractogram has no significant difference, as illustrated in Figure 4.16.

### 4.3.2. FTIR Result of Sample 2

Figure 4.17 shows the FTIR peaks comparison between raw Lisinopril Figure 4.15 (a) and 4.15 (c) Lisinopril drug nanocrystals (sample 2).

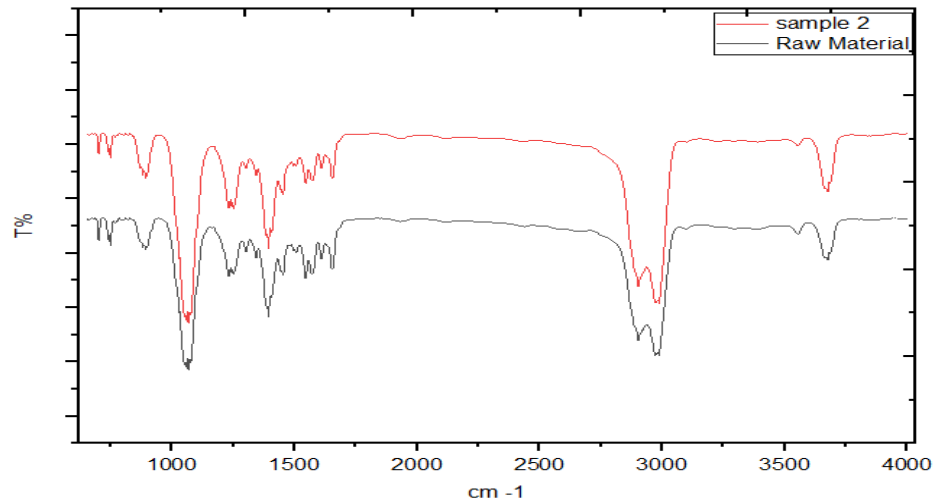


Figure 4.17. IR comparison between raw Lisinopril and prepared Lisinopril drug nanocrystals (sample 2)

According to Figure 4.17, there was no significantly different diffractogram change of FTIR spectrums between raw Lisinopril and prepared Lisinopril drug nanocrystals (sample 2) by antisolvent recrystallization method and pekes completely the same.

### 4.3.3. FTIR Result of Sample 3

The FTIR peaks comparison representation between raw Lisinopril Figure 4.15(a) and 4.15(d) Lisinopril drug nanocrystals (sample 3) illustrated in Figure 4.18.

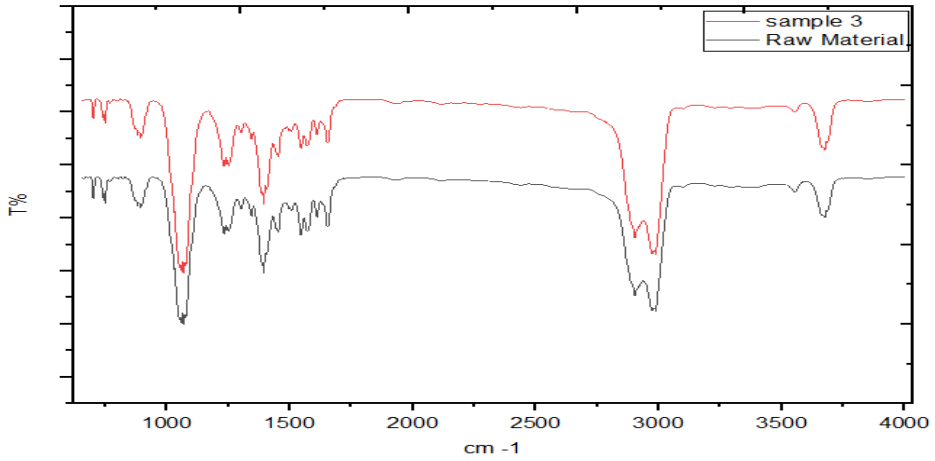


Figure 4.18. IR comparison between raw Lisinopril and prepared Lisinopril drug nanocrystals (sample 3)

According to Figure 4.18, there is no noticeable change of FTIR spectrums between raw Lisinopril and Lisinopril drug nanocrystals (sample 3) of both raw and recrystallized nanoparticles (sample 3), pekes identically same.

As plotted in Table 7.1, the three prepared samples of lisinopril drug nanocrystals had the same functional groups of raw Lisinopril, which means there's no change in the chemical formula, and the action of the stabilizer keeps the chemical structure stable during the process.

Table 4.1The functional groups of Lisinopril

| Absorption | Group | Class | Absorption | Group | Class |
|---|---|---|---|---|---|
| 3700-3584 | O-H | Alcohol | 1420-1330 | O-H | Alcohol |
| 3000-2800 | N-H | Amine salt | 1310-1250 | C-O | Aromatic ester |
| 1662-1626 | C=C | Alkene | 1085-1050 | C-O | Primary alcohol |
| 1550-1500 | N-O | Nitro compound | 895-885 | C=C | Alkene |

### 4.4. Water Content Test

According to the KFT water content test, 500 mg of prepared samples was utilized as a water determent specimen. The titration was performed using Karl Fischer pyridine-free reagent, following the guidelines outlined in USP 44, method 1 (921).

The water content test of lisinopril must be within the limit of (8-9.5)%.

The water content result for sample 1 is equal to 9.39. For sample 2, the water content test was 9.34. sample 3 had an 8.64 as a water content result.

The water test results show that all samples are accepted according to the lisinopril water content limit.

### 4.5. Assay Test

According to USP 44, an assay test was applied for all prepared samples, and raw material was analyzed at the same time and under the same conditions by using HPLC.

#### 4.5.1. Assay Test of Sample 1

According to equation (3.1) and the absorption peaks in Figure 4.19, The assay value was 101.8 %. The proposed approach was precise within the accepted limit.

The chromatogram of raw  Lisinopril and Lisinopril drug nanocrystals in 5.066 and 14.980 retention time of the peaks from active ingredient peaks with sample1.

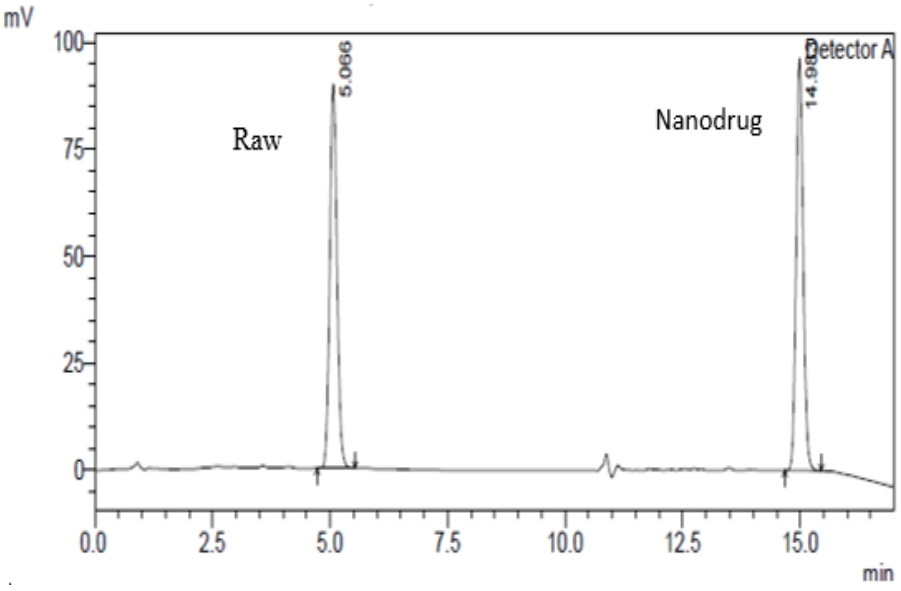


Figure 4.19. Chromatogram of standard solutions for raw and Lisinopril drug

### 4.5.2. Assay Test of Sample 2

The assay value of sample 2 was 101.2 % based on equation (1), and the absorption peaks in Figure 4.20 were within the accepted limit according to USP 44.

The chromatogram of raw Lisinopril and Lisinopril drug nanocrystals in 4.095 and 11.870 retention time of the peaks from active ingredient peaks with the prepared sample.

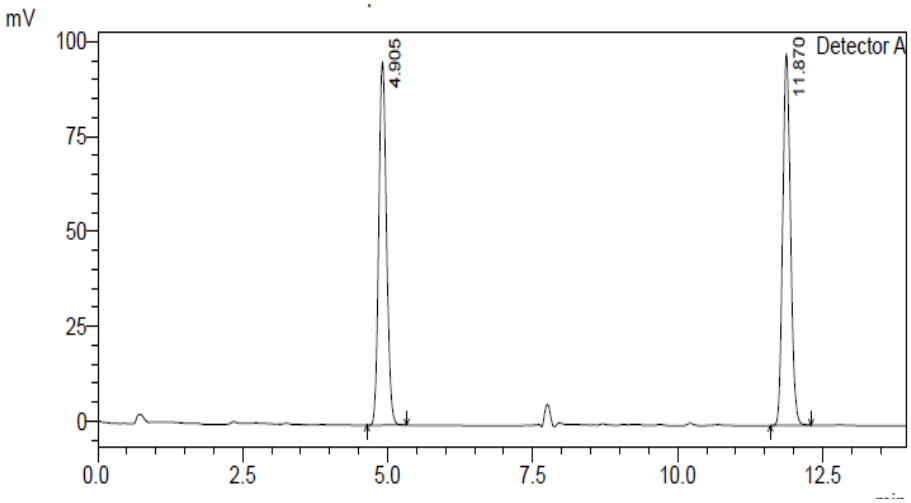


Figure 4.20. Chromatogram of standard solutions for raw and Lisinopril drug nanocrystal (sample 2)

### 4.5.3. Assay Test of Sample 2

The assay value of sample 3 was 100.5 % based on equation (1), and the absorption peaks in Figure 7.16 which were within the accepted limit according to USP 44. The chromatogram of raw Lisinopril and Lisinopril drug nanocrystals in 5.793 and 13.609 retention time of the peaks from active ingredient peaks with the prepared sample.

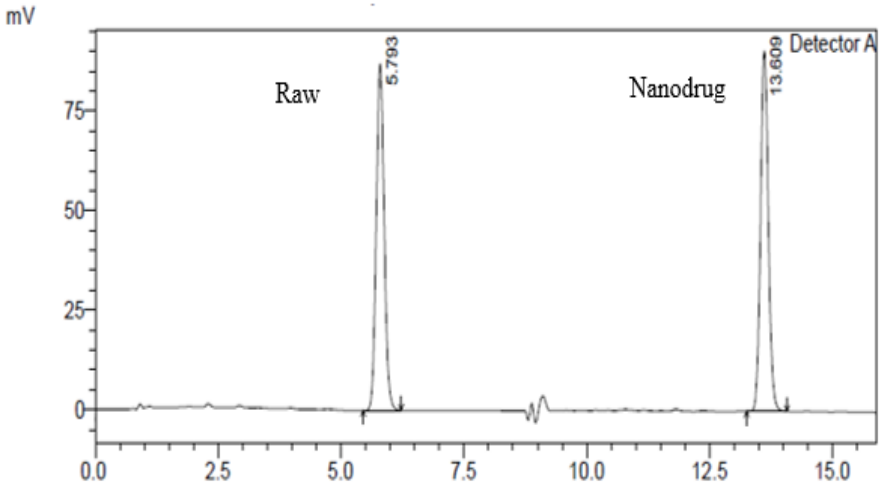


Figure 4.21. Chromatogram of standard solutions for raw and Lisinopril drug nanocrystal (sample 3)

Table 1 summarizes the results of three different concentrations with one repeat at each concentration for accuracy studies. The assay values established that the proposed approach was precise within the limit. The chromatogram of raw 5.066, 4.095, and 5.793 and lisinopril nanocrystals (sample 1, sample 2, and sample 3) in 14.980, 11.870, and 13.609 demonstrated no distortion in peaks from excipient components with active ingredient peaks.

Table 4.2 The assay result of lisinopril nanocrystals with the three different concentrations (sample 1, sample 2, and sample 3)

| Sample no | Ret. Time | Area | Height | Conc. | Assay |
|---|---|---|---|---|---|
| **Sample 1** | 14.980 | 1910073 | 137076 | 50.678 | |
| **Raw** | 5.066 | 1876299 | 142209 | 49.322 | 101.8%. |
| **Sample 2** | 11.870 | 2468460 | 332330 | 50.725 | |
| **Raw** | 4.095 | 243918 | 339228 | 49.275 | 101.2% |
| **Sample 3** | 13.609 | 2534123 | 335479 | 50.620 | |
| **Raw** | 5.793 | 2521516 | 339770 | 49.380 | 100.5% |

### 4.6. Dissolution Test

The bath temperature was set at 37.0 ± 0.5 °C, and the paddle speed was 50 rpm. Separate containers holding 900 ml of sterile water were used to add 10 mg of lisinopril reference standard and lisinopril medication nanocrystal powder, respectively. The drug solubility test was conducted again with 0.1 N hydrochloric acid, and the findings were compared to those obtained with pure water. Once the 30 minutes were up, 2.0 ml of the sample was transferred to a 25 ml volumetric flask, where it was diluted with mobile phase up to volume and filtered using a 0.45 µm syringe filter. Then, a second 25-ml volumetric flask was used to dilute 4.0 ml of this solution to volume with the mobile phase.

The samples were tested for concentration using a high-performance liquid chromatography (HPLC) system at 210 nm (USP 44) using a Shimadzu apparatus, Model LC 2040, with a photodiode array detector. The acceptability threshold for NLT products is 80 %.

### 4.6.1. Dissolution Test of Sample 1

Figure 4.22 shows the absorption peaks of raw and prepared nanodrugs (sample 1). Equation 3.1 was used to calculate the dissolution result of prepared Lisinopril drug nanocrystals. We found the result was 100.6 %, and it was the accepted value according to USP 44.

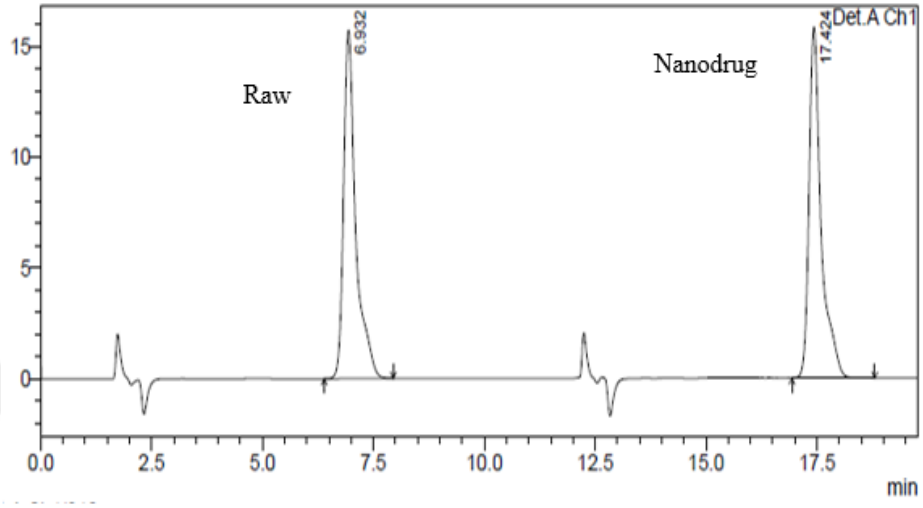


Figure 4.22. Dissolution chromatogram of standard solutions for lisinopril nanodrug and Lisinopril raw material (sample 1)

### 4.6.2. Dissolution Test of Sample 2

Figure 4.23 shows the chromatogram peaks of raw lisinopril and lisinopril drug nanocrystals, respectively.

The area under the curve of both raw Lisinopril and Lisinopril drug nanocrystals was calculated using equation 3.1. The assay result was 98.2 %, which was within the accepted limit.

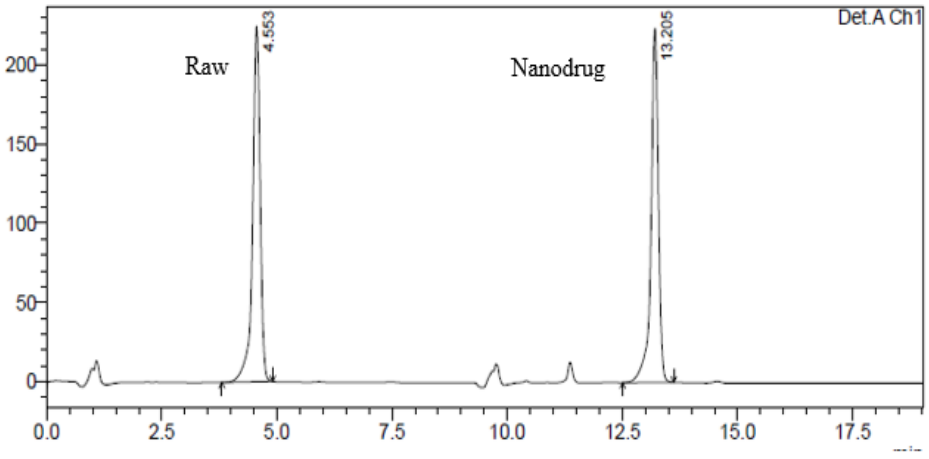


Figure 4.23. Dissolution chromatogram of standard solutions for lisinopril nanodrug and Lisinopril raw material (sample 2)

### 4.6.3. Dissolution Test of Sample 3

Sample 3 was analyzed with respect to raw material as a reference by HPLC to obtain the chromatogram peaks, as shown in Figure 4.24. the dissolution result was 98.8 % by calculating the same for previous samples

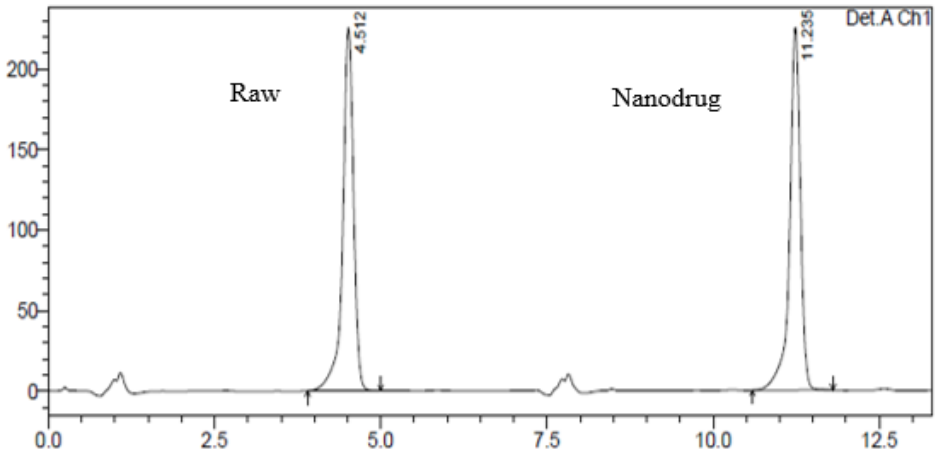


Figure 4.24 Dissolution chromatogram of standard solutions for lisinopril nanodrug and Lisinopril raw material (sample 3)

Table 4.3 The dissolution result of lisinopril nanocrystals with the three different concentrations (sample 1, sample 2, and sample 3)

| Sample no | Ret. Time | Area | Height | Conc. | Dissolution |
|---|---|---|---|---|---|
| **Raw** | 6.932 | 298648 | 15717 | 49.838 | |
| **Sample 1** | 17.424 | 300586 | 15842 | 50.162 | 100.6% |
| **Raw** | 4.553 | 2553730 | 224351 | 50.444 | |
| **Sample 2** | 13.205 | 2508785 | 223558 | 49.556 | 98.2% |
| **Raw** | 4.512 | 2572332 | 225983 | 50.296 | |
| **Sample 3** | 11.235 | 2542092 | 225495 | 49.704 | 98.8 % |

According to absorption peaks illustrated in figures 4.22, 4.23, and 4.24, table 4-3 summarizes the dissolution results of the three samples of prepared lisinopril drug nanocrystals compared with lisinopril raw materials; calculations were made based on eq 1. All the dissolution results were within the accepted limit according to USP 44 guidelines. We observed that the choice of additives was working successfully to produce lisinopril drug nanocrystals without a negative effect. also, the synergic work of stabilizer and ice bathing gives good results in terms of particle size and powder solubility.

### 4.7. Stability Study

For long-term analysis (6 months), an appropriate tight container (a RU MED-Germany stability chamber) was used to store approximately 30 g of each lisinopril medication nanocrystal sample. The sample was then monitored at 30 °C and 15 % relative humidity. If there is a substantial change of 5 % or more in the assay from its initial content of Lisinopril drug nanocrystals API, the stability results will fail, according to the WHO recommendation.

#### 4.7.1. Stability Study of Sample 1

The stability study was made on sample 1 for 6 months. Samples were analyzed at zero time,3 months, and 6 months, as shown in Figure 4.25.

Based on equation 3.1, we calculated the absorption beaks in Figure 7.20

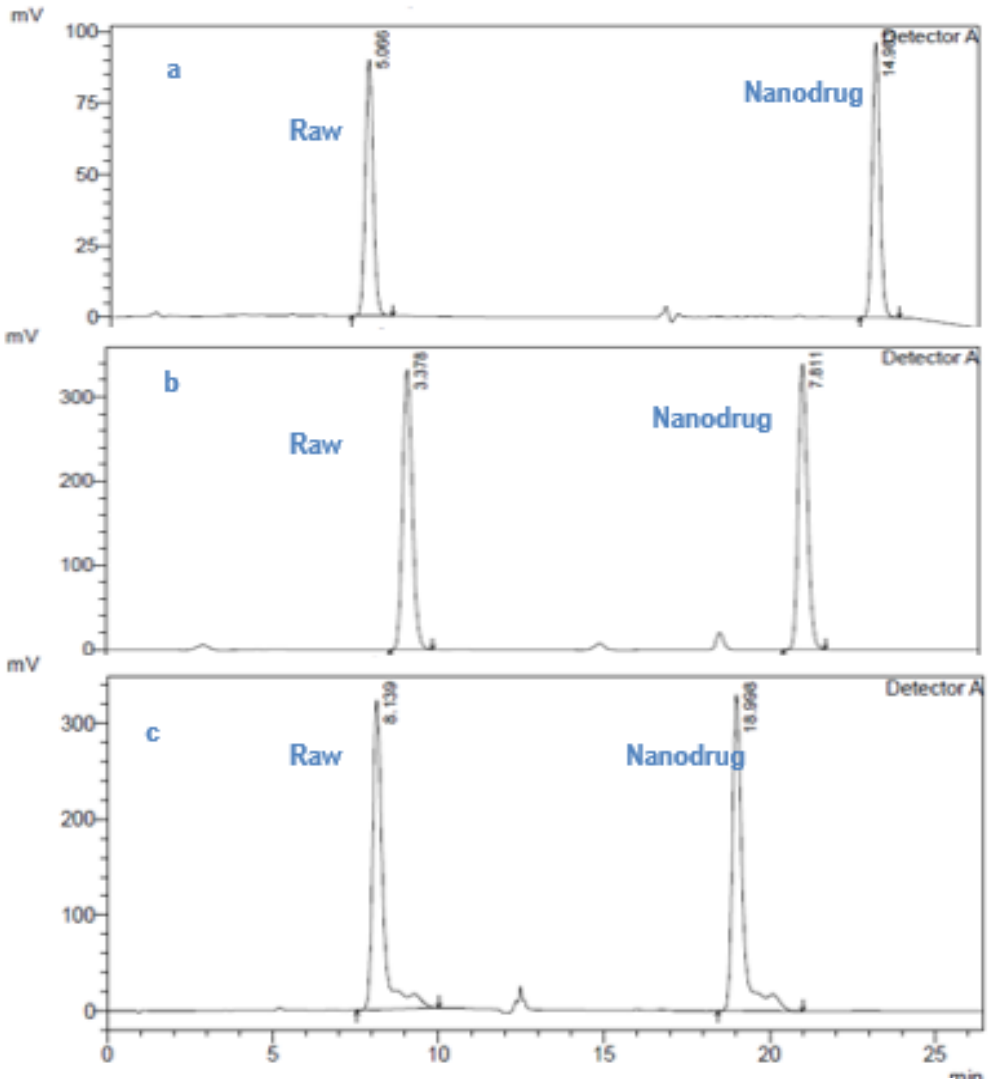


Figure 4.25. Stability study chromatogram of sample 1 at (a) zero time, (b) three months, and (c) six months

according to the area under the curve at the same retention time of raw lisinopril and prepared Lisinopril drug nanocrystals sample 1, we found that the assay at 0 times 101.8 %; after 3 months 100.9 % and after 6 months 100 %. Due to assay results during 6 months of steady stability, the decrease in the assay was 1.8 %.

### 4.7.2. Stability Study of Sample 2

The stability study was made on sample 2 for 6 months. Samples were analyzed at zero time,3 months, and 6 months, as shown in Figure 4.26.

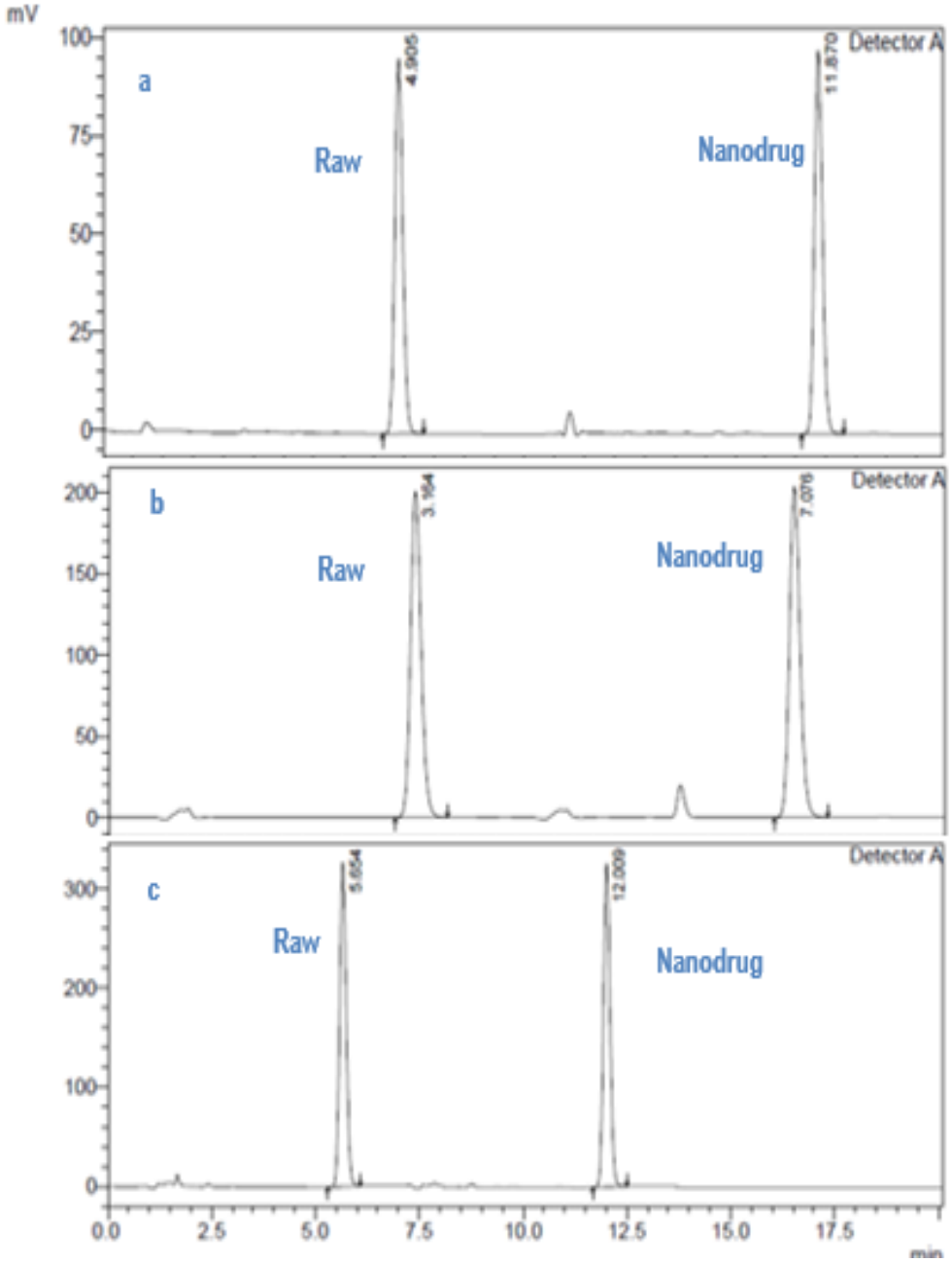


Figure 4.26 Stability study chromatogram of sample 2 at (a) zero time, (b) three months, and (c) six months

Using equation 3.1, we calculated the absorption beaks in Figures 4.26 (a), (b), and (c) according to the area under the curve at the same retention time of raw lisinopril and prepared lisinopril drug nanocrystals sample 2. We found that the assay was at 0 times 101.2 %, after 3 months 99.3 %, and after 6 months 98.2 %. Due to assay results during 6 months of steady stability, the decrease in the assay was 3 %.

### 4.7.3. Stability Study of Sample 3

The stability study was made on sample 3 for 6 months. Samples were analyzed at zero time,3 months, and 6 months, as shown in Figure 4.27.

As for samples 1 and 2, using equation 3.1, we calculated the absorption beaks

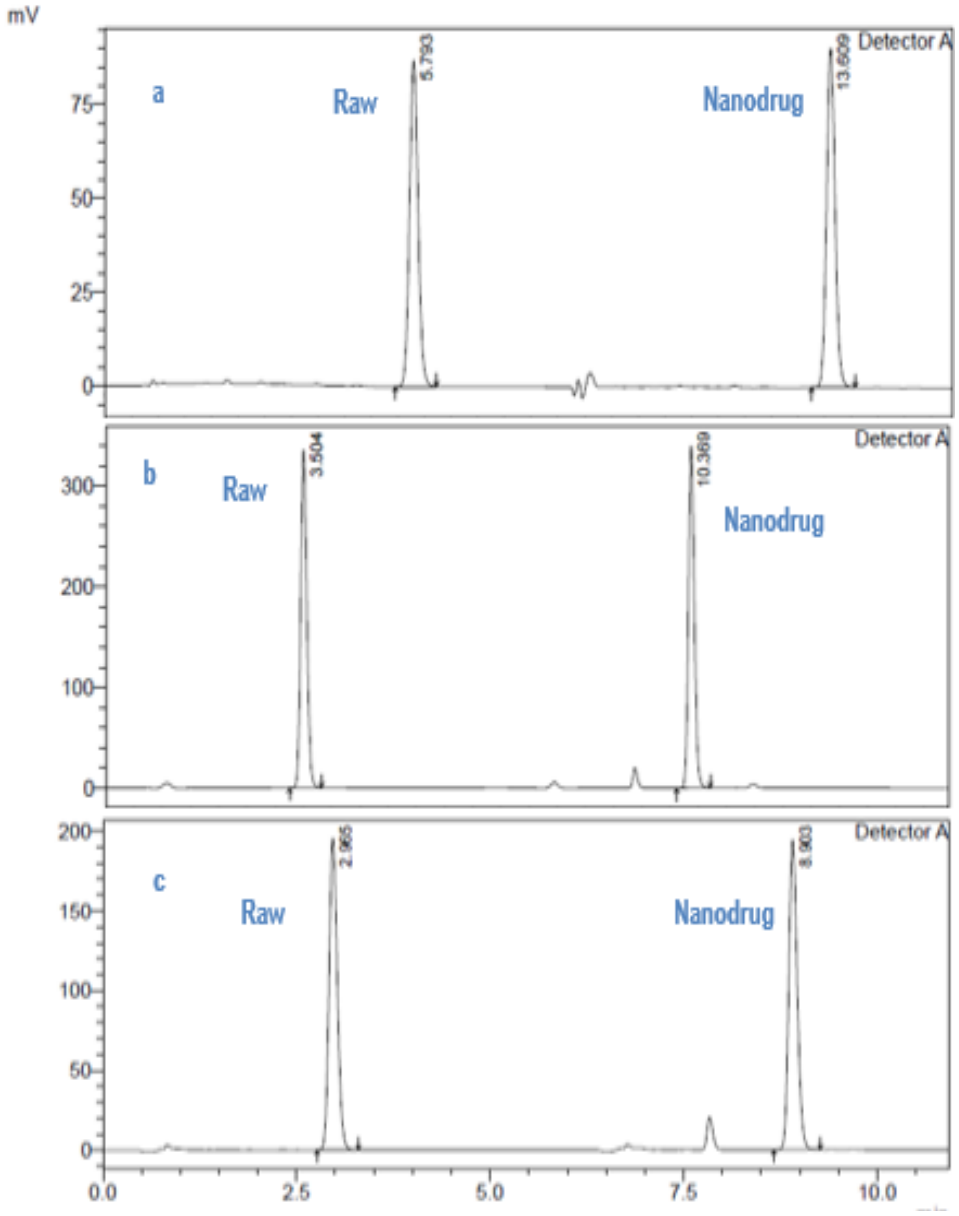


Figure 4.27 Stability study chromatogram of sample 3 at (a) zero time, (b) three months, and (c) six months

in Figure 4.27. (a), (b), and (c) according to the area under the curve at the same retention time of raw Lisinopril and prepared Lisinopril drug nanocrystals sample 2, we found that the assay at 0 time 100.5 %, after 3 months 98.6 % and after 6 months 98.6 %. Due to assay results during 6 months of steady stability, the decrease in the assay was 1.9 %.

Table 4.4 The assay was based on the stability study of sample 1, sample 2, and sample 3 for 6 months

| Sample No | 0 month | 3 month | 6 month | Assay dropping |
|---|---|---|---|---|
| **Sample 1** | 101.8% | 100.9% | 100% | 1.8% |
| **Sample 2** | 101.2% | 99.3% | 98.2% | 3% |
| **Sample3** | 100.5%, | 98.6% | 98.6% | 1.9% |

According to the assay results in Table 4.4, all the prepared samples have good stability due to the decrease in assay after 6 months of the study. We observed that the operations variable can control the stability of the lisinopril drug nanocrystals with different concentrations.

On the other hand, we found that PVP and Tween 20 had effective preservation work to keep the chemical formula without changing more than Tween 80. Further samples had the same operation conditions, the same storage conditions, and the same analysis media ( devices set up solvent, antisolvent solutions, stabilizer, temperature, and operating time).

## 5. CONCLUSION

The antisolvent recrystallization method was successfully used to prepare Lisinopril drug nanocrystals als with three different concentrations. All samples (1, 2, and 3) were prepared with the presence of an ice bath.

For the first sample, the best conditions were a solvent solution of 100 mg/ml lisinopril in distilled water and an antisolvent mixture of acetonitrile and dimethylene formamide. As an additional stabilizing measure, 1 % PVP was employed.

Lisinopril solutions with a supersaturated concentration of 100 mg/ml were prepared. These solutions were filtered using a 0.45 µm inlet filter. The filtered solutions were injected into a beaker that already contained a solution of acetonitrile and dimethylene formamide. The injection was done at a flow rate of 3 ml/min while swirling the mixture at a speed of 1500 rpm.

The fabrication of sample 2 involved dissolving 50 mg of lisinopril in 100 ml of distilled water, using acetonitrile and acetone as antisolvents and 1 % Tween 80 as a stabilizing agent. The solution was then mixed with acetone, acetonitrile, dimethylene formamide, and Tween 80 with dropwise injection. This technique, combined with Scanning Electron Microscopy, provides essential data on scanned specimens.

Sample 3 was placed dropwise in an antisolvent solution containing 1 % Tween, 20, and 99 % acetone at a ratio of 1:3, with a stirring speed of 1300 rpm and a flow rate of 1.5 ml/min. The sample had a concentration of 25 mg/ml of distilled water.

According to SEM results, the particle size of sample 1 ranged between 65.75 nm and 182.26 nm, sample 2 was between 85.60 nm and 197.24 nm, and sample 3 was between 57.75 nm and 145.85 nm. By comparison with the XRD pattern of raw lisinopril, no significant difference was found with respect to prepared drug nanocrystals.

The particle size distribution of sample 1 varied from 100 nm to 120 nm, with a high amount,

For sample 2, the highest amount of prepared nanodrug was between 100 nm and 120 nm, the second amount was between 60nm and 80nm, and the third ranged between 80 nm and 100 nm.

The particle size distribution of sample 3 had the highest nanoparticle size, between 100 nm to 120 nm, second between 80 nm to 100 nm, and third between 60 and 80.

The choice of additives worked successfully to produce Lisinopril drug nanocrystals without a negative effect. also, the synergic work of stabilizer and ice bathing gives good results in terms of particle size and powder solubility.

One of the most important operating variables, the synergic work of stabilizers and ice baths, controls the growth of particles by decreasing the reaction temperature, which works to avoid side reactions and prevent particle agglomerations.

The solvent solution flow rate and antisolvent solution stirring speed were essential variables. An observation was made that increasing the antisolvent's flow rate while decreasing the stirring speed resulted in larger particle size and increased particle agglomeration. To prevent temperature-induced side reactions, it is necessary to maintain a low temperature for the antisolvent solution during the preparation process.

The solvent-to-antisolvent ratio increases or decreases the precipitate sample amount at the end of the process. It was important to increase the antisolvent volume compressing with the volume of solvent solution.

Tween 20 and acetone gave the best results, like regular spherical shape and smallest particle size.

Also, particle size can be controlled using low solvent concentration.

The functional groups of prepared samples were the same as those for raw materials. There was no change in physical or chemical properties based on XRD and FTIR results.

The pharmaceutical results, like assay water content and dissolution, were within the accepted limits according to USP 44 guidelines.

Samples have a stable pharmaceutical formula during 6 months of stability study. The assay drop for sample 1 was 1.9 %, for sample 2, it was 3 %, and for sample 3, it was 1.9 %, which was accepted according to the limitation of WHO.

PVP and Tween 20 had effective preservation work to keep the chemical formula without a change of more than Tween 80. Further samples had the same operation conditions, the same storage conditions, and the same analysis media ( devices set up solvent, antisolvent solutions, stabilizer, temperature, and operating time).

# REFERENCE


Abraham, M. H., Ibrahim, A., Zissimos, A. M., Zhao, Y. H., Comer, J., & Reynolds, D. P. (2002). Application of hydrogen bonding calculations in property based drug design. *Drug Discovery Today, 7*(20), 1056-1063.

Ai, J., Biazar, E., Jafarpour, M., Montazeri, M., Majdi, A., Aminifard, S., Rad, H. G. (2011). Nanotoxicology and nanoparticle safety in biomedical designs. *International journal of nanomedicine*, 1117-1127.

Baravkar, A., Kale, R., & Sawant, S. (2011). FTIR Spectroscopy: principle, technique and mathematics. *International Journal of Pharma and Bio Sciences, 2*(1), 513-519.

Barsagade, P., Khetade, R., Nirwan, K., Agrawal, T., Gotafode, S., & Lade, U. Using RP-HPLC.

Bawa, R., Melethil, S., Simmons, W. J., & Harris, D. (2008). Nanopharmaceuticals: patenting issues and FDA regulatory challenges. *The SciTech Lawyer, 5*(2), 10-15.

Berthomieu, C., & Hienerwadel, R. (2009). Fourier transform infrared (FTIR) spectroscopy. *Photosynthesis research, 101*, 157-170.

Bezalel, S., Mahlab-Guri, K., Asher, I., Werner, B., & Sthoeger, Z. M. (2015). Angiotensin-converting enzyme inhibitor-induced angioedema. *The American journal of medicine, 128*(2), 120-125.

Bitterlich, A., Laabs, C., Krautstrunk, I., Dengler, M., Juhnke, M., Grandeury, A., . . . Kwade, A. (2015). Process parameter dependent growth phenomena of naproxen nanosuspension manufactured by wet media milling. *European journal of pharmaceutics and biopharmaceutics, 92*, 171-179.

Bothiraja, C., Shinde, M. B., Rajalakshmi, S., & Pawar, A. P. (2009). Evaluation of molecular pharmaceutical and in-vivo properties of spray-dried isolated andrographolide—PVP. *Journal of Pharmacy and Pharmacology, 61*(11), 1465-1472.

Brittain, H. G., & Grant, D. J. (1999). Effects of polymorphism and solid-state solvation on solubility and dissolution rate. *Drugs and the pharmaceutical sciences, 95*, 279-330.

Brown, M. J. (2008). Aliskiren. *Circulation, 118*(7), 773-784.

Cabanillas, B., & Novak, N. (2021). Allergy to COVID-19 vaccines: a current update. *Allergology International, 70*(3), 313-318.

Cannavo, A., Bencivenga, L., Liccardo, D., Elia, A., Marzano, F., Gambino, G., . . . Rengo, G. (2018). Aldosterone and mineralocorticoid receptor system in cardiovascular physiology and pathophysiology. *Oxidative medicine and cellular longevity, 2018*.

CESARANO III, J., Aksay, I. A., & Bleier, A. (1988). Stability of aqueous α-Al2O3 suspensions with poly (methacrylic acid) polyelectrolyte. *Journal of the American Ceramic Society, 71*(4), 250-255.

Chang, T.-L., Zhan, H., Liang, D., & Liang, J. F. (2015). Nanocrystal technology for drug formulation and delivery. *Frontiers of Chemical Science and Engineering, 9*, 1-14.

Chen, Y. J., Li, L. J., Tang, W. L., Song, J. Y., Qiu, R., Li, Q., . . . Wright, J. M. (2018). First-line drugs inhibiting the renin angiotensin system versus other first-line antihypertensive drug classes for hypertension. *Cochrane database of systematic reviews*(11).

Chen, Z., Wu, W., & Lu, Y. (2020). What is the future for nanocrystal-based drug-delivery systems? In (Vol. 11, pp. 225-229): Future Science.

Chow, A. H., Tong, H. H., Chattopadhyay, P., & Shekunov, B. Y. (2007). Particle engineering for pulmonary drug delivery. *Pharmaceutical research, 24*, 411-437.

Collins, R., Peto, R., MacMahon, S., Godwin, J., Qizilbash, N., Hebert, P., . . . Fiebach, N. (1990). Blood pressure, stroke, and coronary heart disease: part 2, short-term reductions in blood pressure: overview of randomised drug trials in their epidemiological context. *The Lancet, 335*(8693), 827-838.

Cui, T., Kovell, R. C., Brooks, D. C., & Terlecki, R. P. (2015). A urologist's guide to ingredients found in top-selling nutraceuticals for men's sexual health. *The journal of sexual medicine, 12*(11), 2105-2117.

Danilatos, G. D., & Robinson, V. (1979). Principles of scanning electron microscopy at high specimen chamber pressures. *Scanning, 2*(2), 72-82.

de Leeuw, P. W. (2002). Antihypertensive treatment and the kidney. *Cardiovascular drugs and therapy, 16*(6), 483.

Dhaval, M., Makwana, J., Sakariya, E., & Dudhat, K. (2020). Drug nanocrystals: a comprehensive review with current regulatory guidelines. *Current drug delivery, 17*(6), 470-482.

do Vale, G. T., Ceron, C. S., Gonzaga, N. A., Simplicio, J. A., & Padovan, J. C. (2019). Three generations of β-blockers: history, class differences and clinical applicability. *Current hypertension reviews, 15*(1), 22-31.

Dou, H., Morehead, J., Destache, C. J., Kingsley, J. D., Shlyakhtenko, L., Zhou, Y., . . . Rabinow, B. E. (2007). Laboratory investigations for the morphologic, pharmacokinetic, and anti-retroviral properties of indinavir nanoparticles in human monocyte-derived macrophages. *Virology, 358*(1), 148-158.

Dubey, A., Kotian, B., & Shriram, R. G. (2019). New Drugs and Clinical Trials Rules, 2019: Towards Fast-track Accessibility of New Drugs to the Indian Population. *Indian Journal of Pharmaceutical Education and Research, 53*(4), S451-S459.

Dumbreck, S., Flynn, A., Nairn, M., Wilson, M., Treweek, S., Mercer, S. W., . . . Guthrie, B. (2015). Drug-disease and drug-drug interactions: systematic examination of recommendations in 12 UK national clinical guidelines. *bmj, 350*.

Dwivedi, M., Blech, M., Presser, I., & Garidel, P. (2018). Polysorbate degradation in biotherapeutic formulations: identification and discussion of current root causes. *International journal of pharmaceutics, 552*(1-2), 422-436.

Dwivedi, M., Buske, J., Haemmerling, F., Blech, M., & Garidel, P. (2020). Acidic and alkaline hydrolysis of polysorbates under aqueous conditions: towards understanding polysorbate degradation in biopharmaceutical formulations. *European Journal of Pharmaceutical Sciences, 144*, 105211.

Fatehi, L., Wolf, S. M., McCullough, J., Hall, R., Lawrenz, F., Kahn, J. P., . . . Erdman, A. G. (2012). Recommendations for nanomedicine human subjects research oversight: an evolutionary approach for an emerging field. *Journal of Law, Medicine & Ethics, 40*(4), 716-750.

Felton, L. A. (2016). *Aqueous polymeric coatings for pharmaceutical dosage forms*: CRC Press.

Fischer, K. (1935). A new method for the analytical determination of the water content of liquids and solids. *Angew. Chem, 48*(394), 24.

Folttmann, H., & Quadir, A. (2008). Polyvinylpyrrolidone (PVP)—one of the most widely used excipients in pharmaceuticals: an overview. *Drug Deliv Technol, 8*(6), 22-27.

Food, U., & Administration, D. (2017). Aranesp (darbepoetin alfa) injection, for intravenous or subcutaneous use. Highlights of prescribing information. In.

Ganesh, G., Sureshkumar, R., Jawahar, N., Senthil, V., Venkatesh, D. N., & Srinivas, M. S. (2010). Preparation and evaluation of sustained release matrix tablet of diclofenac sodium using natural polymer. *Journal of pharmaceutical sciences and research, 2*(6), 360.

Gangapure, S. P., & Bhusnure, O. G. (2019). Nanopharmaceuticals. *Journal of Drug Delivery and Therapeutics, 9*(4), 676-687.

Gao, L., Zhang, D., & Chen, M. (2008). Drug nanocrystals for the formulation of poorly soluble drugs and its application as a potential drug delivery system. *Journal of Nanoparticle Research, 10*, 845-862.

Ghosh, I., Schenck, D., Bose, S., & Ruegger, C. (2012). Optimization of formulation and process parameters for the production of nanosuspension by wet media milling technique: effect of vitamin E TPGS and nanocrystal particle size on oral absorption. *European Journal of Pharmaceutical Sciences, 47*(4), 718-728.

Giles, T. D., Berk, B. C., Black, H. R., Cohn, J. N., Kostis, J. B., Izzo Jr, J. L., & Weber, M. A. (2005). Expanding the definition and classification of hypertension. *The Journal of Clinical Hypertension, 7*(9), 505-512.

Go, A. S., Mozaffarian, D., Roger, V. L., Benjamin, E. J., Berry, J. D., Borden, W. B., . . . Fox, C. S. (2013). Heart disease and stroke statistics—2013 update: a report from the American Heart Association. *Circulation, 127*(1), e6-e245.

Gough, W. B., Zeiler, R. H., Barreca, P., & El-Sherif, N. (1982). Hypotensive action of commercial intravenous amiodarone and polysorbate 80 in dogs. *Journal of Cardiovascular Pharmacology, 4*(3), 375-380.

Gupta, P., & Bansal, A. K. (2005). Spray drying for generation of a ternary amorphous system of celecoxib, PVP, and meglumine. *Pharmaceutical development and technology, 10*(2), 273-281.

Hachmann, J., Olivares-Amaya, R., Atahan-Evrenk, S., Amador-Bedolla, C., Sánchez-Carrera, R. S., Gold-Parker, A., . . . Aspuru-Guzik, A. (2011). The Harvard clean energy project: large-scale computational screening and design of organic photovoltaics on the world community grid. *The Journal of Physical Chemistry Letters, 2*(17), 2241-2251.

Hall, E., Wodi, A., Hamborsky, J., Morelli, V., & Schillie, S. (2021). *Epidemiology and prevention of vaccine-preventable diseases*: US Department of Health and Human Services, Centers for Disease Control and ….

Hare, J. I., Lammers, T., Ashford, M. B., Puri, S., Storm, G., & Barry, S. T. (2017). Challenges and strategies in anti-cancer nanomedicine development: An industry perspective. *Advanced drug delivery reviews, 108*, 25-38.

Hatkar, U. N., & Gogate, P. R. (2012). Process intensification of anti-solvent crystallization of salicylic acid using ultrasonic irradiations. *Chemical Engineering and Processing: Process Intensification, 57*, 16-24.

Hecold, M., Buczkowska, R., Mucha, A., Grzesiak, J., Rac-Rumijowska, O., Teterycz, H., & Marycz, K. (2017). The effect of PEI and PVP-stabilized gold nanoparticles on equine platelets activation: Potential application in equine regenerative medicine. *Journal of Nanomaterials, 2017*.

Hey, E. (2003). Vitamin K—what, why, and when. *Archives of Disease in Childhood-Fetal and Neonatal Edition, 88*(2), F80-F83.

Homayouni, A., Sadeghi, F., Varshosaz, J., Garekani, H. A., & Nokhodchi, A. (2014). Promising dissolution enhancement effect of soluplus on crystallized celecoxib obtained through antisolvent precipitation and high pressure homogenization techniques. *Colloids and surfaces B: Biointerfaces, 122*, 591-600.

Hu, M., Li, C., Li, X., Zhou, M., Sun, J., Sheng, F., . . . Lu, L. (2018). Zinc oxide/silver bimetallic nanoencapsulated in PVP/PCL nanofibres for improved antibacterial activity. *Artificial cells, nanomedicine, and biotechnology, 46*(6), 1248-1257.

Ingole, S. A., & Kumbharkhane, A. (2021). Temperature dependent Broadband dielectric relaxation study of Aqueous Polyvinylpyrrolidone (PVP K-15, K-30 & K-90) using a TDR. *Physics and Chemistry of Liquids, 59*(5), 806-816.

Iwashita, N. (2016). X-ray powder diffraction. In *Materials science and engineering of carbon* (pp. 7-25): Elsevier.

Jackson, R., & Bellamy, M. (2015). Antihypertensive drugs. *BJA education, 15*(6), 280-285.

Jalvandi, J. (2016). *Novel chemical and physical approaches for sustainable drug release from biodegradable electrospun nanofibres.* RMIT University,

Jog, R., & Burgess, D. J. (2017). Pharmaceutical amorphous nanoparticles. *Journal of pharmaceutical sciences, 106*(1), 39-65.

Junghanns, J.-U. A., & Müller, R. H. (2008). Nanocrystal technology, drug delivery and clinical applications. *International journal of nanomedicine, 3*(3), 295-310.

Junyaprasert, V. B., & Morakul, B. (2015). Nanocrystals for enhancement of oral bioavailability of poorly water-soluble drugs. *Asian journal of pharmaceutical sciences, 10*(1), 13-23.

Kakran, M., Sahoo, N. G., Li, L., & Judeh, Z. (2013). Particle size reduction of poorly water soluble artemisinin via antisolvent precipitation with a syringe pump. *Powder technology, 237*, 468-476.

Kakran, M., Sahoo, N. G., Tan, I.-L., & Li, L. (2012). Preparation of nanoparticles of poorly water-soluble antioxidant curcumin by antisolvent precipitation methods. *Journal of Nanoparticle Research, 14*, 1-11.

Kannan, M. (2018). Scanning electron microscopy: Principle, components and applications. *A textbook on fundamentals and applications of nanotechnology*, 81-92.

Kannel, W. B. (1991). Left ventricular hypertrophy as a risk factor: the Framingham experience. *Journal of hypertension, 9*, S3-S9.

Kannel, W. B. (1996). Blood pressure as a cardiovascular risk factor: prevention and treatment. *Jama, 275*(20), 1571-1576.

Kerwin, B. A. (2008). Polysorbates 20 and 80 used in the formulation of protein biotherapeutics: structure and degradation pathways. *Journal of pharmaceutical sciences, 97*(8), 2924-2935.

Kesisoglou, F., Panmai, S., & Wu, Y. (2007). Nanosizing—oral formulation development and biopharmaceutical evaluation. *Advanced drug delivery reviews, 59*(7), 631-644.

Khadka, P., Ro, J., Kim, H., Kim, I., Kim, J. T., Kim, H., . . . Lee, J. (2014). Pharmaceutical particle technologies: An approach to improve drug solubility, dissolution and bioavailability. *Asian journal of pharmaceutical sciences, 9*(6), 304-316.

Khan, S. A., Khan, S. B., Khan, L. U., Farooq, A., Akhtar, K., & Asiri, A. M. (2018). Fourier transform infrared spectroscopy: fundamentals and application in functional groups and nanomaterials characterization. *Handbook of materials characterization*, 317-344.

Khan, T. A., Mahler, H.-C., & Kishore, R. S. (2015). Key interactions of surfactants in therapeutic protein formulations: a review. *European journal of pharmaceutics and biopharmaceutics, 97*, 60-67.

Kikuya, M., Hansen, T. W., Thijs, L., Björklund-Bodegård, K., Kuznetsova, T., Ohkubo, T., . . . Ibsen, H. (2007). Diagnostic thresholds for ambulatory blood pressure monitoring based on 10-year cardiovascular risk. *Circulation, 115*(16), 2145-2152.

Kim, S., Ng, W. K., Dong, Y., Das, S., & Tan, R. B. (2012). Preparation and physicochemical characterization of trans-resveratrol nanoparticles by temperature-controlled antisolvent precipitation. *Journal of Food Engineering, 108*(1), 37-42.

Klag, M. J., Whelton, P. K., Randall, B. L., Neaton, J. D., Brancati, F. L., Ford, C. E., . . . Stamler, J. (1996). Blood pressure and end-stage renal disease in men. *New England Journal of Medicine, 334*(1), 13-18.

Klein, D. M., & Cherrington, N. J. (2014). Organic and inorganic transporters of the testis: A review. *Spermatogenesis, 4*(2), e979653.

Klein, T., Buhr, E., & Frase, C. G. (2012). TSEM: A review of scanning electron microscopy in transmission mode and its applications. *Advances in imaging and electron physics, 171*, 297-356.

Law, M., Wald, N., & Morris, J. (2003). Lowering blood pressure to prevent myocardial infarction and stroke: a new preventive strategy. *Health technology assessment (Winchester, England), 7*(31), 1-94.

Levy, G., & Hayes, B. A. (1960). Physicochemical basis of the buffered acetylsalicylic acid controversy. *New England Journal of Medicine, 262*(21), 1053-1058.

Li, C., Li, C., Le, Y., & Chen, J.-F. (2011). Formation of bicalutamide nanodispersion for dissolution rate enhancement. *International journal of pharmaceutics, 404*(1-2), 257-263.

Li, D., & Kaner, R. B. (2006). Shape and aggregation control of nanoparticles: not shaken, not stirred. *Journal of the American Chemical Society, 128*(3), 968-975.

Lin, Y., & Ma, L. (2018). Blood pressure lowering effect of calcium channel blockers on perioperative hypertension: a systematic review and meta-analysis. *Medicine, 97*(48).

Lu, P. J., & Weitz, D. A. (2013). Colloidal particles: Crystals, glasses, and gels. *Annu. Rev. Condens. Matter Phys., 4*(1), 217-233.

Lu, Y., Li, Y., & Wu, W. (2016). Injected nanocrystals for targeted drug delivery. *Acta Pharmaceutica Sinica B, 6*(2), 106-113.

Lu, Y., Qi, J., Dong, X., Zhao, W., & Wu, W. (2017). The in vivo fate of nanocrystals. *Drug Discovery Today, 22*(4), 744-750.

Ma, C., Oketch-Rabah, H., Kim, N.-C., Monagas, M., Bzhelyansky, A., Sarma, N., & Giancaspro, G. (2018). Quality specifications for articles of botanical origin from the United States Pharmacopeia. *Phytomedicine, 45*, 105-119.

Marković, M., & Cucic, B. (2018). Transformer Lifetime Management through Solid and Liquid Insulation Assessment. *Proceedings of the Euro TechCon*.

Martins, R. M., Pereira, S. V., Siqueira, S., Salomão, W. F., & Freitas, L. A. P. (2013). Curcuminoid content and antioxidant activity in spray dried microparticles containing turmeric extract. *Food research international, 50*(2), 657-663.

Medicine, N. L. o. (2000). *Medical subject headings* (Vol. 41): US Department of Health and Human Services, Public Health Service, National ….

Meier, R. J. (2005). Vibrational spectroscopy: a ‘vanishing’discipline? *Chemical Society Reviews, 34*(9), 743-752.

Moldoveanu, S. C., & David, V. (2022). *Essentials in modern HPLC separations*: Elsevier.

Müller, R. H., Gohla, S., & Keck, C. M. (2011). State of the art of nanocrystals–special features, production, nanotoxicology aspects and intracellular delivery. *European journal of pharmaceutics and biopharmaceutics, 78*(1), 1-9.

Mulvihill-Wilson, J., Gaffney, F., Pettinger, W., Blomqvist, C., Anderson, S., & Graham, R. (1983). Hemodynamic and neuroendocrine responses to acute and chronic alpha-adrenergic blockade with prazosin and phenoxybenzamine. *Circulation, 67*(2), 383-393.

Nash, D. (1990). Alpha-adrenergic blockers: Mechanism of action, blood pressure control, and effects on lipoprotein metabolism. *Clinical cardiology, 13*(11), 764-772.

Noyes, A. A., & Whitney, W. R. (1897). The rate of solution of solid substances in their own solutions. *Journal of the American Chemical Society, 19*(12), 930-934.

Oketch-Rabah, H. A., Marles, R. J., Jordan, S. A., & Dog, T. L. (2019). United States pharmacopeia safety review of Willow Bark. *Planta medica, 85*(16), 1192-1202.

Park, M.-W., & Yeo, S.-D. (2012). Antisolvent crystallization of carbamazepine from organic solutions. *Chemical Engineering Research and Design, 90*(12), 2202-2208.

Park*, M.-W., & Yeo, S.-D. (2010). Antisolvent crystallization of roxithromycin and the effect of ultrasound. *Separation Science and Technology, 45*(10), 1402-1410.

Paulino, A., Rauber, G., Campos, C., Maurício, M., De Avillez, R., Capobianco, G., . . . Cuffini, S. (2013). Dissolution enhancement of Deflazacort using hollow crystals prepared by antisolvent crystallization process. *European Journal of Pharmaceutical Sciences, 49*(2), 294-301.

Pavasini, R., Camici, P. G., Crea, F., Danchin, N., Fox, K., Manolis, A. J., . . . Pinto, F. (2019). Anti-anginal drugs: Systematic review and clinical implications. *International journal of cardiology, 283*, 55-63.

Peck, T., & Harris, B. (2021). *Pharmacology for anaesthesia and intensive care*: Cambridge University Press.

Pokharana, M., Vaishnav, R., Goyal, A., & Shrivastava, A. (2018). Stability testing guidelines of pharmaceutical products. *Journal of Drug Delivery and Therapeutics, 8*(2), 169-175.

Popkin, B. M., & Kristen, E. (2010). ’Anci, and Irwin H. Rosenberg. *Water, hydration, and health. Nutrition reviews, 68*(8), 439-458.

Pramanick, S., Singodia, D., & Chandel, V. (2013). Excipient selection in parenteral formulation development. *Pharma Times, 45*(3), 65-77.

Prior, A., Frutos, P., & Correa, C. (2010). *Comparison of dissolution profiles: current guidelines.* Paper presented at the Proceedings of the VI Congreso SEFIG.

Prosapio, V., De Marco, I., & Reverchon, E. (2016). PVP/corticosteroid microspheres produced by supercritical antisolvent coprecipitation. *Chemical Engineering Journal, 292*, 264-275.

Qureshi, S. A. (2004). A new crescent-shaped spindle for drug dissolution testing-but why a new spindle? *Dissolution Technologies, 11*, 13-21.

Ragelle, H., Danhier, F., Préat, V., Langer, R., & Anderson, D. G. (2017). Nanoparticle-based drug delivery systems: a commercial and regulatory outlook as the field matures. *Expert opinion on drug delivery, 14*(7), 851-864.

Rajan, H. (2015). Development and validation of HPLC method-A Review. *International. Journal of current research in pharmacy, 1*(2), 55-68.

Ramalingam, V., Varunkumar, K., Ravikumar, V., & Rajaram, R. (2018). Target delivery of doxorubicin tethered with PVP stabilized gold nanoparticles for effective treatment of lung cancer. *Scientific reports, 8*(1), 3815.

Ran, Q., Wang, M., Kuang, W., Ouyang, J., Han, D., Gao, Z., & Gong, J. (2022). Advances of combinative nanocrystal preparation technology for improving the insoluble drug solubility and bioavailability. *Crystals, 12*(9), 1200.

Rangel-Yagui, C. d. O., Pessoa Jr, A., & Tavares, L. C. (2005). Micellar solubilization of drugs. *J. Pharm. Pharm. Sci, 8*(2), 147-163.

Rao, B. V., Sowjanya, G. N., Ajitha, A., & Rao, V. U. M. (2015). A review on stability indicating HPLC method development. *World journal of pharmacy and pharmaceutical sciences, 4*(8), 405-423.

Rapsomaniki, E., Timmis, A., George, J., Pujades-Rodriguez, M., Shah, A. D., Denaxas, S., . . . Smeeth, L. (2014). Blood pressure and incidence of twelve cardiovascular diseases: lifetime risks, healthy life-years lost, and age-specific associations in 1· 25 million people. *The Lancet, 383*(9932), 1899-1911.

Rasekh, M., Karavasili, C., Soong, Y. L., Bouropoulos, N., Morris, M., Armitage, D., . . . Ahmad, Z. (2014). Electrospun PVP–indomethacin constituents for transdermal dressings and drug delivery devices. *International journal of pharmaceutics, 473*(1-2), 95-104.

Ravindran, R., Juliet, S., Gopalan, A. K. K., Kavalimakkil, A. K., Ramankutty, S. A., Nair, S. N., . . . Ghosh, S. (2011). Toxicity of DMSO, Triton X 100 and tween 20 against Rhipicephalus (Boophilus) annulatus. *Journal of Parasitic Diseases, 35*, 237-239.

Razvi, S. Z. A., Kamm, I., Nguyen, T., Pellett, J. D., & Kumar, A. (2021). Loss on drying using halogen moisture analyzer: An orthogonal technique for monitoring volatile content for in-process control samples during pharmaceutical manufacturing. *Organic Process Research & Development, 25*(2), 300-307.

Reddy, D. N., Singh, A., Shrivastava, B., & Kumar, K. R. (2021). Recent Trends on Regulatory Aspects of Nanotechnology in Indian Pharmaceutical Market. *International Journal of Pharmaceutical Research (09752366), 13*(1).

Regulski, M., Regulska, K., J Stanisz, B., Murias, M., Gieremek, P., Wzgarda, A., & Niznik, B. (2015). Chemistry and pharmacology of Angiotensin-converting enzyme inhibitors. *Current pharmaceutical design, 21*(13), 1764-1775.

Ren, X., Qi, J., Wu, W., Yin, Z., Li, T., & Lu, Y. (2019). Development of carrier-free nanocrystals of poorly water-soluble drugs by exploring metastable zone of nucleation. *Acta Pharmaceutica Sinica B, 9*(1), 118-127.

Reynolds, R. (1989). Principles and techniques of quantitative analysis of clay minerals by X-ray powder diffraction.

Roth, Z., & Brown, M. M. (2006). The seventh report of the Joint National Committee on Prevention, Detection, Evaluation, and Treatment of High Blood Pressure: The JNC report. *Evidence-Based Ophthalmology, 7*(4), 170-171.

Schwartzberg, L. S., & Navari, R. M. (2018). Safety of polysorbate 80 in the oncology setting. *Advances in therapy, 35*, 754-767.

Shen, C., Yang, Y., Shen, B., Xie, Y., Qi, J., Dong, X., . . . Yuan, H. (2018). Self-discriminating fluorescent hybrid nanocrystals: efficient and accurate tracking of translocation via oral delivery. *Nanoscale, 10*(1), 436-450.

Sheskey, R. C. R. P. J., & Quinn, M. E. (2009). *Handbook of pharmaceutical excipients*.

Shete, G., Jain, H., Punj, D., Prajapat, H., Akotiya, P., & Bansal, A. K. (2016). Stabilizers used in nano-crystal based drug delivery systems. *Journal of Excipients and Food Chemicals, 5*(4).

Sinha, B., Müller, R. H., & Möschwitzer, J. P. (2013). Bottom-up approaches for preparing drug nanocrystals: formulations and factors affecting particle size. *International journal of pharmaceutics, 453*(1), 126-141.

Sinko, P. J. (2023). *Martin's physical pharmacy and pharmaceutical sciences*: Lippincott Williams & Wilkins.

Smart, J. D. (2005). The basics and underlying mechanisms of mucoadhesion. *Advanced drug delivery reviews, 57*(11), 1556-1568.

Smith, I., & Jackson, I. (2010). Beta-blockers, calcium channel blockers, angiotensin converting enzyme inhibitors and angiotensin receptor blockers: should they be stopped or not before ambulatory anaesthesia? *Current Opinion in Anesthesiology, 23*(6), 687-690.

Souney, P. F., Cooper, W. D., & Cushing, D. J. (2010). PM101: intravenous amiodarone formulation changes can improve medication safety. *Expert Opinion on Drug Safety, 9*(2), 319-333.

Speakman, S. A. (2011). Basics of X-ray powder diffraction. *Massachusetts-USA, 2011a. Disponível em:< http://prism. mit. edu/xray/Basics% 20of% 20X-Ray% 20Powder% 20Diffraction. pdf*.

Srivalli, K. M. R., & Mishra, B. (2016). Drug nanocrystals: A way toward scale-up. *Saudi Pharmaceutical Journal, 24*(4), 386-404.

Sriyanti, I., Edikresnha, D., Munir, M. M., Rachmawati, H., & Khairurrijal, K. (2017). *Electrospun polyvinylpyrrolidone (PVP) nanofiber mats loaded by Garcinia mangostana L. extracts.* Paper presented at the Materials Science Forum.

Talebi, M., & Armstrong, D. W. (2020). Water determination. In *Specification of Drug Substances and Products* (pp. 459-477): Elsevier.

ten Tije, A. J., Verweij, J., Loos, W. J., & Sparreboom, A. (2003). Pharmacological effects of formulation vehicles: implications for cancer chemotherapy. *Clinical pharmacokinetics, 42*, 665-685.

Teng, H., Chen, L., & Lee, W. Y. (2017). Anti-Solvent Crystallization of L-Alanine and Effects of Process Parameters and Ultrasound. *Food Science and Technology Research, 23*(4), 495-502.

Tocci, G., Battistoni, A., Passerini, J., Musumeci, M. B., Francia, P., Ferrucci, A., & Volpe, M. (2015). Calcium channel blockers and hypertension. *Journal of cardiovascular pharmacology and therapeutics, 20*(2), 121-130.

Tran, T. T.-D., Tran, P. H.-L., Nguyen, M. N. U., Tran, K. T. M., Pham, M. N., Tran, P. C., & Van Vo, T. (2014). Amorphous isradipine nanosuspension by the sonoprecipitation method. *International journal of pharmaceutics, 474*(1-2), 146-150.

Uddin, R., Saffoon, N., & Sutradhar, K. B. (2011). Dissolution and dissolution apparatus: a review. *Int. J. Curr. Biomed. Pharm. Res, 1*(4), 201-207.

Ummadi, S., Shravani, B., Rao, N., Reddy, M. S., & Sanjeev, B. (2013). Overview on controlled release dosage form. *System, 7*(8), 51-60.

Van Vark, L. C., Bertrand, M., Akkerhuis, K. M., Brugts, J. J., Fox, K., Mourad, J.-J., & Boersma, E. (2012). Angiotensin-converting enzyme inhibitors reduce mortality in hypertension: a meta-analysis of randomized clinical trials of renin–angiotensin–

aldosterone system inhibitors involving 158 998 patients. *European heart journal, 33*(16), 2088-2097.

Van Zuylen, L., Verweij, J., & Sparreboom, A. (2001). Role of formulation vehicles in taxane pharmacology. *Investigational new drugs, 19*, 125-141.

Vasan, R. S., Larson, M. G., Leip, E. P., Evans, J. C., O'Donnell, C. J., Kannel, W. B., & Levy, D. (2001). Impact of high-normal blood pressure on the risk of cardiovascular disease. *New England Journal of Medicine, 345*(18), 1291-1297.

Verma, S., Gokhale, R., & Burgess, D. J. (2009). A comparative study of top-down and bottom-up approaches for the preparation of micro/nanosuspensions. *International journal of pharmaceutics, 380*(1-2), 216-222.

Verma, S., Kumar, S., Gokhale, R., & Burgess, D. J. (2011). Physical stability of nanosuspensions: investigation of the role of stabilizers on Ostwald ripening. *International journal of pharmaceutics, 406*(1-2), 145-152.

Villain, G., Thiery, M., & Platret, G. (2007). Measurement methods of carbonation profiles in concrete: Thermogravimetry, chemical analysis and gammadensimetry. *Cement and concrete research, 37*(8), 1182-1192.

Warner, A. M., Stafford, J. D., & Warburton, R. E. (2007). Strategy for active pharmaceutical ingredients. *American laboratory, 39*(12), 15-18.

Warner, N. J., & Rush, J. E. (1988). Safety profiles of the angiotensin-converting enzyme inhibitors. *Drugs, 35*, 89-97.

Whelton, P. K., Carey, R. M., Aronow, W. S., Casey, D. E., Collins, K. J., Dennison Himmelfarb, C., . . . Jones, D. W. (2018). 2017 ACC/AHA/AAPA/ABC/ACPM/AGS/APhA/ASH/ASPC/NMA/PCNA guideline for the prevention, detection, evaluation, and management of high blood pressure in adults: a report of the American College of Cardiology/American Heart Association Task Force on Clinical Practice Guidelines. *Journal of the American College of Cardiology, 71*(19), e127-e248.

Winarni, I., Waluyo, T., & Pasaribu, G. (2020). *Optimization of pulp concentration for bioethanol production from elephant grass (Pennisetum purpureum) using two commercial yeasts with addition of Tween 20.* Paper presented at the IOP Conference Series: Earth and Environmental Science.

Wu, L., Zhang, J., & Watanabe, W. (2011). Physical and chemical stability of drug nanoparticles. *Advanced drug delivery reviews, 63*(6), 456-469.

Xia, D., Quan, P., Piao, H., Piao, H., Sun, S., Yin, Y., & Cui, F. (2010). Preparation of stable nitrendipine nanosuspensions using the precipitation–ultrasonication method for enhancement of dissolution and oral bioavailability. *European Journal of Pharmaceutical Sciences, 40*(4), 325-334.

Xie, Y., Shi, B., Xia, F., Qi, J., Dong, X., Zhao, W., . . . Lu, Y. (2018). Epithelia transmembrane transport of orally administered ultrafine drug particles evidenced by environment sensitive fluorophores in cellular and animal studies. *Journal of Controlled Release, 270*, 65-75.

Yang, S., Liu, J., Chen, Y., & Jiang, J. (2012). Reversal effect of Tween-20 on multidrug resistance in tumor cells in vitro. *Biomedicine & Pharmacotherapy, 66*(3), 187-194.

Yoon, S., Rhee, S.-j., Heo, S. J., Oh, T. Y., Yoon, S. H., Cho, J.-Y., . . . Yu, K.-S. (2017). Comparable pharmacokinetics and pharmacodynamics of two epoetin alfa formulations Eporon® and Eprex® following a single subcutaneous administration in healthy male volunteers. *Drug Design, Development and Therapy*, 3127-3135.

Yu, M., Han, C., Zhou, Q., Liu, C., & Ding, Z. (2017). Clinical effects of prophylactic use of phentolamine in patients undergoing pheochromocytoma surgery. *Journal of Clinical Anesthesia*, *44*, 119-119.

Yusuf, S., Thom, T., & Abbott, R. D. (1989). Changes in hypertension treatment and in congestive heart failure mortality in the United States. *Hypertension, 13*(5_supplement), I74.

Zaky, M., El-Sayedl, M. Y., El-Megharbel, S. M., Abo Taleb, S., & Refat, M. S. (2014). Synthesis, chemical structure elucidation and biological studies on the effect of some vital metal ions on lisinopril. *Journal of the Mexican Chemical Society, 58*(2), 142-151.

Zanchetti, A., Sleight, P., & Birkenhägert, W. H. (1993). Evaluation of organ damage in hypertension. *Journal of hypertension, 11*(8), 875-882.

Zevin, L. S., & Kimmel, G. (2012). *Quantitative X-ray diffractometry*: Springer Science & Business Media.

Zhang, L., Liang, Y., Meng, L., & Wang, C. (2009). Characterization of complexation of PVP copolymer with DNA. *Polymers for Advanced Technologies, 20*(4), 410-415.

Zhang, Z.-B., Shen, Z.-G., Wang, J.-X., Zhao, H., Chen, J.-F., & Yun, J. (2009). Nanonization of megestrol acetate by liquid precipitation. *Industrial & engineering chemistry research, 48*(18), 8493-8499.

Zheng, X., Zhang, T., Song, X., Zhang, L., Zhang, C., Jin, S., . . . Liang, X.-J. (2015). Structural impact of graft and block copolymers based on poly (N-vinylpyrrolidone) and poly (2-dimethylaminoethyl methacrylate) in gene delivery. *Journal of Materials Chemistry B, 3*(19), 4027-4035.

Zhou, W., Apkarian, R., Wang, Z. L., & Joy, D. (2007). Fundamentals of scanning electron microscopy (SEM). *Scanning Microscopy for Nanotechnology: Techniques and Applications*, 1-40.

# CURRICULUM VITEA

Abdulmohsin AL AIROA completed my bachelor's degree from the Department of Chemical Engineering in 2007, followed by my master's in Biomedical Nanoengineering from 2018 to 2020. In 2020, I enrolled in the Department of Nanoscience and Nanotechnology at Ondokuz Mayis University, Samsun.

**Contact Information :**

ORCID ID : 0009-0008-9777-9423

**Publications :**

**1.** Abdulmohsin Al Aıroa, Ibrahim Inanc. (2023). Pharmaceutıcal Preparatıon and Characterızatıons of Lısınoprıl Drug Nanocrystals By Usıng Antı-Solvent Crystallızatıon Methods. Turkey, Academy Global Publishing House

**2.** Abdulmohsin AL AIROA, İbrahim İNANC. (2024). Effect of Antisolvent Recrystallization Method’s Operation Variables on The Particle Size of Produced Lisinopril Drug Nanocrystals. International 7th Usbilim Health, Engineering, and Applied Sciences Congress. Cairo, Egypt, Ubs-Institute of International Scientific Research and Strategy Development Association.